

**International
Progress Report**

IPR-04-23

Äspö Hard Rock Laboratory

EBS Task Force

**Proceedings from Task Force-related
meeting on Buffer & Backfill modelling**

Lund on March 10-11th, 2004

Roland Pusch, Geodevelopment AB

Christer Svemar, Svensk Kärnbränslehantering AB

May 2004

Svensk Kärnbränslehantering AB

Swedish Nuclear Fuel
and Waste Management Co
Box 5864
SE-102 40 Stockholm Sweden
Tel 08-459 84 00
+46 8 459 84 00
Fax 08-661 57 19
+46 8 661 57 19



**Äspö Hard Rock
Laboratory**

Report no.	No.
IPR-04-23	F89K
Author	Date
Roland Pusch	2004-05-06
Christer Svemar	
Checked by	Date
Christer Svemar	2004-07-08
Approved	Date
Christer Svemar	2004-08-26

Äspö Hard Rock Laboratory

EBS Task Force

Proceedings from Task Force-related meeting on Buffer & Backfill modelling

Lund on March 10-11th, 2004

Roland Pusch, Geodevelopment AB

Christer Svemar, Svensk Kärnbränslehantering AB

May 2004

Keywords: Task Force, THMC, buffer, backfill, Prototype Repository, Febex

This report concerns a study which was conducted for SKB. The conclusions and viewpoints presented in the report are those of the author(s) and do not necessarily coincide with those of the client.

Abstract

An overall conclusion from the workshop is that that modelling of some of the major physical processes in buffers and backfills, like the evolution of temperature and hydration, can be made with sufficient accuracy for practical purposes. However, reliable prediction of the hydration process requires that the hydraulic boundaries are well defined, which can not be made today on the basis of geohydrological data. Furthermore, the present theoretical models may not illustrate the true mechanisms in the hydration process. As to the chemical evolution more general models, representing chemically open conditions, are required. A number of important issues for further research in the framework of the Task Force have been identified.

Sammanfattning

En allmän slutsats från workshopen är att modellering av några av de viktigaste fysikaliska processerna i buffert och återfyllning, såsom utveckling av temperatur och bevätning, kan göras med tillräcklig noggrannhet för praktiska ändamål. Emellertid kräver pålitlig förutsägelse av bevättningsprocessen att de hydrauliska gränsvillkoren kan definieras, vilket inte kan ske i dagsläget på basis av geohydrologiska data. Vidare kan det vara så att de nu använda teoretiska modellerna inte helt återspeglar de verkliga mekanismerna som styr bevättningsprocessen. När det gäller den kemiska utvecklingen krävs mer generella modeller som representerar kemiskt öppna system. Ett antal viktiga frågor för fortsatt forskningsarbete för Task Force har identifierats.

Executive Summary

It appears from the workshop that modelling of some of the major physical processes, like the evolution of temperature and the hydration of buffers and backfills under isothermal conditions, can be made with sufficient accuracy for practical purposes. However, this is the case only if the hydraulic boundaries, represented by the EDZ, are such that access to water for saturation is unlimited and well defined with respect to uniformity, while it is not yet known whether the currently used codes are capable of adequately predicting the hydration process in “dry” rock. In fact the models may not illustrate the true mechanisms in the hydration process. As to the chemical evolution the present attempts to describe possible changes require more general models, especially concerning the openness: groundwater flow in the surroundings of deposition holes, bringing in and out chemical species that affect the buffers and backfills, must be introduced.

Putting together the suggestions for further research in the framework of the Task Force one identifies the following major issues, which are similar to those specified in the final report of the Prototype Repository Project respecting modelling of the performance of buffers and backfills:

- Predictions of the access to water from the rock in deposition holes and tunnels for the wetting of the buffer are uncertain and future work related to the role of rock structure on different scales is required for adequate modelling of the hydration of buffers and backfills.
- Predictions and measurements of temperature agree well although some models overestimate the temperature somewhat. The impact of gaps and joints and changes in water content as well as of vapour-driven heat transfer should be further looked into.
- The hydration rate is difficult to predict and both the basic processes in water migration under isothermal conditions and thermal gradients requires further examination.
- The evolution of pressure and mechanical response of the buffer is the most difficult task because it requires that fracturing and displacements in the buffer be included in the models. The issue of interrelation of hydration/dehydration and swelling/consolidation is relevant. Since prediction of the hydration rate is uncertain forecasting of the mechanical response is even more uncertain. More work is required for solving the problem of non-uniform swelling pressure affecting the canisters.

A very important fact is that although the attendants of the workshop represented the modelling groups involved in the various national and EC-supported projects CROP and Prototype Repository Project focusing on EBS, there are additional competent researchers in this and other fields that may represent different opinions. Hence, it is of fundamental importance to let other members of the scientific community examine and review future work.

Contents

1	Introduction	11
2	Synthesis of papers and discussions	13
2.1	Rock mechanics	13
2.2	Geohydrology	14
2.2	Geohydrology	15
2.3	EBS modelling	16
2.4	Basic physical processes in EBS	18
2.5	Chemical processes in buffers and backfills	19
3	General conclusions from the workshop	21
4	Written contributions	23
4.1	Modelling underground mines for rock stability assessment using boundary elements. A new approach for large scale problems.	23
4.2	A new numerical tool for analysis of coupled far-field and near-field processes	33
4.3	Experience with thermo-hydro-mechanical modelling: the tunnel sealing experiment	43
4.4	Experience with hydro-mechanical modelling: the tunnel sealing experiment	53
4.5	Modelling the thermal-hydraulic-chemical-mechanical (THCM) behaviour of bentonite buffers	63
4.6	A perspective of the modelling of Prototype Repository experiment	73
4.7	Mechanisms in buffer hydration – are our modelling attempts OK?	83
4.8	Proposal of an alternative re-saturation model for bentonite buffers - the conceptual model, the numerical model and the data base	95
4.9	Prediction of geochemical changes in the Prototype Repository tunnel backfill	103
	List of Appendices	113

1 Introduction

The ongoing work on developing conceptual and numerical models for describing and forecasting the performance of EBS components in underground laboratories and repositories points to an increasing need for comparing theoretical results with actual experimental data, which are now being accessible from the comprehensive field experiments. Such work, the overall aim of which is to develop improved models, is planned to be made in the framework of a Task Force established by the organizations that are responsible for handling and disposal of radioactive waste products. The basis of the work was planned to be defined in a special workshop on EBS modelling held in Lund, Sweden, in March this year, being a spin-off activity of the more general symposium on Large Scale Field Tests in Granite organized by ENRESA and held in Sitges in Spain in November 2003.

Invitation to take part in the Lund workshop was sent to all the modellers representing the respective waste-handling organizations and to the European Commission as well as to some well-known modellers dealing with similar issues in adjacent research fields, primarily disposal of toxic chemical waste. Their works were expected to provide some new information to the already well-working groups of scientists. The list of participants is enclosed in Appendix 21.

The Lund workshop comprised three sessions: 1) Conceptual models, 2) Codes, and 3) THMC applications. It took one day, starting at noon on March 10 and ending with a Task Force meeting that was terminated in the afternoon of March 11. The subjects were not specified but it was recommended that they should concern EBS performance, including the function of the surrounding rock with respect to its mechanical, hydraulic, and chemical roles.

The presentations were the ones specified in the table below (Table 1) most of them being associated with written contributions that are given in Chapter 4, and with viewgraphs collected in the appendices.

Table 1. List of presentations

Title	Author	Appendix no
Relevant THMC Phenomena and Mathematical description	A. Gens, Technical university of Catalonia	1
Modelling the Thermal-Hydraulic-Chemical-Mechanical (THMC) behaviour of bentonite buffer	H. R. Thomas, P. j. Cleall, T. A. Melhuish and S. C. Seetharam, Geoenvironmental Research Centre	2
Hydraulic Rock-Buffer Interaction	Richard Weston, Lund University Dept. Production and Materials Engineering	3
Conclusions	R Pusch, Geodevelopment AB	4
Influence of water penetration rates on heterogeneous buffer	E. Alonso, Cimne	5
Code-Bright: A THMC numerical simulator	A. Gens, Technical University of Catalonia	6
Numerical Simulation of coupled Heat, Moisture and Salt Transfer in porous Materials	Heiko Fechner, University of Technology	7
A new numerical tool for analysis of coupled far-field near-field processes	Viktor Popov, Wessex Inst. Of Tech.	8
AECL Experiences with HM modelling: Tunnel Sealing Experiment	D. Dixon, R. Guo, AECL	9
A perspective of the modelling of Prototype Repository Experiment	A. Ledsema, G. J. Chen, Cimne	10
Proposal of an alternative re-saturation model for bentonite buffers	Klaus-Peter Kröhn, GRS	11
Pressure distribution versus excavation Disturbed zone in a filled deposition hole - non isothermal two-phase flow in Porous media	Lutz Liedtke, BGR	12
Problem statement and course of work	Lennart Börgesson, Clay Technology	13
Coupled modelling with Rockflow/Rockmech – Current Status	T. Nowak, BGR	14
Predicting THMC Behaviour Of Febex Bentonite At Different Scales	A. Gens, Technical university of Catalonia	15
Modelling gas migration in clay buffers	E. Alonso, Cimne	16
Prediction of geochemical changes in the Prototype Repository tunnel backfill	A. Luukkonen, VTT	17
Proposal for continued modelling work	E. Alonso, UPC	18
Modelling Underground Mines For Rock Stability Assessment Using Boundary Elements A New Approach For Large Scale Problems	Viktor Popov, Wessex Inst. Of Tech.	19

2 Synthesis of papers and discussions

2.1 Rock mechanics

Rock mechanical issues were in focus of one of the papers that described the use of boundary element technique for numerical solution of stability problems in repositories (*Adey and Calaon*). The example provided represented the 400 m deep Stripa mine in granite, the rock structure being generalized to consist of three families of fracture zoned mutually orthogonal and 100 meters distant from each other. The pre- and post-processor GiD and the Boundary Element software Beasy have been used for model preparation, solution and post processing. Modelling technology has been developed to enable the investigation of stability in the presence of a large number of fracture zones while at the same time determining the detailed stress near the repository, considering i.a. the EDZ.

In order to have an idea of the extent of the critical “coulomb” zone and of the mesh dimension necessary to represent it with sufficient precision, a number of simplified models were created with and without EDZ. Rock pressure was applied indirectly to the model, by forcing a compression displacement of the side walls of the model, as in the “full” case with sub-modelling. Since the value of the displacements to be used could not be predicted in advance, two cases were considered and a linear interpolation used to obtain the required values for a third model to confirm the result. The software is designed to automatically interpolate and so map the results on one model to provide the loads and boundary conditions for the other using a radial basis function approximation to ensure accuracy. This makes the detailed study of regions of special interest easy to perform (see figure 2:1). The study definitely shows that BEM provides excellent tools for solving very intricate rock stability problems and is superior to FEM in the sense that more complex problems can be solved with less computer capacity.

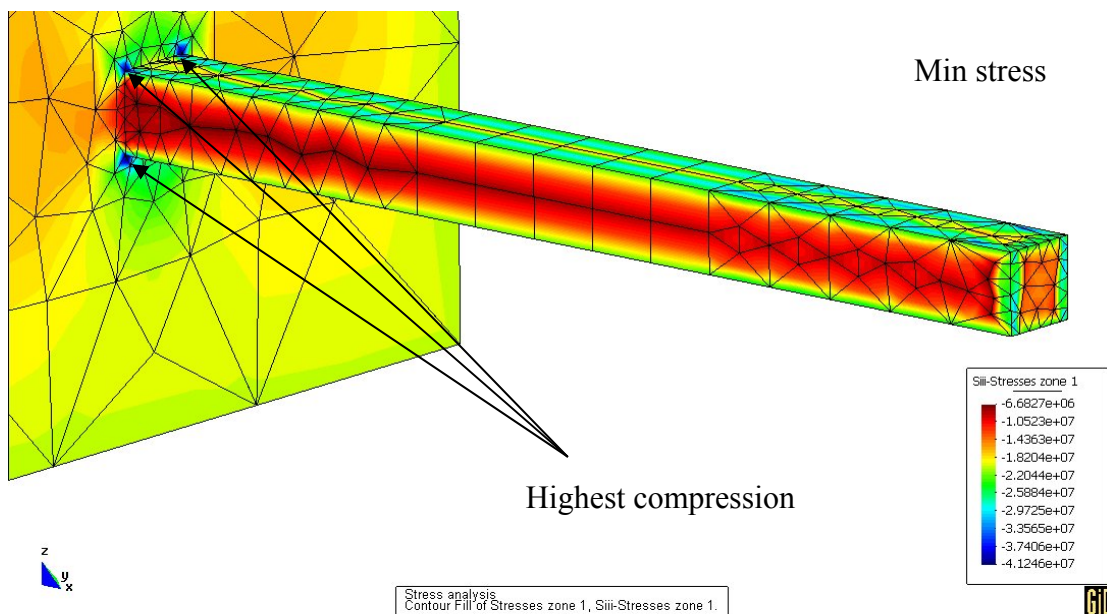


Figure 2:1 Stress conditions in drift connected to a big room in the Stripa mine
[Adey& Calaon]

2.2 Geohydrology

Groundwater flow in rock on scales of interest in the context of waste disposal has been considered in one of the papers (*Popov and Calaon*). A numerical tool, based on BEM, has been developed that can be used for analysis of transport of contaminants from underground repositories and the tool can take into account fracture zones, non-homogeneous domains, and can be used to model the processes in the far-field, near-field and on the interface of the two. Fine details, exemplified by the EDZ, can be included and their role in the transport in the far field of contaminant leaking from a repository evaluated. The study presented shows that the worked-out numerical model and computer code have been developed for estimation of 3D flow and transport from underground repositories. The numerical tool shows high versatility in the sense that domains of different sizes and properties can be used in the same model. Fractures and fracture intersections are added using the discrete fracture approach, while the solution for the rock is obtained by using either fully 3D or by using a 1D representation, as it is usually done in the discrete fracture approach. Fracture intersections are also included in the model and coupled with the solution for the rock and fracture zones. The transport is modelled using advection-diffusion equation with reaction. Any number of chemical reactions as well as different species can be easily modelled using this tool. The figure illustrates concentration gradients in the groundwater flowing along a repository that is intersected by a number of major fracture zones.

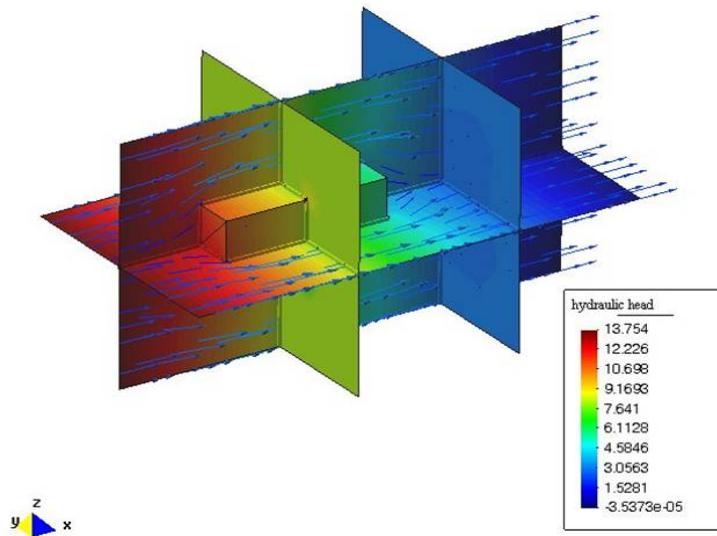


Figure 2:2 Concentration gradients in the groundwater flowing along a repository that is intersected by a number of major fracture zones [Popov & Calaon]

2.2 Geohydrology

A geohydrological case that primarily deals with the performance of plug seals in tunnels under ambient temperature or raised temperature has been investigated by Guo and Dixon. The subject is a field experiment in a sand-filled chamber between two bulkheads consisting of clay-sand blocks and concrete, respectively. The FEM-modelled hydraulic and mechanical responses of the clay bulkhead were compared with the measured data, the major finding being that the numerical simulations generated behaviour patterns that were generally consistent with the field measurements but commonly differing in magnitude. The difference in magnitude highlights the current limitations of using numerical simulations to predict detailed EBS performance. The models can use entirely appropriate physical, mechanical, and thermal formulations and relationships but they are often unable to capture the field constructions “reality”. Features such as construction joints, unanticipated non-homogeneity of materials and other unexpected or unrecognized parameters will affect the field performance while preserving generic patterns of behaviour. Numerical simulations therefore provide a valuable tool in developing designs, preparing construction specifications and predicting general barrier performance but have limitations when it comes to detailed system performance (see Figure).

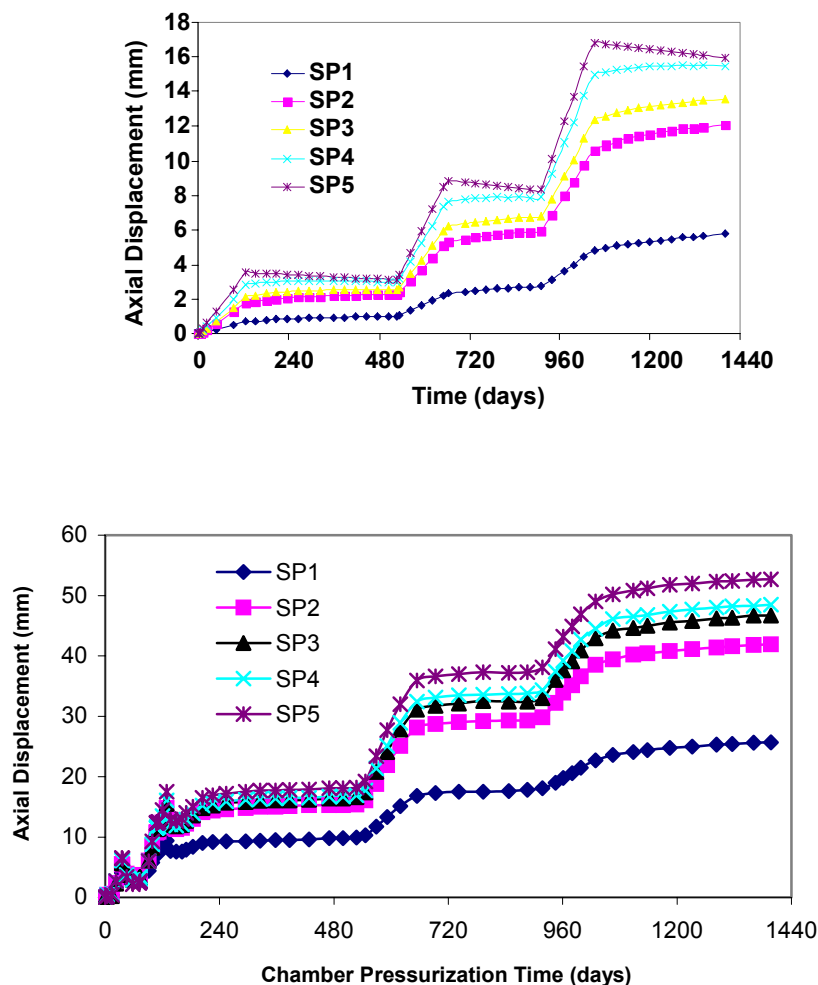


Figure 2:3 The figure shows predicted and the lower the actual strain of the plug system. The difference is up to 300 % [Guo & Dixon]

The same authors also described the performance of the plug system on heating. Modelling of the experiment required a computer program with the capability of describing both thermal convection and conduction (MOTIF). Like most thermal modellings based on relevant data the thermal response in the rock was well simulated. However, the data are different near the open part of the tunnel, which is said to be caused by the EDZ, which was not incorporated in this modelling.

2.3 EBS modelling

Modelling of the buffer and backfill in repositories is of particular interest to the waste-handling organizations and most of the contributions focused on this issue. A contribution by *Thomas et al*, describes a model for the coupled thermal, hydraulic, chemical and mechanical (THCM) behaviour of partly saturated soil and its application to a large scale in-situ test. In particular the results of research work on the inclusion of both the effects of the microstructure on moisture flow and geochemical interactions in models of thermal hydraulic mechanical behaviour are included for simulating the coupled behaviour of the Prototype Repository (Figure 2:4). The simulation results are compared with experimental results. It is found that the model is able to capture both the trends and patterns of behaviour of the system.

The numerical solution of the governing equations is achieved by a combination of the finite element method for the spatial discretisation and a finite difference time stepping scheme for temporal discretisation. The COMPASS code, developed parallel to its application, turns out to give accurate THM predictions.

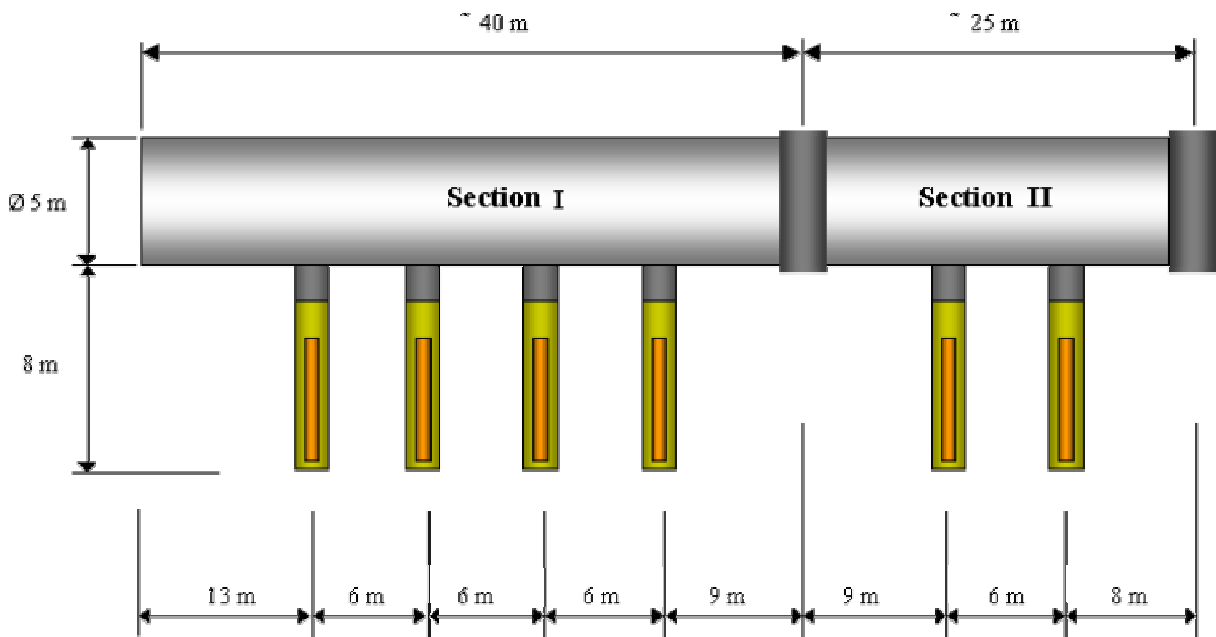


Figure 2:4 The Prototype Repository and deposition holes [Thomas et al]

Another contribution dealing with the same type of problem was provided by *Ledesma and Chen*. They describe the evolution of CODEBRIGHT, which, from the beginning, could not be used for accurate blind predictions of THM processes. However, the experimental data that were available after a couple of years and were fundamental for calibrating the models and the parameters involved, has upgraded the code to give very accurate results.

The preliminary analyses were devoted to the understanding of the role of each parameter and geometry in the physical problem. An example of the need for adequate modelling is that if the geometry and introduction of all components are not made properly the result in terms of temperature may cause differences of up to 100 %. Applying the code to the case of “wet” deposition holes in the Prototype Repository drift gave very accurate prediction of the thermal evolution and the wetting rate. Using it for predicting these processes in a “dry” hole has also given fair agreement but the wetting rate is so low that the capacity of the code to apply to the case of virtually no uptake of water from the rock is not yet validated (Figure 2:5).

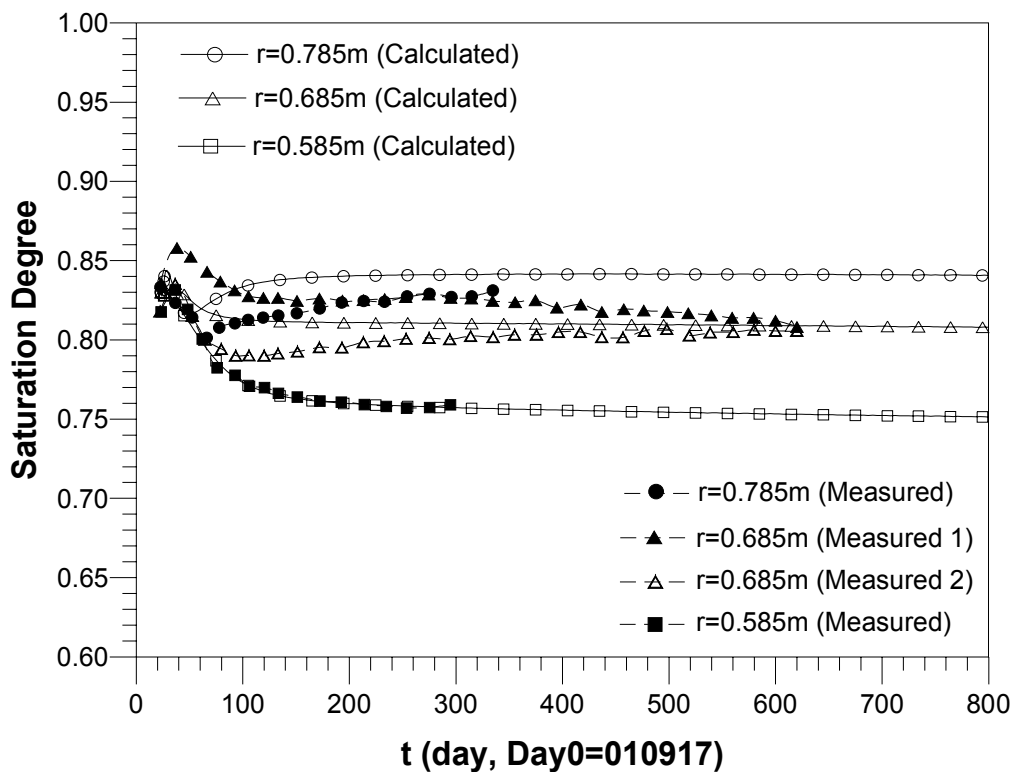


Figure 2:5 Degree of saturation [Ledesma & Chen]

2.4 Basic physical processes in EBS

Numerical codes represent the mathematical form of conceptual models and they can be adjusted and “repaired” to fit experimental data even if the basic conceptual model is totally inadequate. It is therefore essential to investigate whether the true physico/chemical processes are depicted by the conceptual models and one doubt in the present context is that moisture transfer within the buffer and from the rock to the buffer under the prevailing thermal gradient in a deposition hole may not take place as assumed by most modellers. This issue was dealt with in papers by *Pusch et al*, and *Kröhn*, respectively.

In contrast to the current modelling of the rate of water saturation of the buffer clay that surrounds canisters with HLW assuming that suction in the buffer drives in water from the rock and through the buffer, these authors claim that diffusion of water is the dominant hydration process. Microstructural examination suggests that hydration takes place by two parallel mechanisms; migration along particle surfaces from the wet outer boundary and condensation of vapour-transported water from the hot inner part of the buffer. Both processes are of diffusion-type implying that buffer saturation can be described as a quasi-diffusive process.

The second author claims that modelling of vapour diffusion under isothermal conditions gives good agreement with actual determinations of the water content as illustrated by figure 2:6, and he also claims that if vapour diffusion fades to Knudsen-diffusion in an advanced stage of saturation the buffer, saturation can be explained exclusively by vapour flow due to an increased diffusion coefficient.

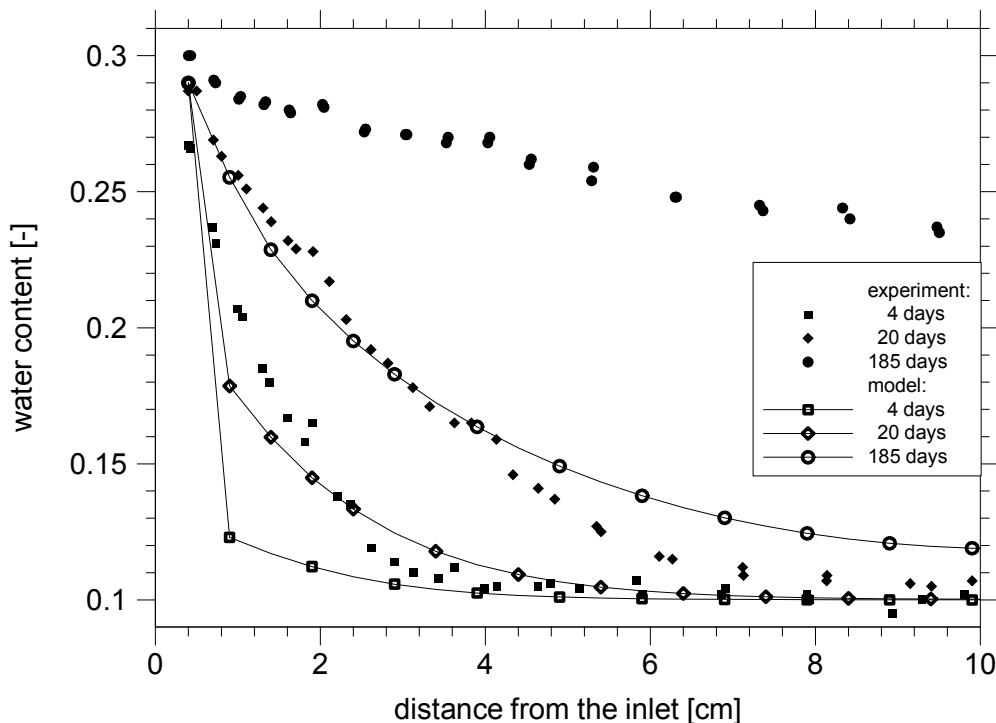


Figure 2:6 Water content as a function of the distance from the wet boundary [Kröhn]

The conclusion from discussions of this theme is that if further analysis of the detailed moisture transport is largely controlled by diffusion processes, new or improved models need to be developed for proper description and prediction of the maturation of buffers and backfills. In fact, a model of this type has been proposed and used in the Prototype Repository project by *Sugita et al* (Code *THAMES*).

2.5 Chemical processes in buffers and backfills

Chemical processes in buffers and backfills are of fundamental importance, both respecting mineral alteration and chemically induced microstructural changes. These issues were dealt with in a contribution by *Luukkonen*. In his study geochemical changes during the wetting of tunnel backfill, and the time-dependent changes at the tunnel boundaries of a repository engineered barrier system were considered. No quantitative coupling to hydrological flow was made and the modelling assumes instant full saturation of a cell volume as soon as infiltrating water first enters the studied element cell. The calculations, which referred to a repository of the Prototype Repository project version, are batch reaction oriented and follow the equilibrium thermodynamic assumption. The initial groundwater sucked into the EBS at the repository boundaries is assumed to be Na-Ca-(HCO₃)-SO₄-Cl -water corresponding to brackish seawater.

The major finding is that one can expect initially present gypsum to be dissolved yielding dissolved sulphate and Ca in the porewater. The role of cation exchange is significant during Ca production and the cation exchange is a partial sink for produced Ca, releasing other major cations into solution. Initially, dissolving calcite causes a marked increase in alkalinity and an increase in pH, while later, calcite will be precipitated at the backfill boundaries.

3 General conclusions from the workshop

It appears from the workshop that modelling of some of the major physical processes, like the evolution of temperature and the hydration of buffers and backfills under isothermal conditions, can be made with sufficient accuracy for practical purposes. However, this is the case if the hydraulic boundaries, represented by the EDZ, are such that access to water for saturation is unlimited and well defined with respect to uniformity, while it is not yet known whether the currently used codes are capable of adequately predicting the hydration process in “dry” rock. In fact, the models may not illustrate the true mechanisms in the hydration process. As to the chemical evolution the present attempts to describe possible changes require more general models, especially concerning the openness: groundwater flow in the surroundings of deposition holes, bringing in and out chemical species that affect the buffers and backfills, must be introduced and this again highlights the role of the EDZ. Putting together the suggestions for further research in the framework of a Task Force one identifies the following major issues, which are similar to those specified in the final report of the Prototype Repository project respecting modelling of the performance of buffers and backfills:

- Predictions of the access to water from the rock in deposition holes and tunnels for the wetting of the buffer are uncertain and future work related to the role of the rock structure on different scales, including the EDZ, is required for adequate modelling of the hydration of buffers and backfills.
- Predictions and measurements of temperature agree well although some models overestimate the temperature somewhat. The impact of gaps and joints and changes in water content as well as of vapour-driven heat transfer should be further looked into.
- Desiccation and accumulation of salt close to the hot canisters are expected to cause significant changes in microstructure and physical performance of the buffer. This is a matter that has not been looked at that needs consideration.
- The hydration rate can not be accurately predicted unless the basic processes in water migration under isothermal conditions and thermal gradients have been clarified.
- The evolution of pressure and mechanical response of the buffer is the most difficult task because it requires that fracturing and displacements in the buffer be included in the models. The issue of interrelation of hydration/dehydration and swelling/consolidation is relevant. Since prediction of the hydration rate is uncertain forecasting of the mechanical response is even more uncertain. More work is required for solving the problem of non-uniform swelling pressure affecting the canisters.

A very important fact is that although the attendants of the workshop represented the modelling groups involved in the EC-supported projects CROP, Prototype Repository and FEBEX project and thereby certifying relevance and professionalism in EBS modelling, there are additional competent researchers in this and other fields that may represent different opinions. Hence, it is of fundamental importance to let other members of the scientific community examine and review future work.

4 Written contributions

4.1 Modelling underground mines for rock stability assessment using boundary elements. A new approach for large scale problems.

Robert Adey & Andrea Calaoon ,
Computational Mechanics BEASY, Ashurst Lodge, Ashurst, Southampton, UK,
r.adey@beasy.com

Abstract

The Boundary Element Method has been applied to calculate stress distribution and stability of underground mines for disposal of chemical waste. A case similar to the Stripa mine in Sweden has been considered. The rock mass was granite, with major fracture zones represented by three families of planes mutually orthogonal and 100 meters distant from each other. The pre and post processor GiD and the Boundary Element software Beasy (<http://www.beasy.com>) have been used for model preparation, solution and result post processing. Modelling technology has been developed to enable the investigation of stability in the presence of a large number of fracture zones while at the same time determining the detailed stress near the mine. Results for stress and stability of the rock are here presented and discussed.

Introduction

This work was performed under the LowRiskDT project which aimed to investigate the suitability of abandoned mines for the storage of toxic waste. A major part of the project was the use computational models to predict the performance of proposed repositories for disposal of chemical waste. The project identified a number of mine types representative of those found in the EU for investigation. The mines were assessed for their stability and isolation capacity (flow and transport) In this paper some results are presented showing the computations performed to determine the rock stability through stress analysis of reference mine repositories which could provide safe and permanent isolation of hazardous waste.

The models were based on the Boundary Element Method (BEM). BEM has a number of advantages over the Finite Element Method (FEM) for modelling media such as rock as only the fracture zones are required to be described with elements. The homogeneous media between the fracture zones can be modelled as blocks of material whose boundary is described by the elements on the fracture zones. The presence of different material properties, the geometry of the Engineering disturbed zone (EDZ), and the extensive fractured media make it necessary to have an efficient tool to generate many “zones” in a single BEM model. (Note: zones are regions of the model with different material properties)

A specialized geometry and input file generator was found in the GiD software. Since GiD is a general tool pre- post processor and solid modeller, an extensive customisation has been necessary to make it able to deal with BEM calculations and with the very special needs of underground modelling, often very different from the ones in mechanics.

Many facilities have been introduced in GiD and a complete problem-type (as the set of customizing files is called inside the GiD environment) have been programmed.

One of the major advantages of using a solid modeller as pre-processor is the possibility to have the critical information (in multi-zonal BEM) about which volume (zone) a surface belongs to. The access to this knowledge (through Tcl functions reading the GiD database) permitted the efficient production of model files with hundreds of zones which otherwise would have been extremely time consuming and costly. Complicated geometries are also possible with the 3D modelling capabilities of GiD. Although some feature not present in GiD would help significantly in underground modelling (and some of them will probably be included in the next release) all the geometries of the present project have been built with GiD only. Some menus and toolbars have been created in the problem-type to speed the model creation and imposition of boundary conditions.

Mohr Coulomb criterion

The modelling of the rock structure provides complete information on the stresses and deformation. However in order to assess the stability a criteria was selected to assess the mine performance, in rock mechanics the most used brittle failure criterion is the Mohr-Coulomb one so this was used. It establishes a limit for the difference between maximum and minimum principal stresses, depending on the maximum itself, often called “confining stress”.

Here the equation representing the critical state used (mechanical convention):

$$\sigma'_1 = -(\sigma_{cm} + k\sigma'_3) \quad (0.1)$$

In equation (0.1) σ'_1 is the minimum principal stress (eigen-value of the stress tensor), and σ'_3 is the maximum. K represents a multiplication factor for the minimum stress and is equal to:

$$k = \left(\frac{1 + \sin \phi}{1 - \sin \phi} \right) \quad (0.2)$$

and σ_{cm} is the uniaxial compressive strength:

$$\sigma_{cm} = \frac{2c_0 \cos \phi}{1 - \sin \phi} \quad (0.3)$$

The field visualized has then a 0 value everywhere apart from the areas where the failure criterion is not respected. There the value of the field changes to 1.

Sub modelling

For any numerical model any small feature where the solution is rapidly varying, embedded in a much bigger and “smooth” part, and presents a modelling challenge. In fact small features need small elements on them, and even smaller if the variation of the result itself is of interest (possible local failure). On the other hand a big part of the model doesn't need a particularly fine mesh since there is very little variation there.

In order to be able to handle the geometry of tunnel and room, each of them crossed by a vertical fracture zone, the EDZ zone is divided in sub-zones and the big “cubes” of rock in the Granite case, a sub-modelling technique was used. The new method uses a technique, which can be used not only for this case, but also in the general interaction between FEM and BEM models.

Some Experiments to Determine the Required Model Details

In order to have an idea of the extent of the critical coulomb zone and of the mesh dimension necessary to represent it with sufficient precision, a number of simplified models were created. They represent a section of the rock with a tunnel in it, split by a fracture zone. Models with and without EDZ were assessed, at the normal tectonic pressure of 20 MPa and at an increased one (not shown in here). The tectonic pressure was applied indirectly to the model, by forcing a compression displacement of the side walls of the model, as in the “big” case with sub-modelling. Since the value of the displacements to be used could not be predicted in advance, two cases were considered and a linear interpolation used to obtain the required values for a third model to confirm the result.

The first experiment was performed without the EDZ zones and with a tectonic pressure of 20 MPa in all horizontal directions. This experiment showed that for the Mohr-Coulomb criterion all the tunnel, walls, ceiling and floor and their surrounding are instable (see Figure 1). The principal reason is that the so-called “confining stress” cannot reach the walls. A small tension stress appears in the rock and endangers the local stability. In the present case not only the sides (where the tension develops) of the tunnel are unstable, but the ceiling and the floor as well (on the floor the max principal stress is practically 0 everywhere).

This experiment shows also that the necessary mesh resolution around the whole tunnel should be not less than the one used in the example.

A second experiment was performed using the same geometry, but with a 1 meter deep EDZ divided in sub-zones. The new mesh is shown in Figure 2.

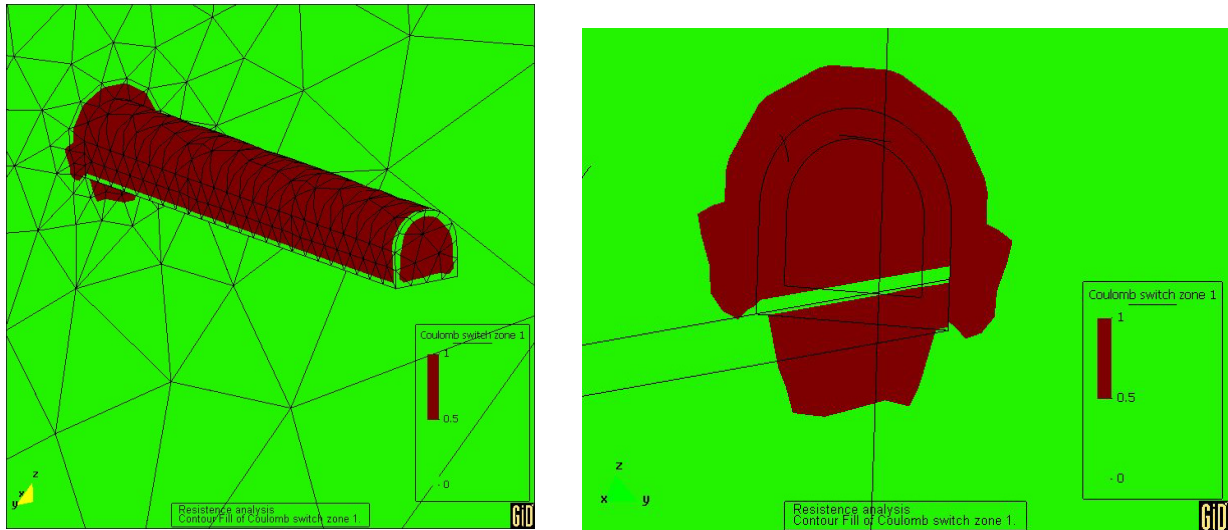


Figure 1. Mohr-Coulomb criterion result near the crossing fracture zone in the first model without EDZ.

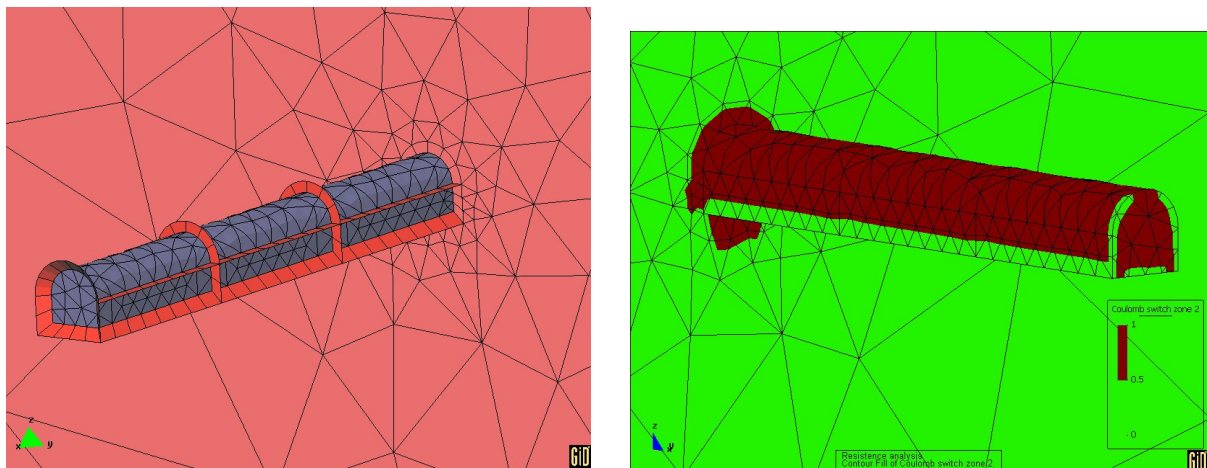


Figure 2. Mesh of the second model with EDZ on the left and Mohr-Coulomb result on the right.

The Mohr-Coulomb result is shown in Figure 2; it is practically the same of the case without EDZ and the shape of the failure area in the fracture zone is also identical. A comparison can be made between Figure 1 and Figure 2. If we look at the max stress (not pictured here) in the two cases, although showing the same pattern, is slightly higher in the second, due to the presence of a minimal support of the EDZ internal layer. The minimum (maximum for geological conventions) is for engineering purposes practically identical in the two cases. This explains also why the extension of the “Mohr-Coulomb failure zone” is identical for the two cases, and is the principal reason why we decided that the result of models *without* EDZ, can be taken as valid and representative for the same geometry and BC but with EDZ. So we assumed: in practice the presence of the EDZ doesn’t change the stability problem.

Full scale model

The rock mass surrounding room and tunnel was modelled to a depth 800 meters below the ground level (see Figure 3). A square area of 600 by 600 meters represents a horizontal cross section of a parallelogram enclosing the whole model. The rock mass is cut by 3 ortho-normal fracture zone families, 2 vertical and 1 horizontal. For all of them the distance between the discontinuity planes is 100 meters, so the rock matrix around room and tunnel is made up by a 3 dimensional array of cubes with a 100 meters long edge. A room and a tunnel, both empty, are located inside three blocks in the “middle” of the model, with the room ceiling depth at 425 meters. Both room and tunnel are crossed by only one vertical fracture zone.

The room dimensions are:

Cross section: 50 [m] x 50 [m]

Length: 100 [m]

The tunnel dimensions are:

Cross section: 5 [m] x 5 [m]

Length: 150 [m]

The tunnel is parallel to the length of the room and departs from it starting from the centre of a bottom edge.

Without sub-modelling the number of dof in the model would be too large to be solved in a reasonable time. This conclusion still applied when attempts were made to limit the mesh refinement using techniques like the transition mesh for passing from a coarse to a refined one. Therefore the sub-modelling strategy was chosen, and two different models prepared from the large model.

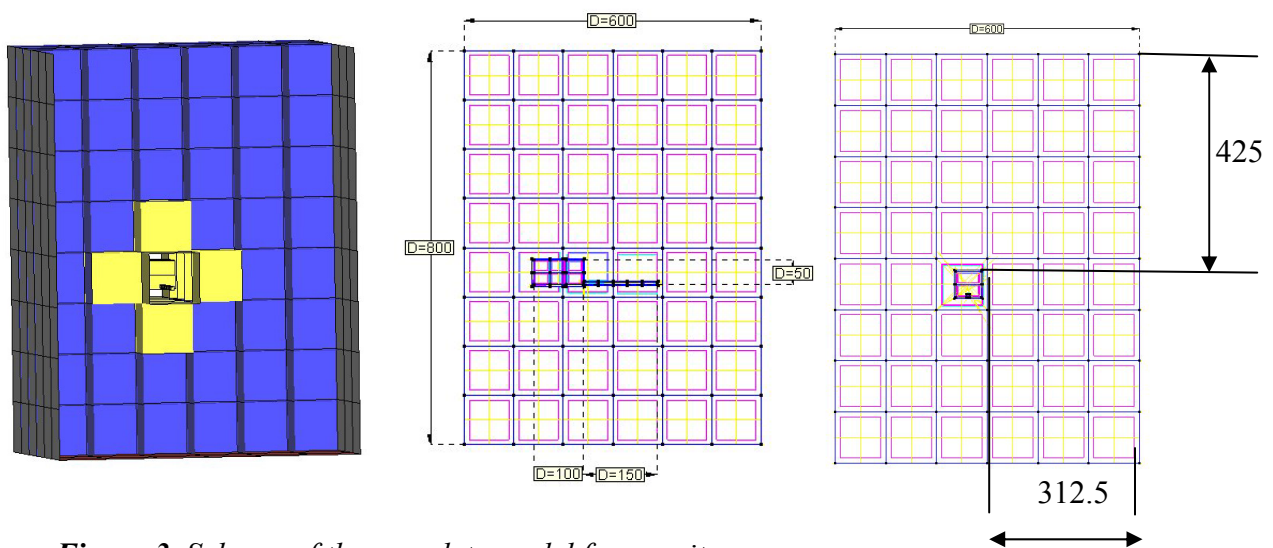


Figure 3. Scheme of the complete model for granite.

Global (outer) model

An “outer” model was created starting from the complete one where only the “rock cubes” were represented. The model consists of 288 volumes and is shown in Figure 4.

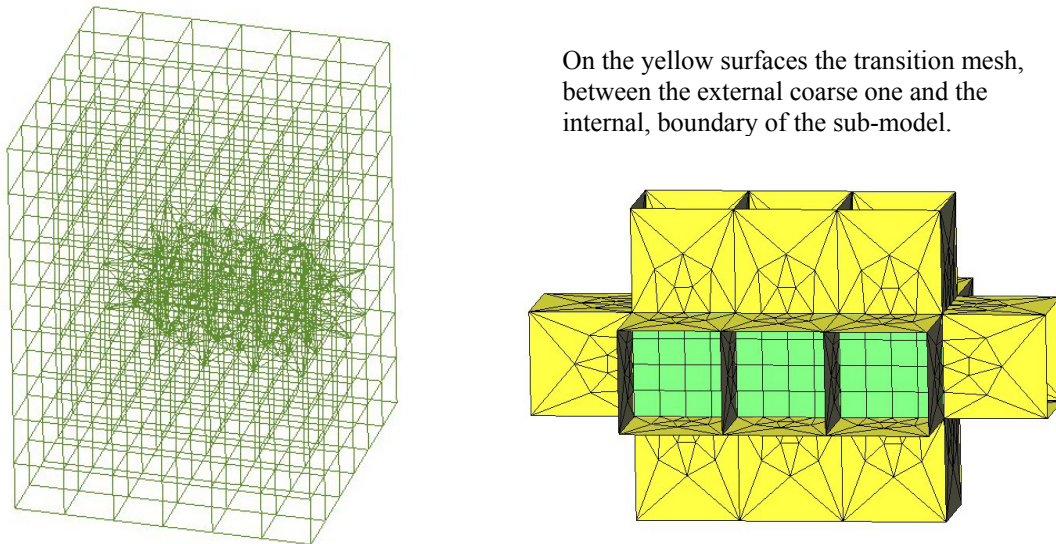


Figure 4. Outer model with refined mesh in the part surrounding the sub-model.

The bottom surface has been constrained vertically, and the sides moved inward, squeezing the rock blocks. To have an equivalent stress of about 20 MPa on the sides, a normal displacement of few centimetres was applied to the eternal “walls” of the model.

Sub model

The sub-model, sharing its external surface with the “outer” one, is depicted in Figure 5. Since the experiments previously described showed that the presence of the EDZ wouldn’t sensibly change the stability conditions, a simplified model was prepared in which no EDZ was modelled, assuming so a worst case.

The displacement boundary conditions have been calculated from the “big” model and introduced in the data file. This model was solved successfully.

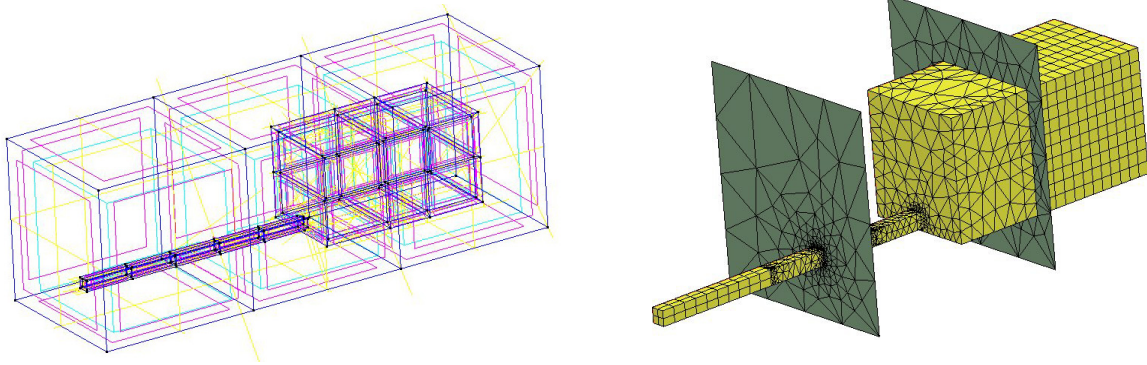


Figure 5. Geometry and mesh of the sub-model.

The material properties used for all the models are: $E = 50 \text{ GPa}$; $\nu = 0.3$; $c_0 = 1 \text{ MPa}$, $\varphi_0 = 35^\circ$.

Results

Global Model

The results of the global model are very simple to interpret, since the whole geometry shrinks horizontally, and, due to the confining pressure, it raises up slightly in the upper part (orogenesis). A lateral compressive stress linearly increasing with the depth results from the calculation, and its intensity varies from about 14.3 MPa near the surface, to about 23.4 MPa at the bottom.

Sub-model

The displacement of the outer model on the surface shared with the sub-model was applied as boundary conditions to the sub-model without EDZ, assuming the presence of room and tunnel does not have any influence on the outer model solution. The software is designed to automatically interpolate and so map the results on one model to provide the loads and boundary conditions for the other using a radial basis function approximation to ensure accuracy. This makes the detailed study of regions of special interest easy to perform. The model was solved and the stress results are presented in the following figures.

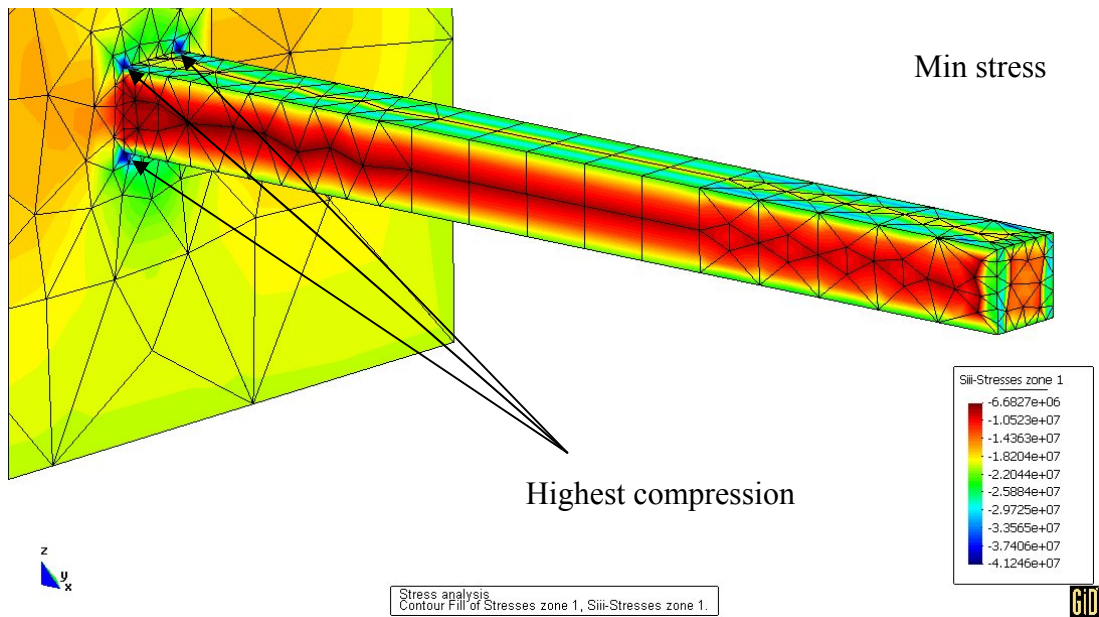


Figure 6. Min stress distribution in the sub-model. Here the end side of the tunnel is visible.

In Figure 6 the principal stresses on the tunnel far from the room are shown. As previously seen in the experimental models, a light tension (max principal stress) develops along the walls of the tunnel and the min principal stress is maximal there, so limiting the effect of the tension for the Mohr-Coulomb failure.

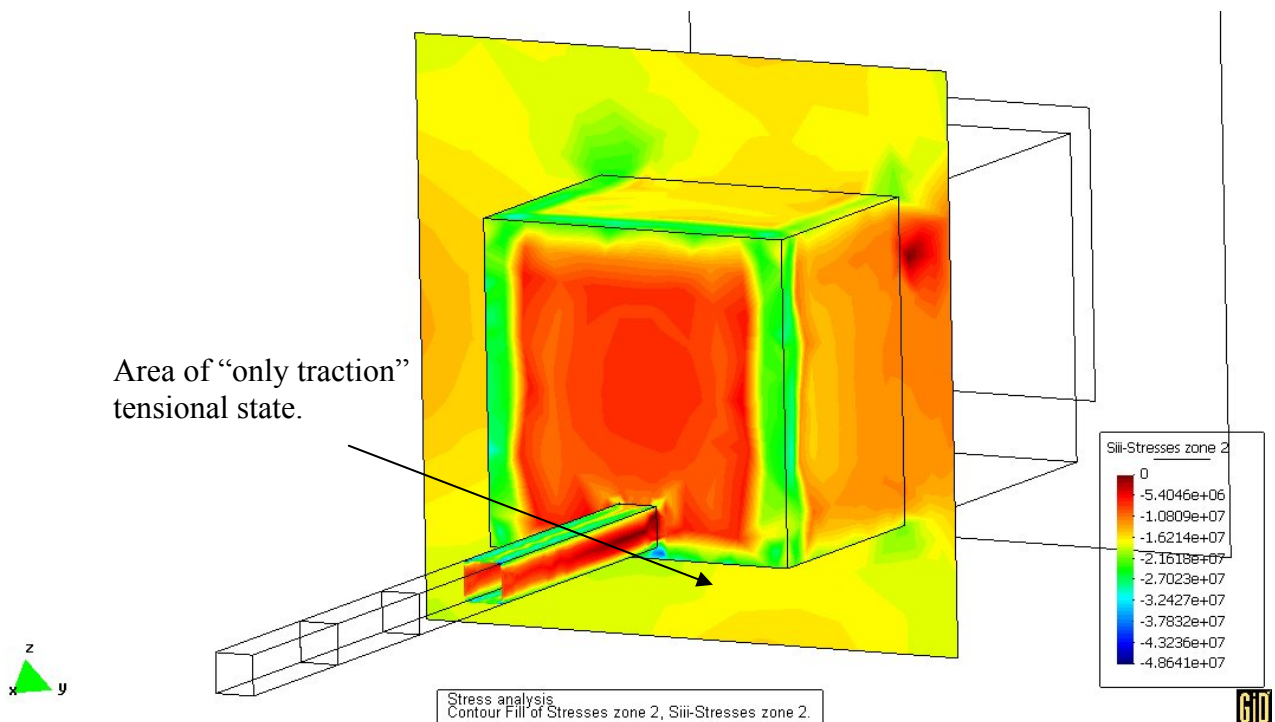


Figure 7. Max and min stress distribution in the sub-model. Here the room entrance side is visible.

The max principal stress in the “face wall” of the room near the tunnel shows some tension around the room walls, but its value is very low (in the order of 0.2 MPa).

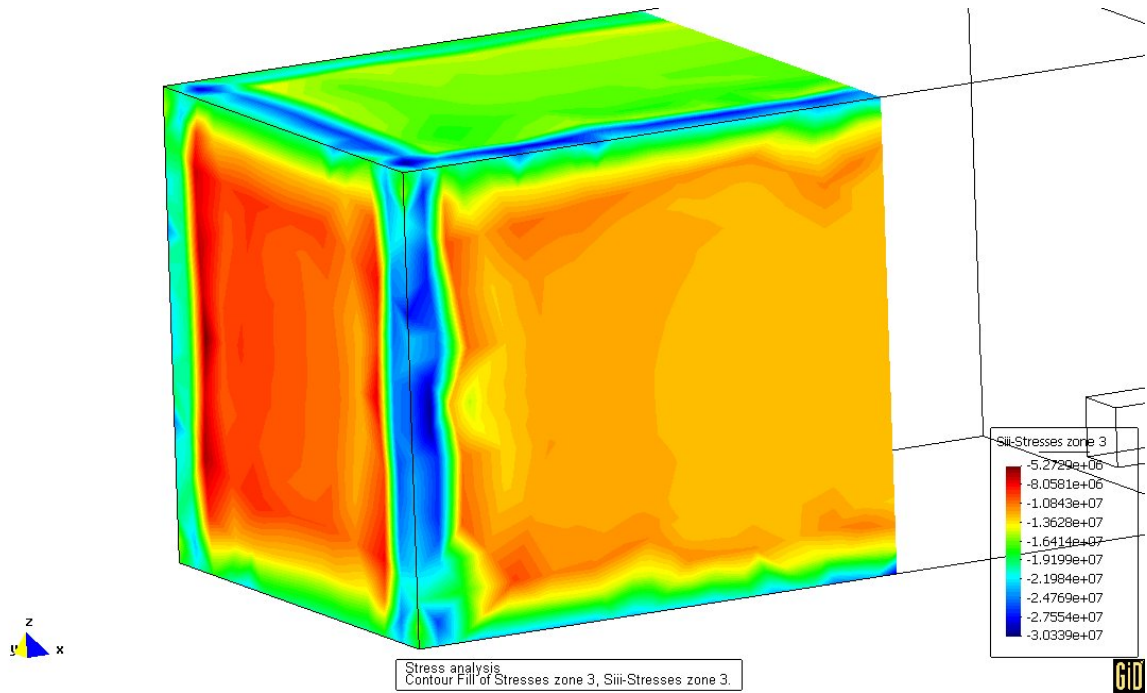


Figure 8. Min stress distribution in the sub-model. Here the end wall of the room is visible.

The max principal stress is particularly high on the side walls of the tunnel (Figure 6, max value 3.7 MPa tension and Figure 7, max value 6.5 MPa).

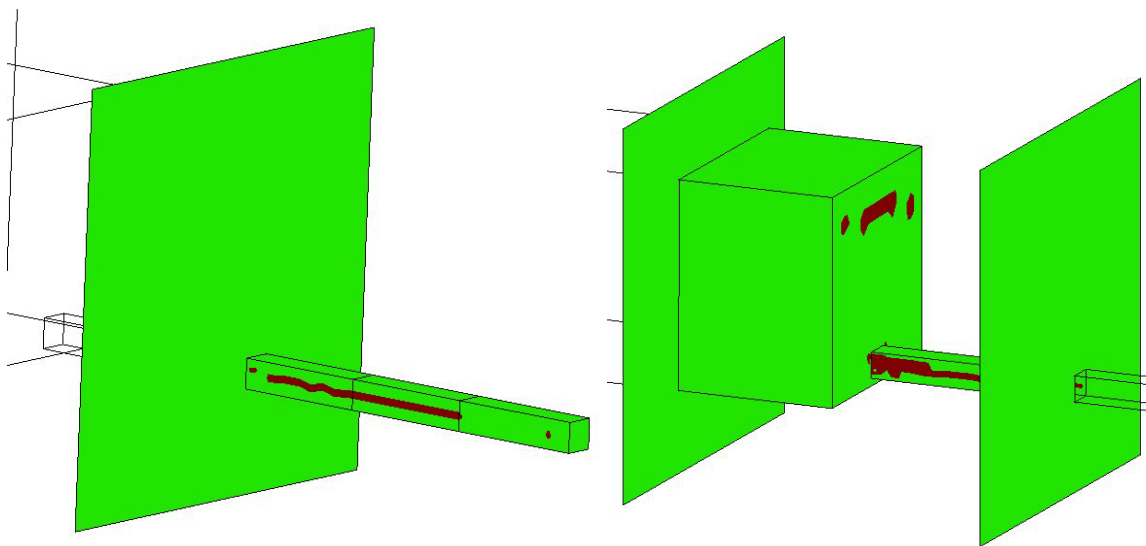


Figure 9. Mohr-Coulomb criterion on the tunnel and the front part of the room.

The Mohr-Coulomb results are shown in Figure 9. The walls of the tunnel appear to be damaged almost on their entire length, and the most critical part is the one near the room, where the extension of the “red part” goes from ceiling to the floor.

Around the room, the more dangerous area appears to be the entrance wall, in correspondence with the tunnel access. The upper part of the wall shows failure, and would probably be the first to cause dangerous rock fall. The rest of the room appears to be safe, but another calculation not shown here, with an increased tectonic stress (30 MPa), shows it completely collapsing. The results suggest that the state calculated with 20 MPa tectonic stress is very near the load at which the instability propagates from the front wall to the rest of the room walls and ceiling.

Conclusions

Tools have been developed to investigate the stability of potential mine repository sites. Combining the facilities of BEASY for modelling fractured structures and extensive customization of the GiD program a convenient tool has been developed to model the stability of mine repository sites in highly fractured materials like crystalline rock.

One reference mine has been investigated. It was a mine in a crystalline rock with a fractured matrix (100 m distance between the fracture zones). Experiments on small detailed models showed that there was no influence of practical significance with the presence or absence of the EDZ. Therefore it was concluded that there is no need in this case to model the EDZ when assessing the stability.

A sub modelling approach was developed to map results and data from the large “regional” based model to the smaller but much more detailed local model. The big “regional” model was analysed first with the major tectonic boundary conditions applied. The results were then transformed to the sub model, which was solved to reveal the detailed stress and deformation in the immediate vicinity of the mine.

The stability analysis performed using the Mohr-Coulomb failure criterion shows that the tunnel and some part of the room are unstable. A second model with increased tectonic forces 30MPa indicated substantial instability with the room totally damaged. With this configuration the mine at tectonic loads of 20MPa or more would require strengthening.

4.2 A new numerical tool for analysis of coupled far-field and near-field processes

Viktor Popov & Andres Peratta
Wessex Institute of Technology, Southampton, UK

Abstract

A numerical tool has been developed that can be used for analysis of transport of contaminants from underground repositories. The tool can take into account fracture zones, non-homogeneous domains, and can be used to model the processes in the far field, near field and on the interface of the far field and near field. In the paper we show results of the influence of the excavation-disturbed zone (EDZ) on the flow and transport in the far field, as well as large-scale long-term analysis of flow and contaminant leak from a repository. The results show the effectiveness of the approach for such analysis.

Introduction

A numerical tool has been developed for modelling flow and transport in fractured porous media [1]. The numerical tool is based on the discrete-fracture model [2] for both flow and transport. The flow model is based on the Darcy law and the transport model is based on the advection-diffusion equation with reaction. The numerical approach used to solve the partial differential equations is the multi-domain boundary element dual reciprocity method [3], [4]. The numerical model was used to estimate the significance of the thickness of the EDZ in the case of underground repositories. It has been assumed that a number of fractures intersect the repository/EDZ.

Numerical solver used for flow and transport simulation

Bellow the main features of the developed computer code are summarized:

- The solver is based on the discrete fracture model;
- The model for flow is based on the Darcy flow and for the transport on the advection-dispersion equation with reaction;
- The rock (3D entities), the fractures (2D entities), the fracture intersections (pipes - 1D entities) and pipe intersections (0D entities), have been implemented and coupled in a 3D code;
- The numerical approach used is the boundary element method (BEM) with domain decomposition for the flow and boundary element - dual reciprocity method multi domain approach (BE DRM-MD) for the transport;
- The computer code is implemented in such way that many sub-domains with different geometries properties can exist in a single model;

- The way in which the scheme is implemented offers unique flexibility to decide whether certain sub-domain, 3D or 2D, would be discretized on the boundary only, or would be discretized by volume;
- Manual or automatic fracture intersection detection is implemented;
- Automatic 3D block merging and detection is implemented;
- Automatic time step selection is implemented;
- The code is linked to the commercial package GID for pre- and post-processing;
- The code shows high accuracy and capability to integrate geometry with small details inside large-scale models.

Figure 1 shows the way that matrix blocks, fractures and fracture intersections interact. Fractures can be modelled as 2D or 3D entities.

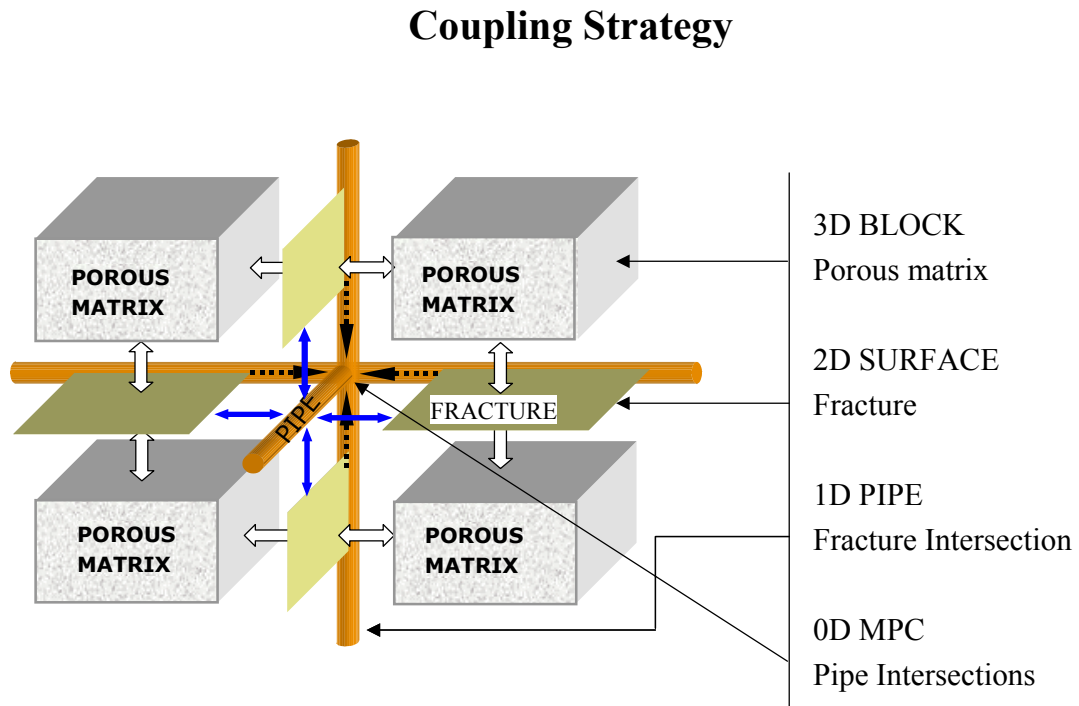


Figure 1. Coupling of matrix blocks, fractures and fractures intersections

The following solvers and pre-conditioners for sparse system of equations were implemented:

Direct solvers:

- LU (Gauss + Pivoting + dropping technique to keep the sparsity pattern)

Iterative Solvers (Sparskit):

- GMRES – FGMRES – PGMRES
- CG
- FOM
- BICG

Preconditioners:

- ILUT, ILTP, ILUT(n)
- MC64
- Physical and Geometrical Scaling

Figure 2. shows different possibilities available for representing 3D porous volumes. The 3D sub-domains can either be discretised by volume using linear or quadratic tetrahedrons or hexahedrons, or can be discretized over the surface of the volume.

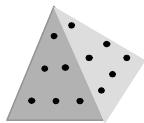
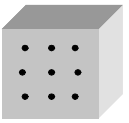
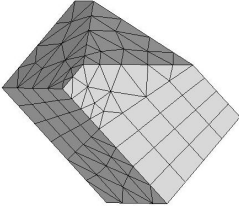
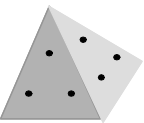
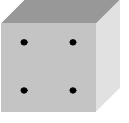
Shape Functions	Automatic Subdomains (FEM – like mesh generator)		Manual subdomains (geometry modeller & Surface mesher)
Quadratic Discontinuous Elements			Optional internal nodes for the DRM 
Linear Discontinuous Elements			

Figure 2. Various possibilities for discretization of porous blocks

Influence of the EDZ on the flow in the near-field

The excavation-disturbed zone (EDZ) was included in the model by considering it as a 2D layer wrapping-up the repository. The main assumption taken into account for modelling the EDZ is that its thickness is very small in comparison with its typical length and width, and that the flow is parallel to the main plains of the EDZ. In this way, the EDZ can be seen as a two dimensional discontinuity embedded in a three dimensional space.

The example consists of room of size 100m×100m×150m, see Figure 6, filled with chemical embedded in clay. Three fracture zones intersect the EDZ. The size of the domain is 300m×300m×450m. The hydraulic conductivities used were: for the EDZ E-7 m/s, for the clay E-10 m/s, for the rock E-9 m/s, for the fracture zones E-7 m/s and for fracture intersections 1E-6m/s.

The first example tests the assumption that the flow in the EDZ and fracture zones is parallel to the plains of the EDZ/fracture zones. In Figure 3 the part of the modelled domain, which includes clay from the repository, EDZ, fracture zone and rock are shown. Figure 4 shows the velocity field as well as the equipotential lines of the solution for the flow. It can be seen that the flow in the fracture zones and the EDZ are indeed parallel to the sides of the fractures/EDZ.

Figure 5(a) shows the time variation of the concentration profile found along the line DC. It can be seen that the transport in the EDZ layer is faster than in the rocks and the clay, which is expected due to much higher permeability. Figure 5(b) shows the concentration profile along the EDZ, from $x = 0$ to $x = 20\text{m}$, at $y = 6.5\text{m}$.

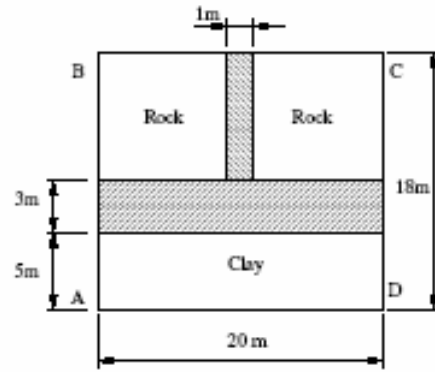


Figure 3. Part of the modelled domain, which includes clay from the repository, EDZ, fracture zone and rock

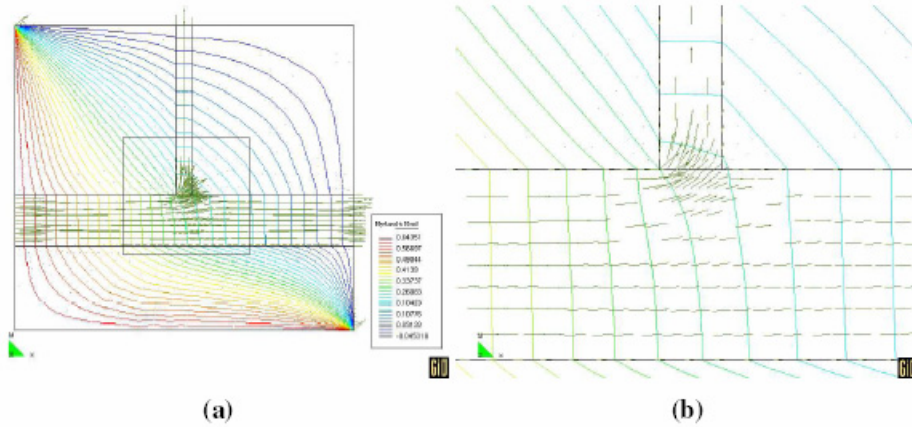


Figure 4. Velocity field and equipotential lines for the flow

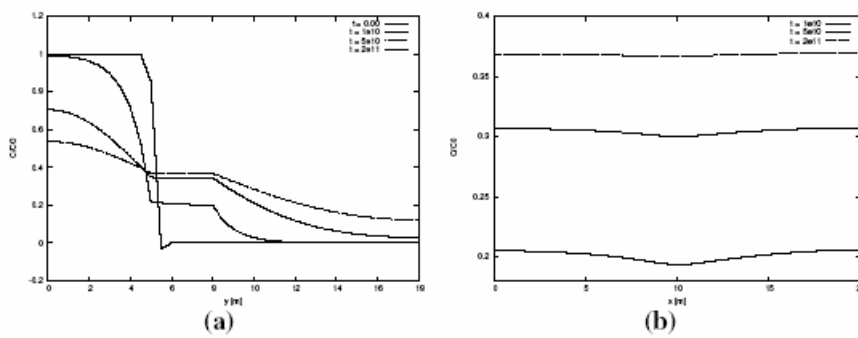


Figure 5. (a) Concentration profiles along boundary DC; (b) Concentration profiles along the EDZ

In Figure 6(a) the flow is shown around the room, which is filled with clay. In this case the EDZ is not included in the model. It can be seen that the velocity field around the room has got a component that is directed away from the room. The reason is the lower permeability inside the room, which makes most of the flow be diverted around the room.

The effect of the EDZ is obvious in Figure 6(b) where the flow velocity has got a component, which is directed towards the room. The reason for this effect is that the EDZ has got higher permeability than the surrounding rock so part of the fluid that would otherwise flow through the surrounding rock is diverted towards this zone.

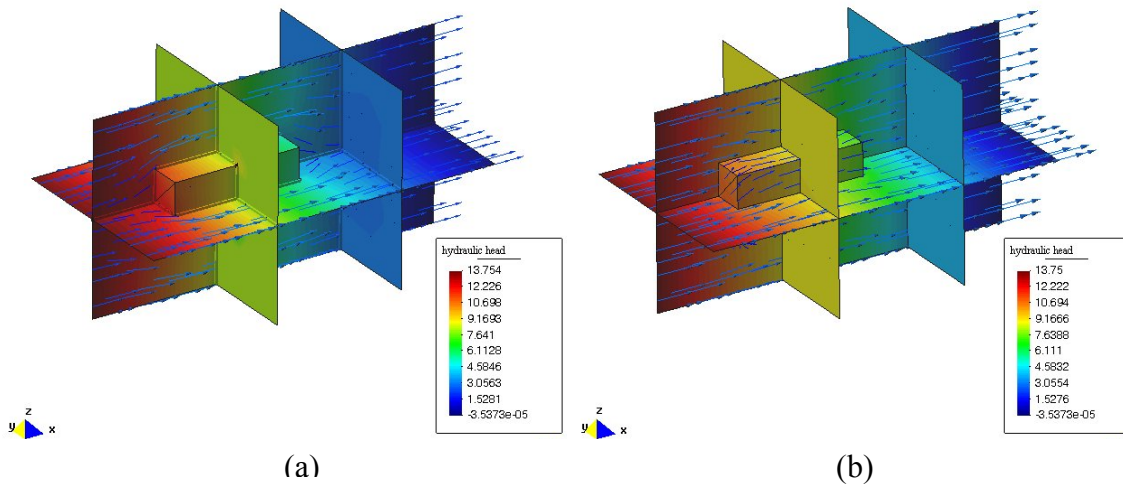


Figure 6. (a) Flow around a room embedded in rock, when the EDZ is not included in the model; (b) Flow around a room embedded in rock, when the EDZ is included in the model.

Large scale example

Figure 7 shows a room with tunnel filled with hazardous chemical embedded in clay. The dimension of the room is 100m×50m×50m. The size of the modeled domain is 700m×800m×600m. The length of the tunnel is 150m and the cross section is 5×5m. Around the room and the tunnel there is EDZ with thickness of 3m around the room and 1m around the tunnel. The vertical and horizontal lines in Figure 7(b) represent fracture intersections. It can be seen that there are 18 fracture zones in the model, with an aperture of 1m. The fracture zones are perpendicular to each other, separating in this way large porous rock blocks. For each porous block the average hydraulic properties are considered. This is considered to be a conservative case since three fractures intersect the EDZ of the room and two intersect the EDZ of the tunnel, which speeds up the transport of the chemicals, which would leak out of the repository.

The boundary conditions for flow are: on the top surface atmospheric pressure; on the bottom surface impermeable boundary conditions; one of the vertical surfaces has got 5% overpressure in respect to the hydrostatic pressure, while the other three vertical surfaces are with hydrostatic pressure. Saturated flow is assumed.

The results for the flow in the case of crystalline rock are shown in Figure 8(a). The hydraulic head is represented as a density plot over the fracture network, whereas the velocity field is represented as a vector plot. Typical values of the velocity in the rock matrix are two orders of magnitude lower than in the fracture network, which is due to the difference in hydraulic conductivities in rock and fractures. The influence of the EDZ can be seen in Figure 8(b). Because of the higher hydraulic conductivity the flow is directed towards the room on the inflow part of the room/EDZ, in the figure bottom-left side of the room, and away from the room on the outflow part of the room/EDZ, in the figure top-right side of the room.

Next, results for the transport are shown. The transport is calculated for the 2,2-dichloroacetic acid (DCA), product of decomposition of Dichlorvos. The distribution coefficient K_d is taken to be $= 0$, therefore, the retardation factor R is 1. The initial concentration inside the repository is 10000ppm.

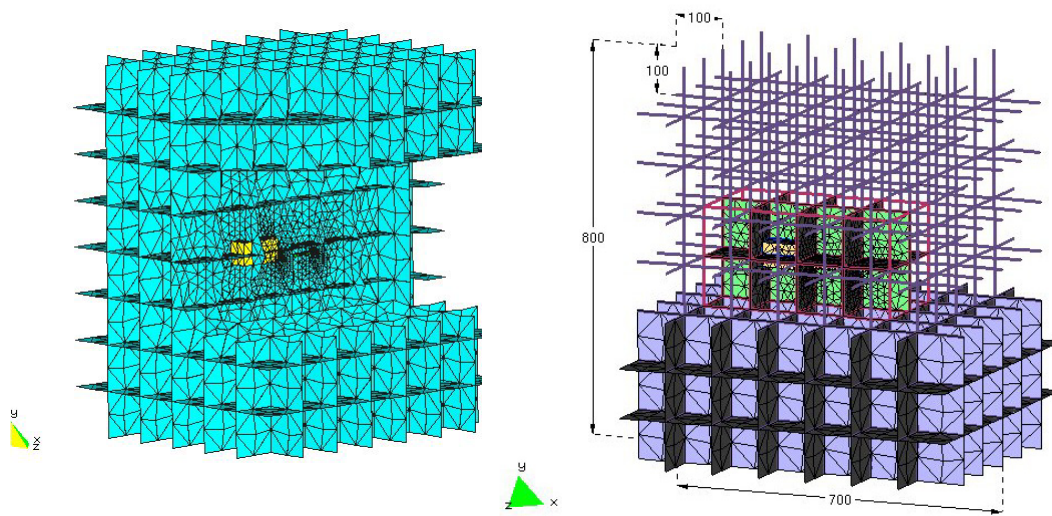


Figure 7. Position of the room, the tunnel and fracture zones in the model

As a test of the accuracy of the simulation we use the plot of the concentration in the “pipe”/fracture intersection, shown in Figure 9(a) as a parallel bright line above the tunnel. The concentration of DCA in Figure 9(a) has been normalized, where 1 corresponds to 10000ppm. The concentration plot, Figure 9(b), starts after the room and finishes after the second perpendicular fracture that intersects the tunnel. It is evident that there is a jump in the concentration related to the point where the second perpendicular fracture connects the pipe with the tunnel. Though there were many tests of the 3D solver towards various 1D analytical solutions that verified the accuracy, this example confirms the accuracy of the model in real 3D conditions.

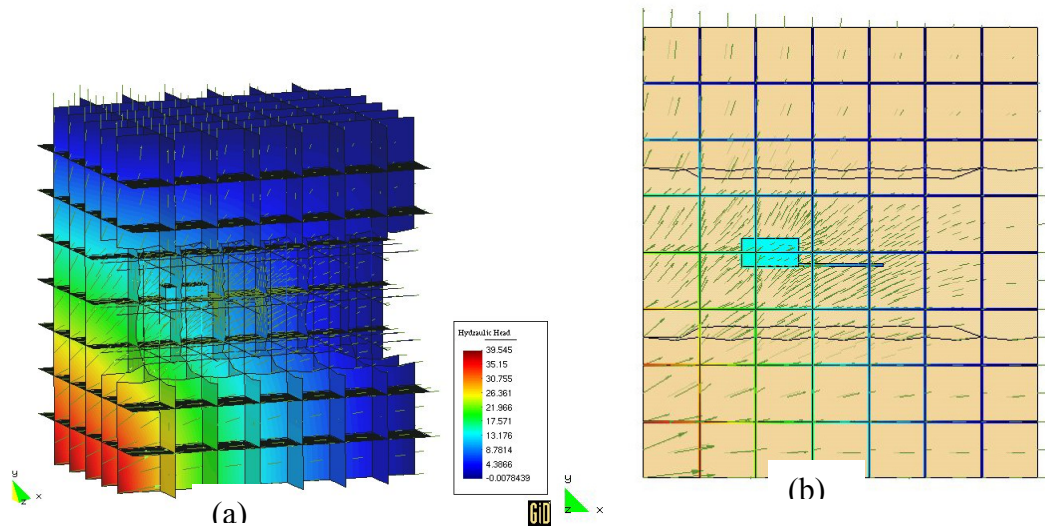


Figure 8. Density plot of hydraulic head and vector plot of Darcy velocity in the fracture network

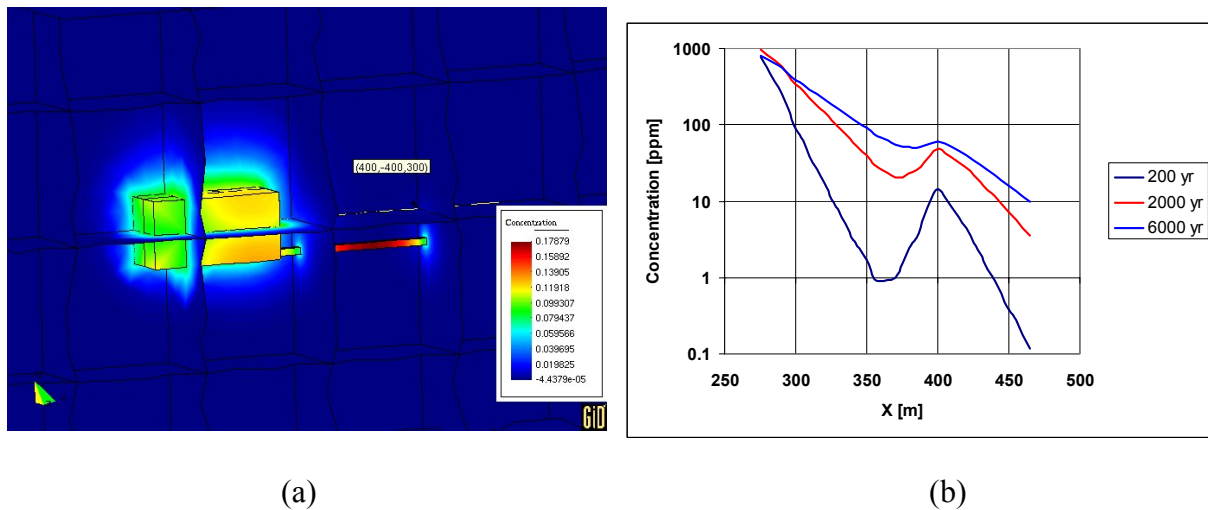


Figure 9. (a) Close view of transport of DCA after 1000 years in vicinity of the repository; (b) The effect of the tunnel in the crystalline case, where a vertical fracture is crossing the tunnel at $x = 400\text{m}$ and affecting the transport in the fracture intersection under observation

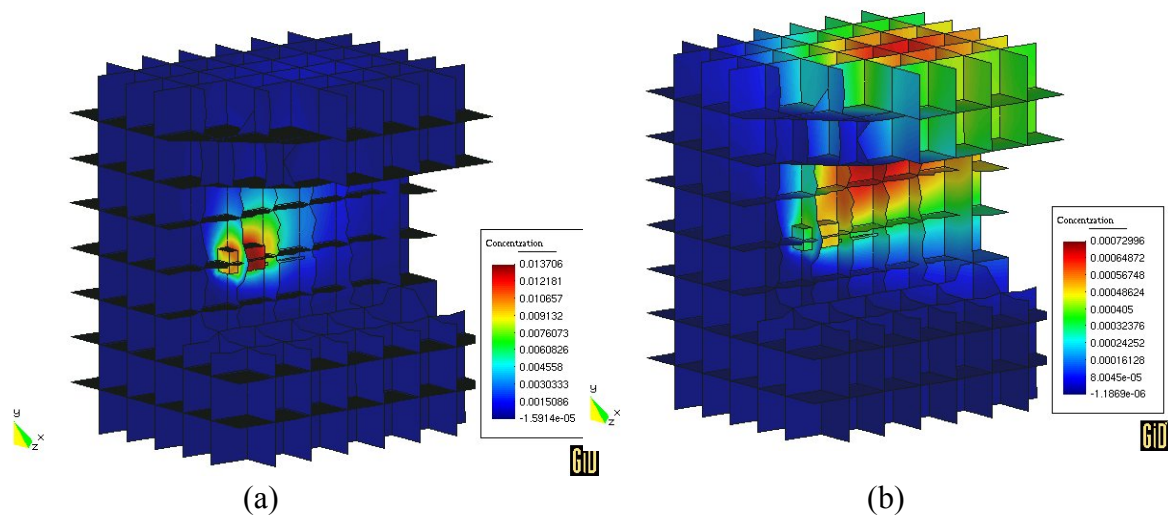


Figure 10. (a) Normalized concentration distribution of DCA in the considered domain after 127000 years; and (b) after 317000 years

Figures 10(a) and 10(b) show the character of the transport. In this case the transport of the contaminant is different than the transport of plume of contaminant in groundwater. In the case of transport of plume in groundwater, due to dispersion, the size of the plume increases while the concentration decreases, but preserves its shape. In this case, since the hazardous waste is embedded in clay of low hydraulic conductivity, the chemical is slowly released in time, the process having little resemblance with transport of contaminant plume in groundwater. It can be seen that by $t=100000$ years the maximum concentration in the rock is still close to the repository since the concentration gradient inside the repository is still high enough to induce significant flux of contaminant. At $t=300000$ years the leakage from the room has decreased significantly, so the highest concentration in the rock is away from the room, due to transport of contaminant, which leaked at some previous time. Both effects in the transport of the chemicals are evident, the advection and the dispersion. The timescale of the whole process of release of the chemical from the repository is of the order of magnitude of 600000 years.

In Figure 11(a) long term analysis of the transport of chemicals from the repository to the top of the rock, inside the vertical fracture zone that intersects the EDZ, is shown. The maximum concentration is less than 10 ppm and is obtained after approximately 200000 years. Figure 11(b) shows the change of concentration in time in two different points. One of them is in the middle of the room, concentration shown on the left-hand axis, and the other is 110m from the end of the tunnel, inside the fracture zone that intersects the EDZ.

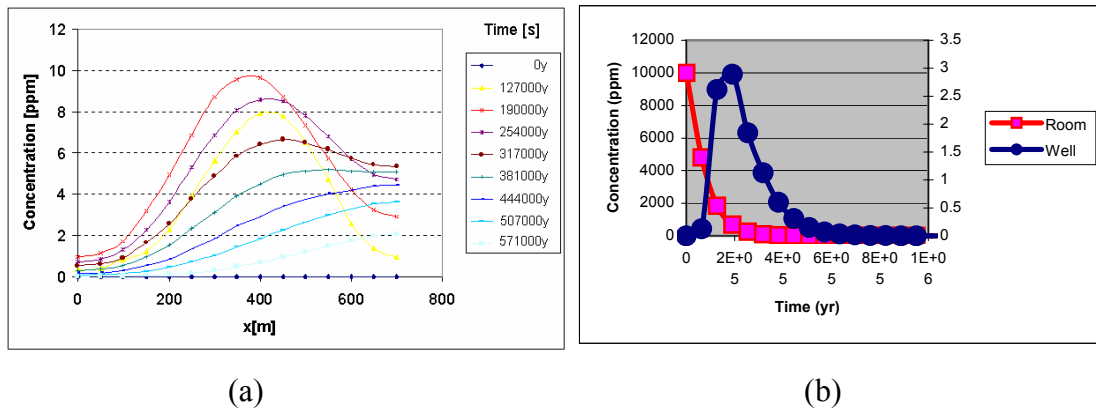


Figure 11. (a) Long term analysis of DCA concentration variation on the ground level in the fracture zone that intersects the EDZ; (b) DCA concentration variation in time in the middle of the room, shown on the left axis, and in point 110 metres from the end of the tunnel, shown on the right axis

Conclusions

A numerical model and computer code has been developed that can be used for estimation of 3D flow and transport from underground repositories. The numerical tool shows high versatility in sense that domains of different sizes and properties can be used in the same model. Fractures and fracture intersections are added using the discrete fracture approach, while the solution for the rock is obtained by using either fully 3D or by using a 1D representation, as it is usually done in the discrete fracture approach. Fracture intersections are also included in the model and coupled with the solution for the rock and fracture zones. The transport is modelled using advection-diffusion equation with reaction. However, any number of chemical reactions as well as different species can be easily modelled using this tool.

References

- [1] Peratta, A., Popov, V., ‘A new scheme for numerical modelling of flow and transport processes in 3D fractured porous media’, submitted to *Advances in Water Resources*.
- [2] Steefel, C.I. and Lichtner, P.C. (1997), “Multicomponent reactive transport in discrete fractures: I. Controls on reaction front geometry”, *Journal of Hydrology*, 209, 186-199.
- [3] Popov, V., Power, H. (1999), “The DRM-MD Integral equation method: An efficient approach for the numerical solution of domain dominant problems”, *International Journal for Numerical Methods in Engineering*, 44, 327-353.
- [4] Popov, V., Power, H. (1999), “DRM-MD approach for the numerical solution of gas flow in porous media, with application to landfill”, *Engineering Analysis with Boundary Elements*, 23/2, pp. 175-188.

4.3 Experience with thermo-hydro-mechanical modelling: the tunnel sealing experiment

R. Guo, AECL Underground Research Laboratory. Pinawa, Manitoba, Canada

D. Dixon, AECL Underground Research Laboratory. Pinawa, Manitoba, Canada

Abstract

The Tunnel Sealing Experiment (TSX) is an international project developed by Japan, France, the United States of America and Canada. The TSX consists of 11.45-m-long sand-filled chamber between two bulkheads. At one end, a clay bulkhead was constructed of 9000 clay-sand blocks (360x105x170 mm) and at the other end a concrete bulkhead was constructed of 76 m³ of low-heat, high-performance concrete. The experiment is operated in two distinct phases. The first phase was the stepwise pressurization of the chamber to 4 MPa in order to investigate the ability of the two bulkheads to resist hydraulic flow. The second phase involved circulating heated water through the chamber in order to raise the temperature of the sealing system and to evaluate the influence of elevated temperature on the performance of the bulkheads. This paper focuses on interpretation of results from fully coupled thermo-hydro-mechanical modelling of the clay bulkhead and the adjacent rock during heating and the differences between the simulated and measured results. Numerical analyses to simulate the thermo-hydro-mechanical evolution of the clay bulkhead and the surrounding rock of the TSX were performed using MOTIF finite element program and compared with the measured data.

Introduction

In situ experiments to test various components of the engineered barriers system have been performed at Atomic Energy of Canada Limited's (AECL's) Underground Research Laboratory (URL). The Tunnel Sealing Experiment (TSX) is designed to evaluate the performance of clay-based materials and concrete, which are expected to be the main components of tunnel and room bulkheads and other repository seals. The TSX is an international project funded by a partnership of nuclear waste management organizations from Japan, France, the United States of America and Canada. The clay bulkhead is composed of highly-compacted sand-bentonite blocks, and the concrete bulkhead was constructed using mass-poured, low-heat, high-performance concrete (Figure 1). A permeable sand fill was placed in the chamber between these bulkheads. After construction of the bulkheads, the chamber was pressurized with water in a stepwise manner to 4 MPa so that the ability of each of the bulkheads to resist hydraulic flow could be evaluated under ambient (isothermal) conditions. On completion of the isothermal phase of testing the temperature of the sand-filled chamber was increased by circulating hot water through the sand, gradually elevating the temperature within the bulkheads and the surrounding rock.

Guo and Dixon (2004) discussed the results of numerical simulations of the isothermal hydro-mechanical evolution of the clay bulkhead as they compare to the physical measurements collected. This paper focuses on the fully coupled thermo-hydro-mechanical modelling for the clay bulkhead and adjacent rock during heating.

The initial hydraulic conditions for this model were based on the results from Guo et al. (2003) who described the modelled response associated with the pressurization of the water in the TSX chamber under ambient temperature conditions using the MOTIF finite element computer program (Chan et al. 1999a, 1999b). The original plan was to increase the temperature of the water in two steps: first, to increase the temperature at the upstream surface of the bulkheads to 50°C and hold the temperature constant for a year; and second, the temperature of the upstream surface of the bulkheads was to be increased to 80°C over the next year (Guo and Chandler 2002; Guo et al. 2002). However, the duration of the experiment was shortened by running the first heating stage for only approximately 6 months and then increasing the chamber temperature to 80°C and running the experiment for an additional 6 months before cooling, draining and dismantling.

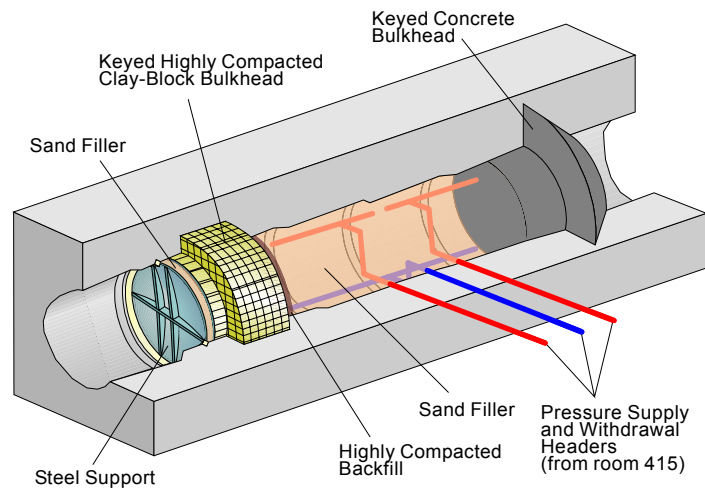


Figure 1. Configuration of the Tunnel Sealing Experiment.

Model and parameters

In order to help understand the thermo-hydro-mechanical (T-H-M) evolution in the TSX, the fully-coupled T-H-M modelling was done using MOTIF. The three-dimensional schematic of the TSX clay bulkhead model is illustrated in Figure 2. The axial dimension is 24 m. The radial dimension is 25 m. The tunnel is assumed to have a circular cross-section with a radius of 2 m. The chamber length is 5.75 m. There are 8520 elements, 9734 nodes and five kinds of materials. They are the rock surrounding the tunnel, the sand-bentonite (clay) bulkhead, the sand-bentonite (clay) backfill (a 300-mm-thick, 90%-sand and 10%-clay wall between the chamber and the clay bulkhead), the chamber sand and the sand filler located at the downstream side of the bulkhead. Table 1 shows the parameters used in this modelling.

Output of modelling and test results

Thermal response to heating

The evolutions of the originally simulated, best-fit simulated and actual measured temperatures at PSY47T, PZ5T, and PZ6T in the clay bulkhead are illustrated in Figure 3 for 328 days of heating. PSY47T is located near the upstream side of the clay bulkhead. PZ5T and PZ6T are located at horizontal axis of the clay bulkhead 0.63 m and 1.86 m from the upstream side of the clay bulkhead.

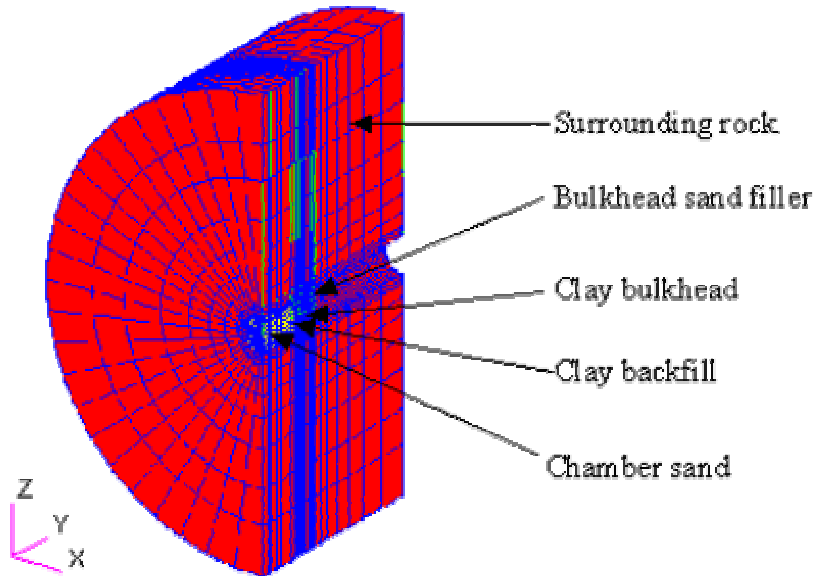


Figure 2. Finite element discretization of the TSX clay model

Table 1. Thermal and mechanical properties of components

	Bulkhead sand filler	Clay bulkhead	Clay backfill	Rock	Chamber sand
Hydraulic conductivity (m/s)	6.25×10^{-5}	3×10^{-12}	6.25×10^{-5}	2×10^{-16}	6.25×10^{-5}
Thermal conductivity (W/(m°C))	2.0	1.8	1.8; 0.5; 0.36; 0.26	3.5	2
Specific heat (J/(kg°C))	820	1400	1400	1015	820
Young modulus (MPa)	600	100	200	5.759×10^4	100
Poisson's ratio	0.3	0.315	0.315	0.207	0.3
Thermal expansivity (1/°C)	1.9×10^{-5}	1.0×10^{-5}	1.0×10^{-5}	1×10^{-6}	0
Dry density (kg/m ³)	2000	1900	1900	2650	1850
Porosity	0.24	0.315	0.315	0.005	0.287
Biot's coefficient	1.0	1.0	1.0	0.2	1.0

For the first 50 days of heating, the simulated results match the measured data well. After 50 days the measured and the original simulated temperatures based on the original thermal conductivity of 1.8 W/(m°C) for the clay backfill showed increasing divergence with increasing temperature. The difference between predicted and measured temperature at PSY47T was 7.5°C after 165 days of heating and 20°C after 328 days of heating. A similar behaviour is noted for thermistors PZ5T and PZ6T. The best fit between the measured and simulated temperatures was obtained by using 1.8 W/(m°C) as the thermal conductivity for the clay bulkhead. The clay backfill was required to have a thermal conductivity that varied over time (0.5 W/(m°C) for the first 51 days, 0.36 W/(m°C) from 52 days to 165 days, and 0.26 W/(m°C) from 166 to 328 days of heating) in order to maintain a consistent relationship between the measured and simulated results. While the thermal conductivity assumed for the clay bulkhead (1.8 W/(m°C)) was appropriate based on known thermal properties for this type of material, the values used for the thermal conductivity for the clay backfill are too low to be realistic and need to be varied with temperature/time.

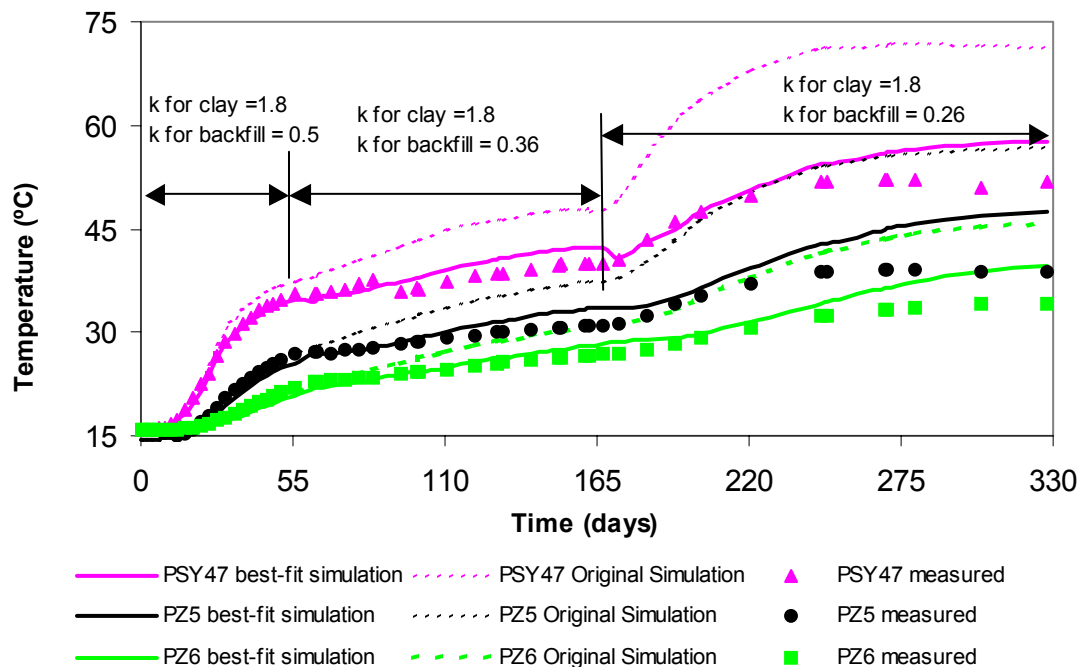


Figure 3. Measured and simulated temperatures at three locations in the clay bulkhead

The simulated temperatures generated using MOTIF are compared in Figure 4 with the measured temperatures in the rock at different depths below the floor of the TSX chamber. EXT2-2T, EXT2-3, EXT2-4T, EXT2-5 and EXT2-6 are located in the rock below the chamber 8.873 m, 5.873 m, 3.873 m, 2.873 m and 2.173 m from the axis of the chamber, respectively. The computed results matched the measured results well. This suggests that the thermal parameters used in modelling the rock are reasonable.

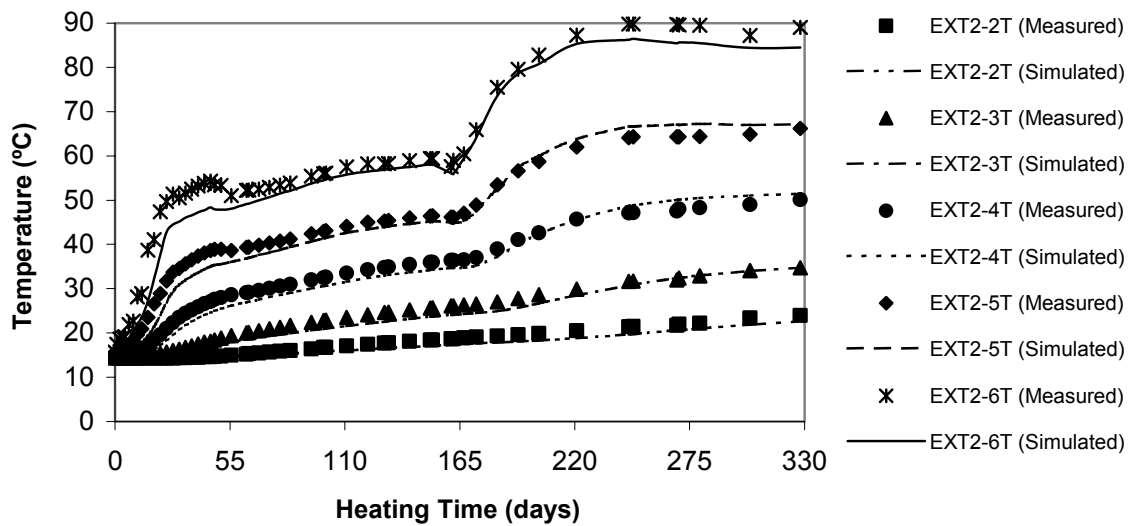
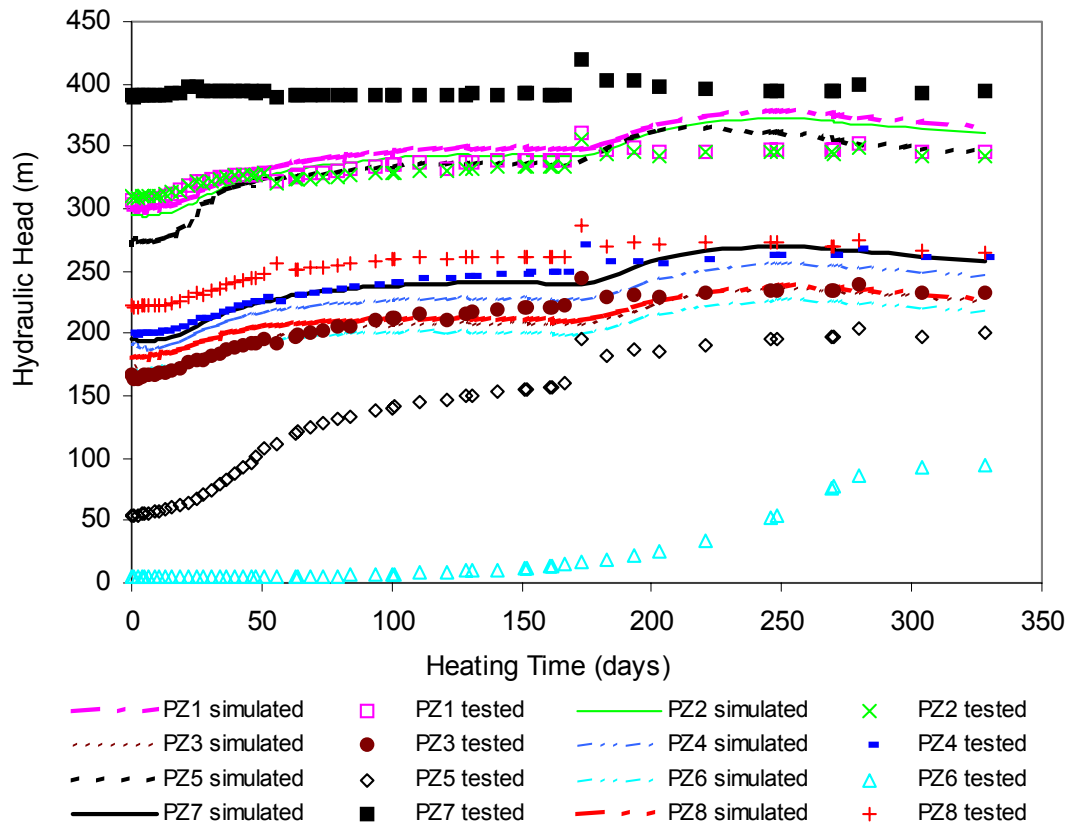


Figure 4. Measured and simulated temperatures in the rock below the floor of the TSX chamber

Given that the numerical simulation worked well for the rock mass, the observed large differences between the predicted and the measured temperatures for the clay bulkhead continuing to increase with increasing temperature may likely be due to some physical cause rather than a flaw in the numerical simulation. One possible explanation is that air bubbles formed in the TSX chamber or within the backfill portion of the clay bulkhead. As previously noted thermal conductivity values of 0.5, 0.36 and 0.26 W/(m°C) required in the best-fit simulation are not reasonable for water-saturated clay backfill. The water in the hot water supply system was not deaired. When the temperature was low, the air remained dissolved in the water. With increasing temperature, the air could have come out of solution and formed air bubbles at the top of the chamber. The trapped air bubbles may have effectively formed a layer of insulation on the upstream side of the clay backfill. Therefore, the best-fit values of the thermal conductivity derived in the modelling for the clay backfill could be a combination of the thermal conductivities for the backfill and an insulating layer of air bubbles.

Hydraulic response to heating

The comparison of the simulated thermally-induced hydraulic heads to the measured



data is shown in Figure 5.

Figure 5. Comparison of the simulated to the measured thermally-induced hydraulic heads in the clay bulkhead at different locations

The simulated hydraulic heads are shown to have a good match with the measured data for piezometers PZ1, PZ2, PZ3 and PZ4, located at 0.656 m, 0.659 m, 1.598 m, 1.601 m, respectively, from the upstream surface of the bulkhead. The simulated hydraulic head has a similar pattern to that of the measured data for piezometer PZ8 (1.488 m), but the value is less than the measured hydraulic head. The reason may be that PZ8 was located in the interface of the rock/clay bulkhead and this interface may have a hydraulic conductivity greater than the main body of the clay bulkhead. The model did not take into account the possibility of a greater hydraulic conductivity at the interface. Similar to PZ8, the simulated hydraulic head for PZ7 (0.597 m) was less than the measured data, which was almost the same as the hydraulic head in the chamber. There may be a pathway with a greater hydraulic conductivity between PZ7 and the chamber along the clay bulkhead-rock interface. Piezometers PZ5 and PZ6 (0.671 m and 1.568 m, respectively) were in the central part of the clay bulkhead and but were saturated later than the other piezometers. The patterns of the simulated results for PZ5 and PZ6 are similar to the measured data. A material model for water transport through unsaturated sand-bentonite material should be implemented within the simulation.

The simulated and measured hydraulic heads at locations of HGT1-1 to HGT1-5 during heating are shown in Figure 6 using 2×10^{-16} m/s as the hydraulic conductivity for the intact rock. (HGT1-1 to HGT1-5 are located in the rock above the chamber 17.75 m, 12.75 m, 7.75 m, 4.75 m and 2.67 m from the axis of the chamber). Generally, the patterns of the simulated hydraulic heads during heating follow those of measured data, but the simulated values at HGT1-2 to HGT1-4 are less than the measured data as temperature increases.

From the comparison of the simulated and the measured hydraulic heads in the clay bulkhead, the simulated hydraulic-head increases tended to match the measured data. In the intact rock, differences between the simulated and the measured hydraulic heads existed. The possible reason is that the actual hydraulic conductivity of the intact rock may be less than 2×10^{-16} m/s.

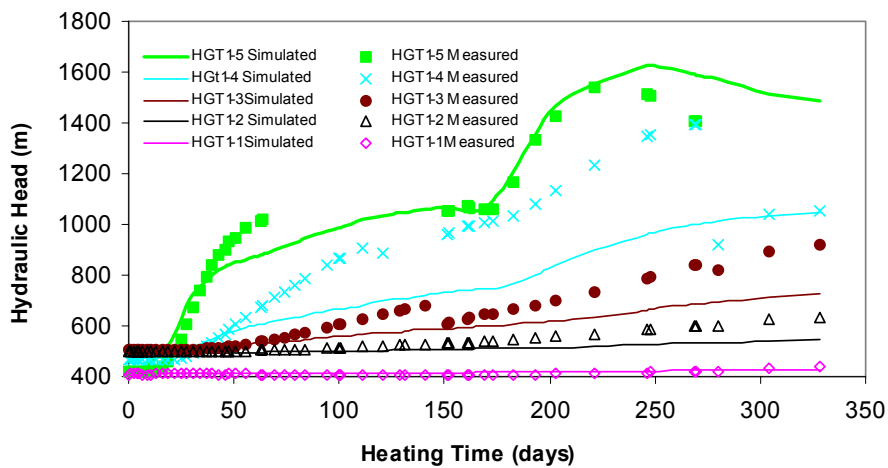


Figure 6. Simulated hydraulic heads in the rock at different locations along HGT1

Mechanical response to heating

The axial displacement of the clay bulkhead was measured using a sonic probe extensometer with 5 measurement segments (SP1 through SP5). SP1 through SP5 are located at 0.46 m, 1.19 m, 1.39 m, 1.76 m and 2.15 m, respectively, from the downstream face of the clay bulkhead. In addition to physically measuring bulkhead displacement, a series of simulations was done. Figure 7 shows the simulated and measured axial displacements at five locations in the clay bulkhead during heating. Differences in the magnitude of the simulation and observed data may be attributed to the differences between the assumed initial saturation state before heating and the known initial conditions.

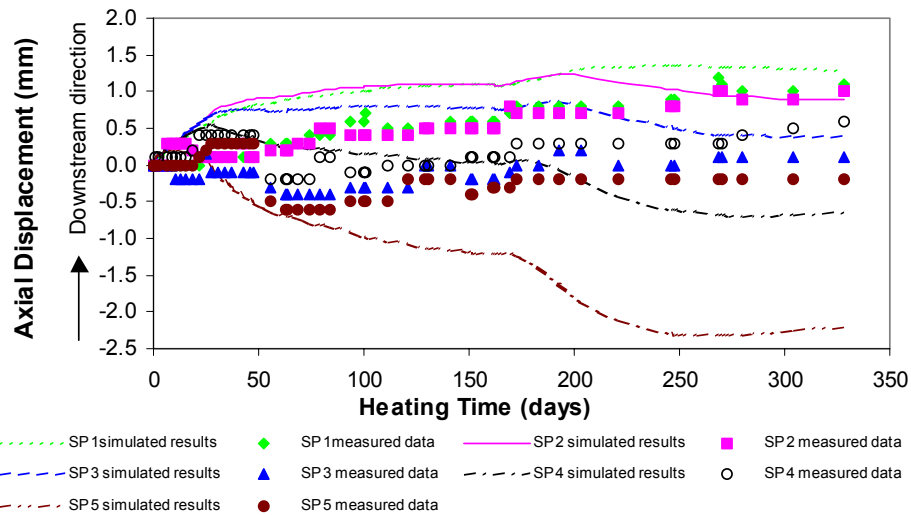


Figure 7. Comparison between the displacements predicted for different locations in the clay bulkhead and the measured results

Summary

The TSX was heated by thermal convection in the sand-filled chamber and thermal conduction in the bulkheads and the surrounding rock. Modelling the experiment required a computer program with the capability of modelling thermal convection as well as conduction. MOTIF was successfully used to model both heating processes in the TSX chamber and the bulkhead.

The thermal response in the rock was well simulated. The good match of the thermal response for different locations in the rock means that the thermal parameters used in this modelling for the rock are reasonable.

One cause of differences between modelled and measured thermal response of the clay bulkhead is that there may be air trapped on the upstream side of the bulkhead, resulting in very low thermal conductivities in this region and an over-prediction of the rate of temperature change in the clay bulkhead.

The pattern of the simulated thermally-induced hydraulic heads in the rock matched the measured hydraulic heads. The difference in magnitude between the simulated and the measured data for the intact rock indicates that the parameters used in this modelling should be refined.

The increase in hydraulic head in the clay bulkhead was simulated using MOTIF. The differences between the simulated and the measured data for PZ5 and PZ6 were caused by the unsaturated state of the clay bulkhead at the start of the TSX and a resultant low actual initial pore pressure at the start of heating. A material model for water transport through unsaturated sand-bentonite material should be implemented.

Acknowledgements

The Tunnel Sealing Experiment was jointly funded by the Japanese Nuclear Cycle Development Institute (JNC), the Agence Nationale pour la Gestion de Déchets Radioactifs (ANDRA) of France, the United States Department of Energy Carlsbad Area Field Office through Sandia National Laboratories, their Science officer for the Waste Isolation Pilot Plant (WIPP) and Atomic Energy of Canada Limited (AECL). Ontario Power Generation (OPG) has supported activities related to the reporting of the results of the TSX.

References:

Chan T., Scheier N. W., and Stanchell F. W., 1999a. MOTIF code version 3.2 user's manual. Ontario Hydro, Nuclear Waste Management Division Report No: 06819-REP-01200-0090-R00.

Chan T., Scheier N. W., and Guvanase V., 1999b. MOTIF version 3.2 theory manual. Ontario Hydro, Nuclear Waste Management Division Report No. 06819-REP-01200-0091-R00.

Chandler, N., Martino J., and Dixon D., 2002a. The Tunnel Sealing Experiment. In Proc. of 6th International Workshop on Design and Construction of Final Repositories. Session 4, Number 11. Brussels. ONDRAF-NIRAS.

Chandler N., Cournut A., Dixon D., Fairhurst C., Hansen F., Gray M., Hara K., Ishijima Y., Kozak E., Martino J., Masumoto K., McCrank G., Sugita Y., Thompson P., Tillerson J., and Vignal B., 2002b. The five year report of the Tunnel Sealing Experiment: -an international project of AECL, JNC, ANDRA and WIPP. Atomic Energy of Canada Limited Report AECL-12727.

Guo R. and Chandler N. 2002. Thermal-hydraulic numerical model of the flow of heated water through a sand-filled tunnel in granite. In Proc. 55 Canadian Geotechnical Engineering Conference, 3rd Joint IAH/CGS Conference. Niagara Falls. Oct. 20-25, 2002.

Guo R. and Dixon D., 2004. Experience with Hydro-Mechanical modelling: The Tunnel Sealing Experiment. Presented at Task Force-Related Meeting on Buffer and Backfill Modelling, Lund, Sweden, March 10-11, 2004.

Guo R., Chandler N.A. and Dixon D.A., 2002. Modelling the thermally induced hydraulic and mechanical response for the heated phase of the Tunnel Sealing Experiment. Ontario Power Generation Inc., Nuclear Waste Management Division Report 06819-REP-01200-10095-R00.

Guo R., Chandler N., Martino J. and Dixon D., 2003. Thermo-hydro-mechanical numerical modelling of the TSX with comparisons to measurements during stage 1 heating. Ontario Power Generation Inc., Nuclear Waste Management Dixon Report 06819-REP-01300-10070-R00.

4.4 Experience with hydro-mechanical modelling: the tunnel sealing experiment

R. Guo, AECL Underground Research Laboratory. Pinawa, Manitoba, Canada

D. Dixon, AECL Underground Research Laboratory. Pinawa, Manitoba, Canada

Abstract

The Tunnel Sealing Experiment (TSX) is an international project developed by Japan, France, the United States of America and Canada. The TSX consists of 11.45-m-long sand-filled chamber between two bulkheads. At one end a clay bulkhead was constructed of 9000 clay-sand blocks (360x105x170 mm) and at the other end a concrete bulkhead was constructed of 76 m³ of low-heat, high-performance concrete. The experiment operated in two distinct phases. The first phase was the stepwise pressurization of the chamber to 4 MPa in order to investigate the ability of the two bulkheads to resist hydraulic flow. The second phase involved circulating heated water through the chamber in order to raise the temperature of the sealing system and to evaluate the influence of elevated temperature on the performance of the bulkheads. This paper focuses on our experience with numerical modelling tools (MOTIF, COMPASS, CODE_BRIGHT and CLEO) to simulate the hydro-mechanical (H-M) evolution of the clay bulkheads and surrounding rock under isothermal (ambient) conditions as well as during pressurization of the chamber. The modelled hydraulic and mechanical responses of the clay bulkhead were compared with the measured data.

Introduction

The waste emplacement configurations proposed for a deep geologic repository for used nuclear fuel in Canada have a number of features in common with those proposed by other nations. The Canadian concept for waste isolation includes a horizontal array of waste emplacement rooms at a nominal depth of 500 to 1000 m in plutonic rock of the Canadian Shield. Used fuel within corrosion-resistant containers would be placed and sealed in these rooms. The containers would be positioned either vertically within boreholes drilled into the floors of the emplacement rooms (in-floor borehole emplacement method) or horizontally within the confines of each room (in-room emplacement method) (Russell and Simmons 2003).

The long-term safety of an underground repository for heat-generating used fuel relies on the ability of a series of natural and engineered barriers to limit to very low values the rates of container corrosion, used fuel dissolution and radionuclide release. Engineered barriers include bulkhead seals placed at strategic locations in tunnels and shafts and at the entrance to each waste emplacement room. The purpose of these seals would be to limit the flow of water and any water-borne radionuclides along the length of the excavated openings as well as to provide mechanical restraint to the sealing and backfilling materials in the waste emplacement rooms for the period prior to complete repository closure.

The Tunnel Sealing Experiment

In situ experiments to test various components of the engineered barriers system have been performed at Atomic Energy of Canada Limited's (AECL's) Underground Research Laboratory (URL). The Tunnel Sealing Experiment (TSX) is designed to test the performance of clay-based materials and concrete, which are expected to be the main components of tunnel and room bulkheads and other repository seals. The TSX is an international project funded by a partnership of nuclear waste management organizations from Japan (JNC), France (ANDRA), the United States of America (WIPP) and Canada (AECL). The clay bulkhead was constructed from highly-compacted sand-bentonite blocks, and the concrete bulkhead was constructed using mass-poured, low-heat, high-performance concrete (Figure 1). A permeable sand fill was placed in the chamber between these bulkheads. After construction of the bulkheads, the chamber was pressurized with water so that the ability of each of the bulkheads to resist hydraulic flow could be evaluated under ambient (isothermal) conditions.

In addition to evaluating the ambient temperature response of the clay and the concrete bulkheads, the influence of elevated temperatures on the sealing performance of the bulkheads was evaluated (Chandler et al. 2002). To accomplish this, the temperature of the chamber was increased during the second phase of the TSX by circulating heated water through headers installed in the sand-filled chamber (Figure 1).

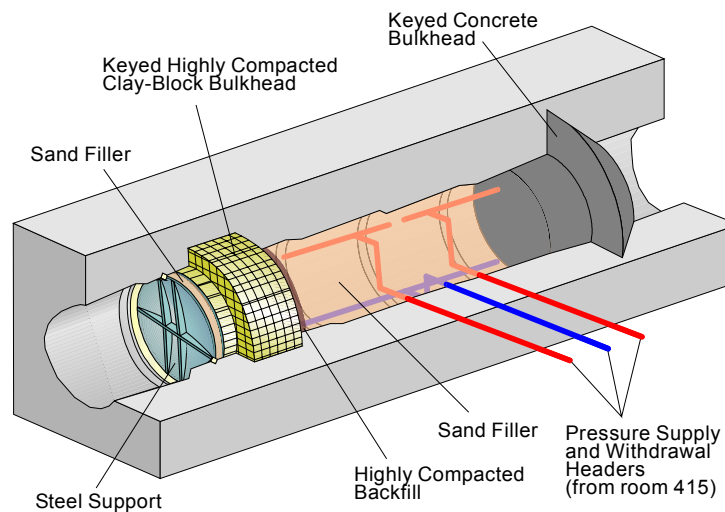


Figure 1. Configuration of the Tunnel Sealing Experiment.

Numerical simulations performed for the TSX

Extensive numerical simulations related to the TSX have been performed using the numerical finite element programs: CODE_BRIGHT, CLEO, COMPASS and MOTIF. These simulations were primarily intended to provide means for assessing and understanding the thermal, hydraulic and mechanical responses of the clay bulkhead and the surrounding rock.

Sensitivity analyses were carried out by the Universidad Politecnica de Catalunya (UPC) using CODE_BRIGHT and by Eurogeomat using CLEO to estimate the effects of the relative permeability of the clay bulkhead, the boundary conditions and initial conditions on the process of saturation within the clay bulkhead. The effect of the water retention curve for the clay used in the construction of the clay bulkhead on the saturation process was also modelled.

Moisture movement within the clay bulkhead during system saturation was modelled by Thomas et al. (2003) using COMPASS (COde for Modelling PARTly Saturated Soil). It is a fully coupled thermo-hydro-mechanical (T-H-M) program. Preliminary non-coupled, three-dimensional analyses of the TSX clay bulkhead were performed in order to assess the hydraulic behaviour of the host granite rock prior to chamber pressurization. Investigation of the more complex coupled T-H-M behaviour occurring in the heating phase was also carried out using three-dimensional geometries (Guo and Dixon 2004).

In order to provide design guidance for the heating stage of the TSX, a fully coupled T-H-M predictive modelling of the TSX was performed using MOTIF (Model Of Transport In Fracture/porous media) (Chan et al. 1999) and FLAC (Fast Lagrangian Analysis of Continua), a finite difference program. MOTIF was developed by AECL to model coupled groundwater flow, heat transport, solute transport and mechanical response in saturated/unsaturated, fractured/porous media. MOTIF was used to back analyze the TSX tunnel excavation and chamber pressurization, to predict T-H-M responses in the clay bulkhead, the concrete bulkheads and the surrounding rock using the heating plan proposed from the MOTIF T-H modelling (Guo et al. 2003), and to model temperature change in the TSX and coupled T-H-M effects. This modelling was performed in parallel with FLAC modelling in order to calculate the heat loss to the rock from the heated water supply and withdrawal headers (Guo et al. 2002; Guo et al. 2003a).

Modelling and test results

An objective of the ambient temperature phase of the TSX was the performance of numerical simulations to estimate the time required to achieve water saturation and to predict the distribution of pore water pressures within the clay bulkhead.

Numerical modelling of clay bulkhead hydration

Part of the TSX design process was to simulate the effects of varying the degree of saturation, density and key shape on the hydraulic evolution of the clay bulkhead in the TSX. These numerical simulations were used to determine how the sand-filled chamber would be pressurized (i.e., wetting from one face, wetting from two faces), to assess the effect of hydraulic head (e.g. ranging from 0 to 5 MPa) on the saturation rate and to provide an estimate of the time required for the bulkhead to achieve full saturation. Sensitivity assessment of hydraulic evolution provided a means for determining which parameters are likely to dominate the uptake and transmission of water in the clay bulkhead.

Pre-construction modelling was performed using CODE_BRIGHT and CLEO to estimate water uptake for the degree of saturation at the downstream face of the key after two years of water supply as well as the time required to achieve 95% saturation throughout the bulkhead.

Within the constraints of the numerical approaches used, these simulations provided estimates of the time required for water saturation to be achieved under a variety of hydraulic heads. Most estimates predicted saturation in 2.5 to 5 years if wetting was assumed to occur from the upstream face only. Although not considered to be particularly relevant at the time of performing the numeric simulations, a case was run where wetting was defined to occur via both faces of the bulkhead. This simulation predicted that saturation of the clay bulkhead would occur within one year. The range of results obtained for the various simulations wetting from 1 face only are provided in Figure 2.

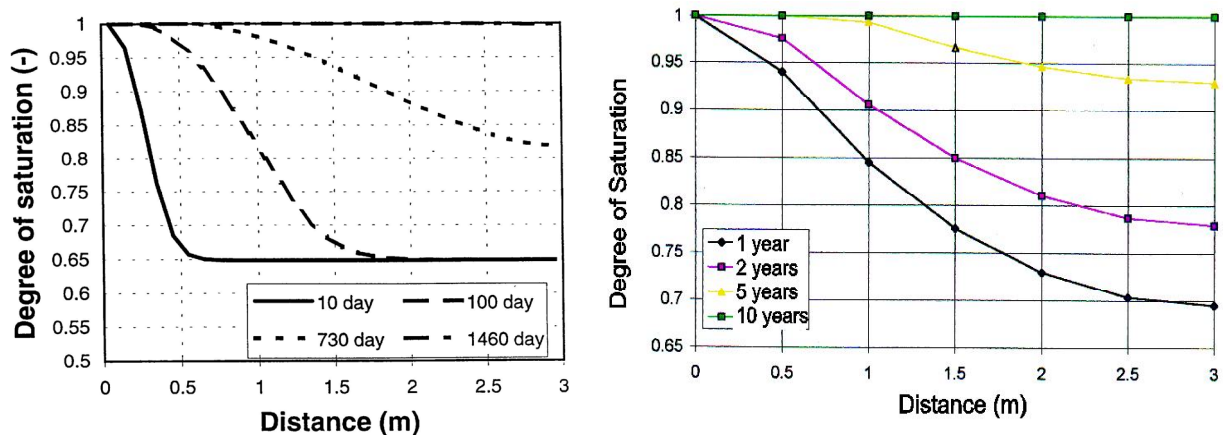


Figure 2. Saturation Profile Predictions for the Clay Bulkhead (by UPC (left) and Eurogeomat (right))(Chandler et. al 2002b)

The clay bulkhead was predicted to gradually saturate from upstream to downstream in a very uniform pattern. The constructed clay bulkhead essentially reached full saturation in approximately the time predicted by these scoping calculations but by a very different mechanism than was assumed for the numerical models. The joints between the clay blocks and the unsaturated shotclay between the blocks and surrounding rock were highly preferential flow paths for water in the initial stages of the saturation process. As a result of this water movement, numerical models, as constructed, were unable to simulate the actual field performance of the clay bulkhead in the early stages of system saturation. Following the rapid influx of water into portions of the clay bulkhead and the saturation of the upstream and downstream faces of the bulkhead as well as the perimeter, the final stages of bulkhead saturation continued in the manner initially defined for the numerical models. Full saturation was achieved within 3 years of beginning the saturation process (Figure 3).

Thomas et al. (2003) provided a hydro-mechanical (H-M) prediction for water uptake using the COMPASS program. The water uptake and distribution predicted for the clay bulkhead is provided in Figure 4. The COMPASS H-M analysis predicted that in 2.8 years, the core of the clay bulkhead would reach 99.9% of saturation. This modelling was performed using the same material parameters as the previously described simulations but was done after the start of the ambient temperature phase.

Thomas et al. used the knowledge that water had contacted the downstream face of the clay bulkhead so that wetting was assumed to progress from both ends but no other “in-progress” water distribution information was used in their modelling. Given that the water collection system on the downstream face of the clay bulkhead was saturated and could provide water to the bulkhead via its downstream face, this assumption of two-face wetting was considered to be appropriate. This analysis did not take into account any water supplied to the perimeter of the clay bulkhead via the shotclay. Figure 4 shows a similar pattern at the upstream end of the bulkhead to that seen in Figure 3 but it assumed that the saturation of the clay bulkhead progressed via both the upstream and the downstream ends, so that the core was last to saturate.

Hydraulic head and axial displacement within the clay bulkhead

The development of hydraulic pressures within the clay bulkhead was numerically simulated using MOTIF to estimate the total pressures acting on the restraint system, the displacements in the clay bulkhead and the pore pressure change in the surrounding rock mass as they affect the mechanical performance of the bulkhead. In this model, clay was assumed to be saturated and the gaps between the clay blocks were not incorporated. A small value of Young’s modulus for the clay bulkhead was used to reflect the gap closure.

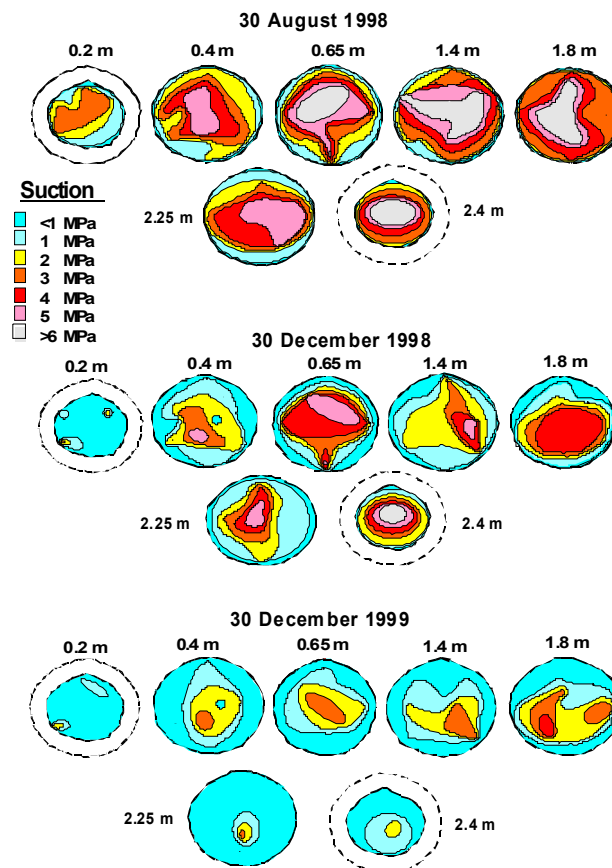


Figure 3. Suction Contours Through the TSX Clay Bulkhead (August 1998 – December 1999) (Note: Cross-sections are measured from the upstream face of the clay blocks)

Figure 5 compares the simulated hydraulic heads with measurements from 8 piezometers in the clay bulkhead (PZ1 to PZ8) during the first 1403 days of chamber pressurization (Guo et al. 2003a). In this simulation, the clay bulkhead was assumed to be saturated at the start of chamber pressurization and this assumption resulted in calculated hydraulic heads in the clay bulkhead that were much higher than the measured heads where the clay bulkhead was not saturated during the first 1000 days. After 1000 days of chamber pressurization, the numerical results show a similar pattern of pressure change to the measured results, except for PZ5 and PZ6, which are located in the central part of the clay bulkhead. The measured hydraulic heads at these two locations began to increase after 1300 days of chamber pressurization, indicating that the central part of the clay bulkhead was just achieving saturation at the time the chamber pressure reached 4 MPa. The similar patterns for the development of observed and predicted piezometric pressure for the remaining six piezometers suggest that the parameters chosen for the clay bulkhead are reasonable and can be used in future modelling exercises.

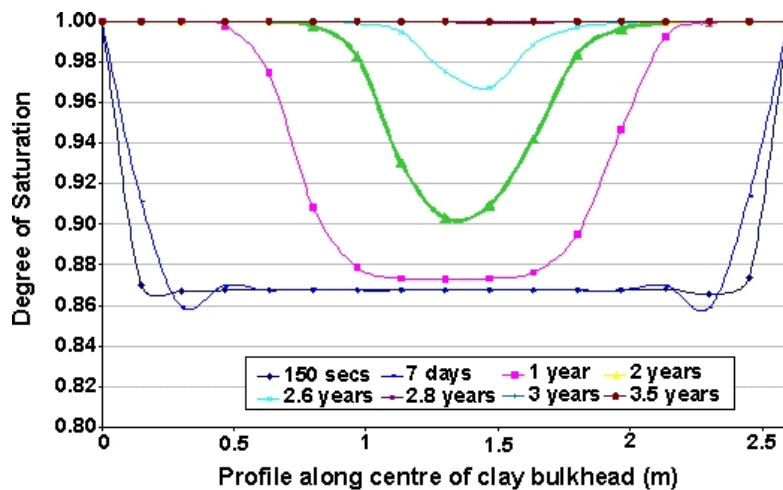


Figure 4. Degree of Saturation Along the Tunnel Axis (Thomas et al. 2003)

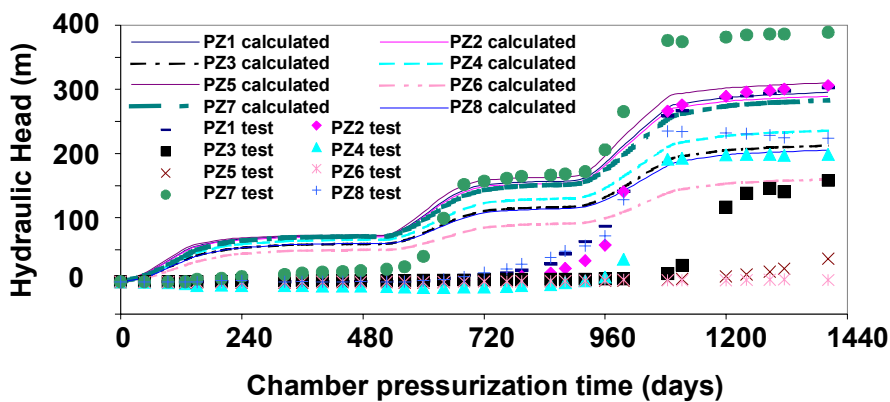


Figure 5. Comparison of Simulated and Measured Hydraulic Heads in the Clay Bulkhead During the Ambient Temperature Phase

The axial displacements of the clay bulkhead at the locations of five sonic probe extensometer segments SP1 to SP5 were simulated using MOTIF and the results are presented in Figure 6. The assumed Young's modulus for the clay bulkhead was 100 MPa (Guo et al. 2003b). Compared with the measured data provided in Figure 7, the simulation results shown in Figure 6 have a similar pattern of displacement, but their magnitudes are considerably less. The greater measured displacement (Figure 7) (i.e., 2 to 4 times larger than predicted by the numerical simulation) of the clay bulkhead may be explained by the closure of the construction gaps between the steel plate at the downstream face of the bulkhead and the gaps present between the clay blocks. These gaps are known to have existed to some degree at the time of bulkhead construction and their gradual closing under the pressures applied at the upstream face of the bulkhead and swelling of the clay blocks would have resulted in larger than anticipated compression. These gaps were not incorporated in this numerical modelling. There may also be some refinement required of the numerical model as it predicts some rebound of the bulkhead following each pressure increment while the field measurements did not detect any such rebound.

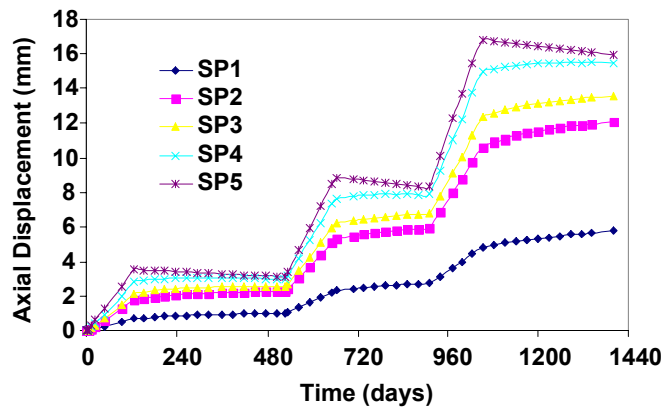


Figure 6. Simulated Axial Displacements at Sonic Probe Extensometer Locations During Chamber Pressurization (Young's modulus for clay = 100 kPa)

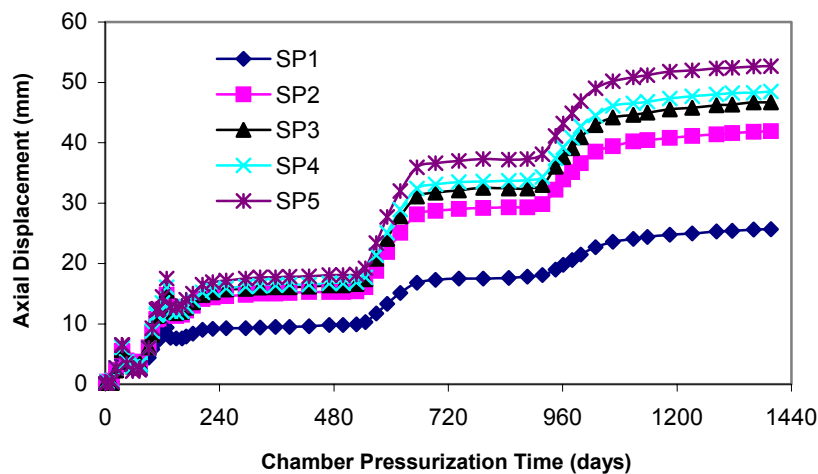


Figure 7. Measured Axial Displacements at Different Locations in the Clay Bulkhead during Chamber Pressurization

Summary

The numerical simulations described in this paper generated materials behaviour patterns that were generally consistent with the field measurements obtained in the TSX, but commonly differed in their magnitudes. These differences in magnitude highlight the current limitations of using numerical simulations to try and predict detailed bulkhead performance. The models can use entirely appropriate physical, mechanical, and thermal formulations and relationships but they are often unable to capture the field constructions “reality”. Features such as construction joints, unanticipated non-homogeneity of materials and other unexpected or preciously unrecognized parameters will affect the magnitudes of the field performance while preserving generic patterns of behaviour. Numerical simulations therefore provide a valuable tool in developing designs, preparing construction specifications and predicting general barrier performance but have limitations when it comes to detailed system performance. With improved experience in numerical modelling and an improving ability to recognize the most important parameters controlling field performance, they have the potential to greatly aid in developing tools that can be used to assist in assessing system performances. However, if numerical simulations that are based on inadequate representations of an actual system or do not recognize the key processes active, the potential exists for a field (or repository) construction to be incorrectly deemed as not functioning properly (e.g. straining too much, saturating too quickly).

In some cases the numerical simulations are limited by uncertainty in the parameter values needed for the conduct of these simulations. In such cases carefully controlled laboratory tests are required to determine these input parameters. This will also contribute to improved comparability between the simulations and field performance. In the future, an appropriate numerical model including the clay bricks, the gaps between the bricks, and the shotclay between the bricks and the surrounding rock should be developed to simulate the TSX clay bulkhead.

Acknowledgements

The Tunnel Sealing Experiment was jointly funded by the Japanese Nuclear Cycle Development Institute (JNC), the agence nationale pour la gestion de déchets radioactifs (ANDRA) of France, the United States Department of Energy Carlsbad Area Field Office through Sandia National Laboratories, their Science officer for the Waste Isolation Pilot Plant (WIPP) and Atomic Energy of Canada Limited (AECL). Ontario Power Generation (OPG) has supported activities related to the reporting of the results of the TSX.

References

Chan T., Scheier N.W., and Stanchell F.W., 1999. MOTIF code version 3.2 user's manual. Ontario Hydro, Nuclear Waste Management Division Report No: 06819-REP-01200-0090-R00.

Chandler N., Cournut A., Dixon D., Fairhurst C., Hansen F., Gray M., Hara K., Ishijima Y., Kozak E., Martino J., Masumoto K., McCrank G., Sugita Y., Thompson P., Tillerson J., and Vignal B., 2002. The five year report of the Tunnel Sealing Experiment: -an international project of AECL, JNC, ANDRA and WIPP. Atomic Energy of Canada Limited Report AECL-12727.

Guo R. and Dixon D., 2004. Experience with Thermo-Hydro-Mechanical Modelling: The Tunnel Sealing Experiment, Presented at Task Force-Related Meeting on Buffer and Backfill Modelling, Lund, Sweden, March 10-11, 2004.

Guo R., Chandler N.A. and Dixon D.A., 2002. Modelling the thermally induced hydraulic and mechanical response for the heated phase of the Tunnel Sealing Experiment. Ontario Power Generation Inc., Nuclear Waste Management Division Report 06819-REP-01200-10095-R00.

Guo R., Chandler N., and Dixon D., 2003a. Thermo-Hydro-Mechanical modelling of the Tunnel Sealing Experiment clay bulkhead at the Underground Research Laboratory. In Proceedings of the 56th Canadian Geotechnical Society Conference, Winnipeg.

Guo R., Chandler N., Martino J. and Dixon D., 2003b. Thermo-hydro-mechanical numerical modelling of the TSX with comparisons to measurements during stage 1 heating. Ontario Power Generation Inc., Nuclear Waste Management Dixon Report 06819-REP-01300-10070-R00.

Russell S.B. and Simmons G.R., (2003). Engineered barrier system for a deep geologic repository. In Proc. 2003 International High-Level Radioactive Waste Management Conference. Las Vegas, USA.

Thomas H.R., Cleall P.J. and Melhuish T.A., 2003. Simulation of the Tunnel Sealing Experiment using THM modelling. Ontario Power Generation Inc., Nuclear Waste Management Dixon Report 06819-REP-01200-10112-R00.

4.5 Modelling the thermal-hydraulic-chemical-mechanical (THCM) behaviour of bentonite buffers

H.R. Thomas, P.J. Cleall, T.A. Melhuish and S.C. Seetharam
*Geoenvironmental Research Centre, Cardiff School of Engineering,
Cardiff University, UK*

Abstract

This paper describes a model for the coupled thermal, hydraulic, chemical and mechanical (THCM) behaviour of partly saturated soil and its application to a large scale in-situ test. In particular the results of research work on the inclusion of both the effects of i) the microstructure on moisture flow and ii) geochemical interactions in models of thermal hydraulic mechanical behaviour are presented. The presented model is then applied to simulate the coupled behaviour of the Prototype Repository. The simulation results are compared with experimentally measure results. It is found that the model is able to capture both the trends and patterns of behaviour in the system.

Introduction

The engineering performance of high level nuclear waste disposal repositories is a problem of international major importance. Currently deep geological repositories, in which waste will be placed within a multibarrier system employed to control the migration of the radionuclides, are under consideration by a number of organisations (Swedish Nuclear Fuel Supply Co, 1983; EU, 1999).

The proposed concept involves the placement of a partly saturated engineered clay barrier to form one layer of the multibarrier system. The performance of this barrier is affected by a number of phenomena including i) elevated temperatures due to heat energy emitted by the waste, ii) ground water recovery after closure tending to resaturate the engineered barrier, iii) a build up of gas pressure as the barrier resaturates and iv) geochemical behaviour of both the barrier and the host environment. To carry out a suitable assessment of the barrier system each of these phenomena needs to be taken into account.

The behaviour of partly saturated soil in relation to i) the flow of moisture, heat, gases and chemicals and ii) the stress-strain response of the medium is therefore of great importance. An analysis of the bi-directional non-linear coupling between each of the flow fields and the stress strain field is required. For example the effects of the chemical composition of the system on the hydraulic and mechanical response and the influence of the microstructure need to be addressed.

The authors and co-workers have been actively involved in the development of such models for a number of years. Initially the prediction of the coupled movement of heat and moisture was addressed (Thomas and King, 1991). A coupled flow and deformation model, utilising a non-linear elastic constitutive relationship was then developed (Thomas and He, 1995). Later an elasto-plastic constitutive relationship was included in the model (Thomas and He, 1998) allowing collapse and swelling of the soil under wetting to be simulated.

The next step was to attempt to include the effect of chemicals on the soil behaviour, to extend the THM models to THCM. This development is necessary because of possible effects of the geochemistry on the flow and deformation behaviour of bentonitic soils (Yong, 1999).

In the approach presented here three main components of behaviour are addressed: i) flow of chemical solutes in pore fluid, ii) effect of the presence of solutes on the stress–strain behaviour of the soil and iii) geochemical interaction of solute with other species and soil solid. The first component has been attempted herein via a coupled advection–diffusion mass balance equation (Bear and Verruijt, 1987). Initial attempts at including the second component based on an osmotic potential term, have been presented previously (Thomas and Cleall, 1999). The final component, geochemical interaction of the solute with other species and the soil solid is attempted herein via the integration of the existing flow model with a geochemical model. Moisture and chemical solute flow are linked in a sequential manner to a suitable geochemical model.

Further study (Thomas et al, 2003) has found that the expansion of the microstructure of the bentonite, as the material saturates, has a significant influence on the resaturation behaviour of bentonite based buffer materials. Inclusion of this micro / macro structural interaction on moisture flow is also addressed here.

This paper presents the theoretical approach developed, the numerical methods employed and finally application of the model to simulate the Prototype Repository experiment.

Theory

Unsaturated soil can be considered a three-phase porous medium consisting of solid, liquid and gas. A set of coupled governing differential equations has been developed to describe the flow and deformation behaviour of the soil. The development of these equations is dealt with below. The primary variables of the model are pore water pressure, u_l , pore air pressure, u_a , temperature, T , chemical concentration, c_d and deformation, \mathbf{u} .

Heat transfer

Conservation of heat energy can be defined via a classical conservation equation:

$$\frac{\partial \Omega_H}{\partial t} = -\nabla \cdot Q \quad (1)$$

where, the heat content of unsaturated soil per unit volume, Ω_H , includes latent heat of vaporisation and the classical components of heat capacity. The heat flux per unit area, Q , includes conduction, convection and transfer of latent heat of vaporisation.

Moisture transfer

The governing equation for moisture transfer in an unsaturated soil can be expressed as:

$$\frac{\partial(\rho_l n S_l)}{\partial t} + \frac{\partial(\rho_v n (S_l - 1))}{\partial t} = -\rho_l \nabla \cdot \mathbf{v}_l - \rho_l \nabla \cdot \mathbf{v}_v - \nabla \cdot \rho_v \mathbf{v}_a \quad (2)$$

where, n is the porosity. The velocities of pore liquid and pore air are based on a generalised Darcy's law. The definition of vapour velocity is based on the flow law proposed by Philip and de Vries (1957) and follows the approach presented by Thomas and King (1991).

Micro-macro moisture transfer

Recent research has shown that the micro and macro structure of a bentonite buffer material may have a pronounced effect on the saturation rates of the material (Thomas et al., 2003). It was postulated that as water enters the buffer the majority of it becomes adsorbed within the micropores and hence is unavailable for further flow. This adsorption of water results in swelling of the micropore in the buffer. Depending on the degree of mechanical restraint swelling of the micropore will lead to some reduction in the size of the macropores (Pusch, 1998). As the only water available for flow is contained in the macropores, the swelling of the micropore in a restrained material would thus tend to 'choke' moisture flow and further reduce the effective hydraulic conductivity of the material. Thomas et al., (2003) presented an approach to modify the hydraulic conductivity relationship accordingly. The buffer in the Prototype Repository is relatively free to deform, compared to the buffer investigated in Thomas et al., (2003), therefore the effect of microstructural swelling choking of the macro structure is modified here. This has led to the following relationship being assumed, as a first approximation, for simulation of the influence of the microstructure in the MX-80 bentonite buffer present in the Prototype Repository:

$$k = k_{unsat} k_l \cdot [S_a + 0.06 S_l (\exp(0.01(1 - 0.06) S_l))] \quad (3)$$

Dry air transfer

Air in unsaturated soils is considered to exist in two forms: bulk air and dissolved air. In this approach the proportion of dry air contained in the pore liquid is defined using Henry's law:

$$\frac{\partial[S_a + H_s S_l] n \rho_{da}}{\partial t} = -\nabla \cdot [\rho_{da} (\mathbf{v}_a + H_s \mathbf{v}_l)] \quad (4)$$

where, S_a represents the degree of pore air saturation and the dry air density can be defined via the use of Dalton's law of partial pressures.

Multicomponent reactive chemical transport

The mechanisms for chemical transport considered are advection, hydrodynamic dispersion and geochemical reactions such as speciation, aqueous complexation, acid-base, redox, ion exchange and mineral precipitation/dissolution. The effect of geochemical reactions is included here via a sink/source term in the governing chemical transport equation. In this study, the sink/source term is evaluated using a geochemical model, MINTEQA2. The governing equation for multicomponent reactive chemical transport can be represented as:

$$\frac{\partial (nS_i c_d^i)}{\partial t} + \frac{\partial (nS_i s_s^i)}{\partial t} = -\nabla \cdot [c_d^i \mathbf{v}_1] + \nabla \cdot [nS_i D_h^i \nabla c_d^i] + \nabla \cdot [nS_i D_d^i S^i \nabla T] \quad (5)$$

where, c_d^i is the dissolved concentration and s_s^i is the sink/source term expressed in terms of mass per unit volume of the solution for the i^{th} chemical component. D_h^i represents the hydrodynamic dispersion which is a summation of dispersion and molecular diffusion (D_d^i) effects for the i^{th} chemical component. S^i represents the sorpt coefficient for the i^{th} chemical component.

Deformation behaviour

A number of constitutive stress-strain models for soils can be used which include the effects of suction, temperature, chemical solute and net mean stress variations (for example the model proposed by Alonso et al., 1990). Generally for problems in unsaturated clays, the total strain can be given in an incremental form, without loss of generality, as:

$$d\boldsymbol{\varepsilon} = d\boldsymbol{\varepsilon}_\sigma + d\boldsymbol{\varepsilon}_T + d\boldsymbol{\varepsilon}_s + d\boldsymbol{\varepsilon}_{c_s} \quad (6)$$

where, the subscripts σ , T , s and c_s refer to net stress, temperature, suction and chemical solute concentration contributions.

Modelling approach

The numerical solution of the governing equations is achieved by a combination of the finite element method for the spatial discretisation and a finite difference time stepping scheme for temporal discretisation. A computer code known as COMPASS (COde for Modelling PARTly Saturated Soil) has been developed to implement the numerical approach (Thomas and He, 1995, 1998; Thomas and Cleall, 1999). During the course of the development of COMPASS, an extensive verification and validation program has been undertaken. It is recognised, however, that validation of the code is a process rather than a series of events and as such, continued work on this aspect is envisaged.

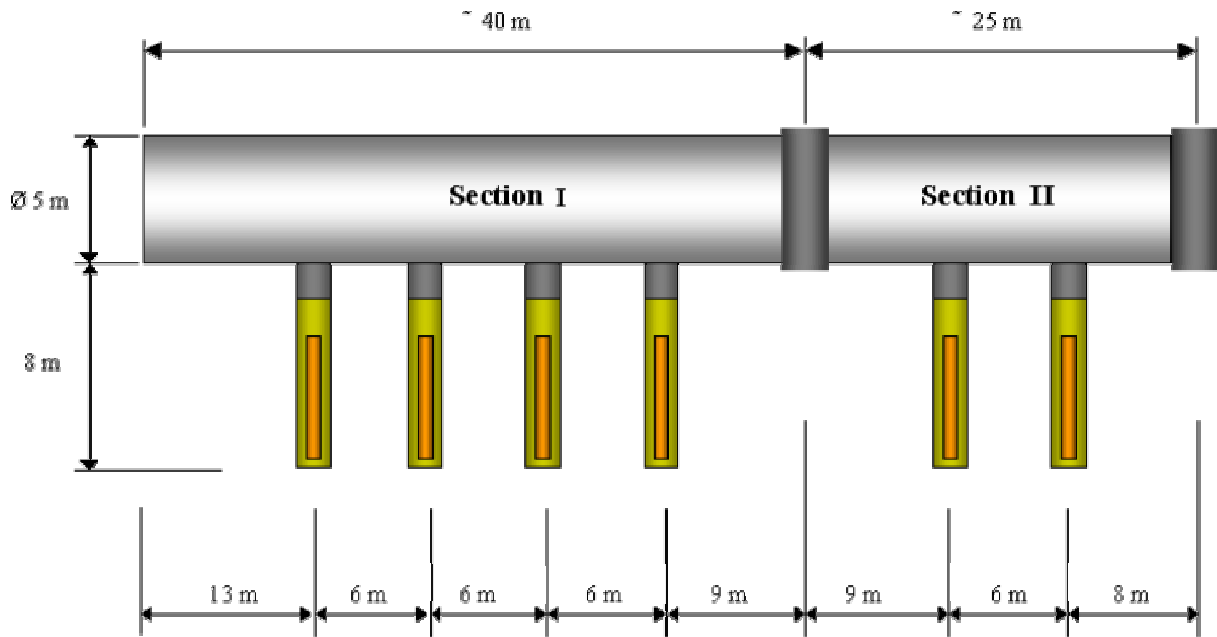


Figure 1: Schematic layout of the Prototype Repository and deposition holes

Modelling the THM behaviour of the Prototype Repository

The Prototype Repository is an international, EC-supported project with the objective to investigate, on a full-scale, the integrated performance of engineered barriers and near-field rock of a deep repository intended for the disposal of high-level nuclear waste. It is located at SKB's Äspö Hard Rock Laboratory, in Sweden (Dahlström, 1998). It has been constructed in a 65m long TBM drift at approximately 450m below the ground surface in crystalline rock. It consists of six 1.75m diameter, 8m deep full-scale deposition holes. Heater canisters have been placed in these holes with a combination of bentonite blocks, bentonite pellets and backfill material used to form a series of engineered barriers in accordance with the Swedish reference concept for disposal (KBS-3). A schematic can be seen in Figure 1. The experiment is currently running and a range of results have been published (Goudarzi and Börgesson, 2003).

A full three-dimensional model of SKB's Prototype Repository incorporating all of the primary features of the tunnel has been developed. The model domain measures 200m by 100m by 200m. This model has been discretised using 8 noded hexahedral elements and consists of 158,175 elements and 146,380 nodes. The mesh has been refined in and around the buffer with a coarser mesh discretisation used in the far-field rock.

Thermal-Hydraulic-Mechanical Results

A large number of coupled thermal-hydraulic-mechanical analyses have been performed to investigate the complex behaviour that occurs in the Prototype Repository following heater activation with a step-wise approach to the modelling being adopted. A full range of 3D tunnel section and 2D axisymmetric analyses have been undertaken with the results being presented previously (Thomas et al., 2002). However, more recently full three-dimensional analyses of the Prototype Repository have been performed.

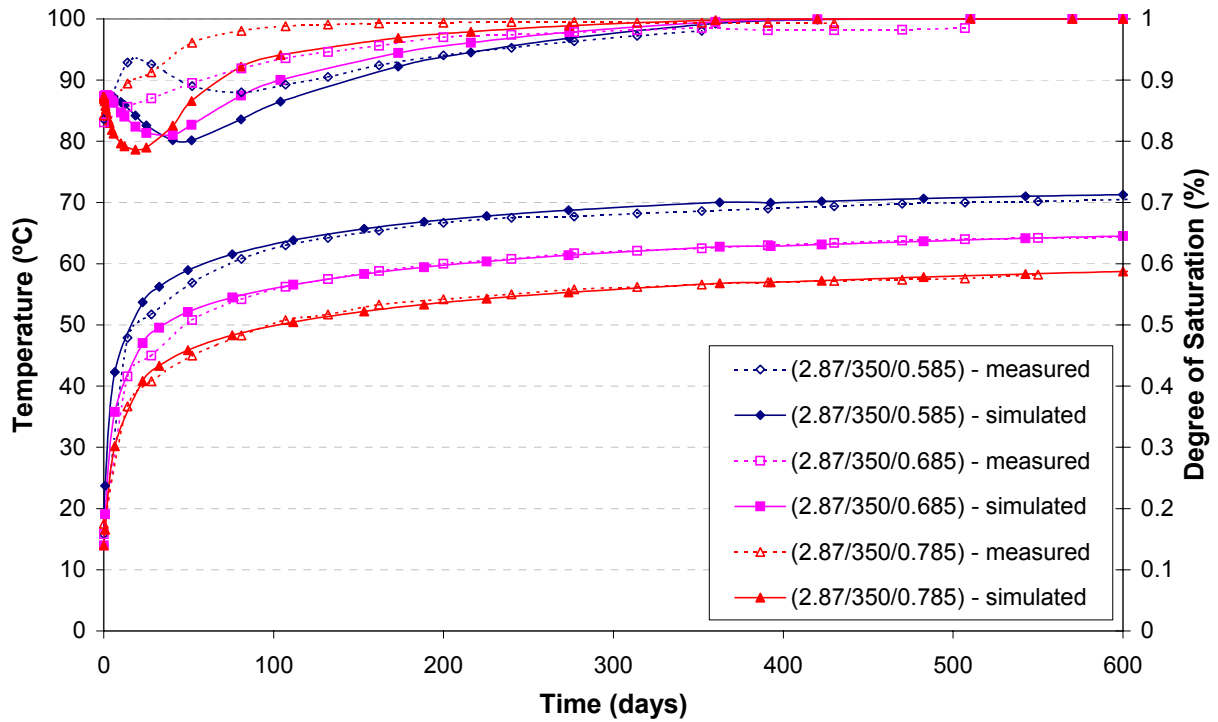


Figure 2: Measured and simulated temperature and degree of saturation plots for Borehole 1/Ring 5

Figure 2 shows both the simulated and experimentally measured temperature and degree of saturation after 600 days for the 3 different radii positions in Borehole 1 at the mid-height of the canister. The experimentally measured values are taken from the Vaisala measurements. It can be seen that there is excellent agreement in the temperature results and illustrate that the temperature regime is well understood and captured by the model in Borehole 1. In terms of degree of saturation it can be seen that initially there is an over prediction of drying in the buffer whereas experimentally the buffer closest to the rock exhibits immediate recharge following heater activation. The pellet filled region appears to have little effect in terms of retarding the rate of resaturation in the more centrally located buffer. After 100 days the correlation between the experimental and simulated results is much improved, with almost complete saturation being achieved after approximately 400 days in both cases.

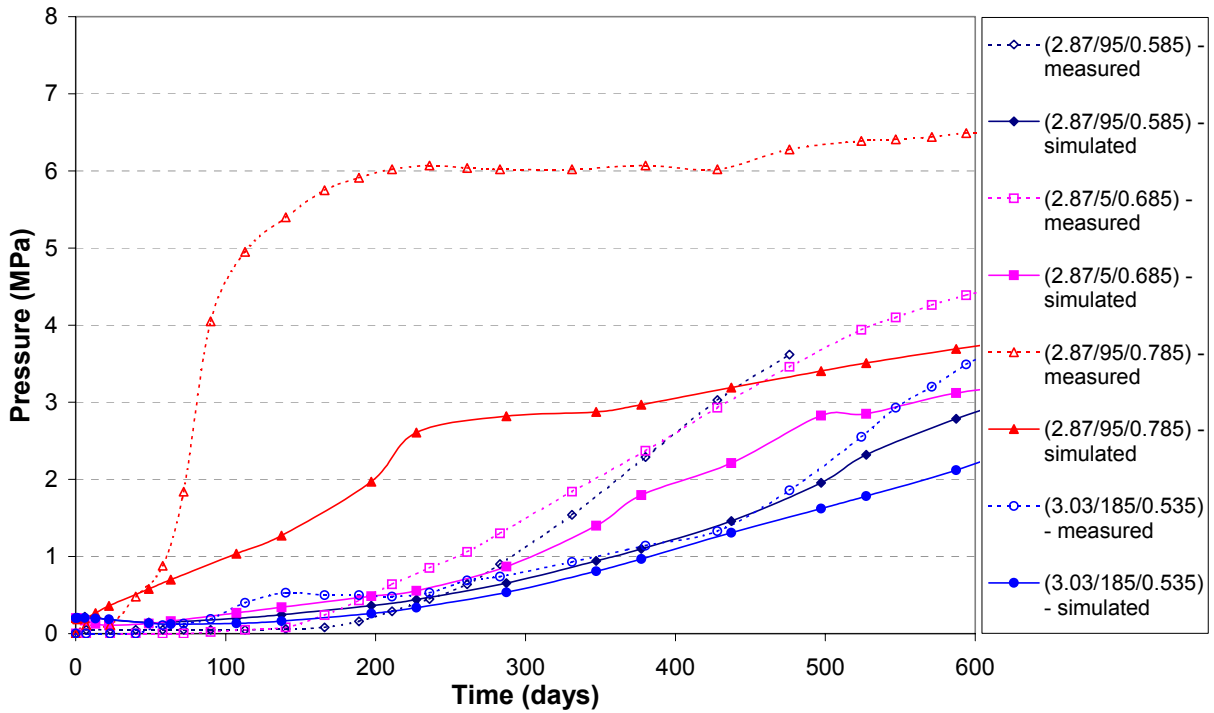


Figure 3: Measured and simulated total pressure plots for Borehole 1/Ring 5

Figure 3 shows both the simulated and experimentally measured total pressure plots in the buffer at 4 different positions in Borehole 1. It can be seen that there is good qualitative correlation between the results. Quantitatively the simulation has captured the development of swelling pressures in the buffer well, with the exception of the point closest to the rock/buffer interface. In both cases the buffer closer to the rock experiences the highest swelling pressure as a result of the recharge from the granite. It is believed that this difference in these results is due to an overestimation of the compressibility of the pellet region. This leads to a relief of some of the swelling pressure being developed on saturation.

Figure 4 shows both the simulated and experimentally measured temperature and degree of saturation after 600 days for 3 different radii positions in Borehole 3. The simulated results accurately capture the rate of increase in temperature of the measured results and again illustrate that the temperature regime is well understood and captured by the simulation. In terms of degree of saturation it can be seen that the simulation captures the overall hydraulic behaviour of the experiment well. In all regions initial drying is observed before resaturation begins to take place up to 600 days.

Figure 5 shows the simulated and experimentally measured total pressure plots in the buffer at 3 different positions in Borehole 3. It can be seen that very little swelling pressure develops in the first 600 days and that there is no major change from the initial conditions. These patterns follow the slow rate of resaturation in the buffer as illustrated in Figure 4. It is expected that as the buffer in Borehole 3 further resaturates the swelling pressures will increase accordingly.

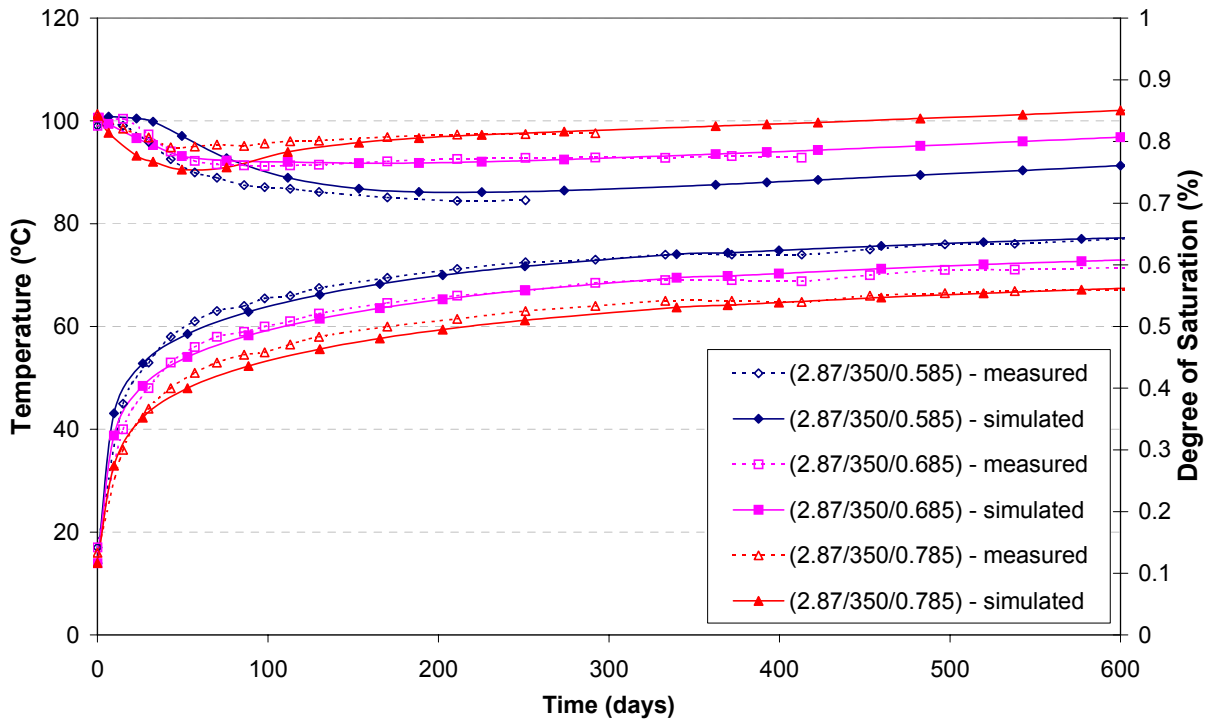


Figure 4: Measured and simulated temperature and degree of saturation plots for Borehole 3/Ring 5

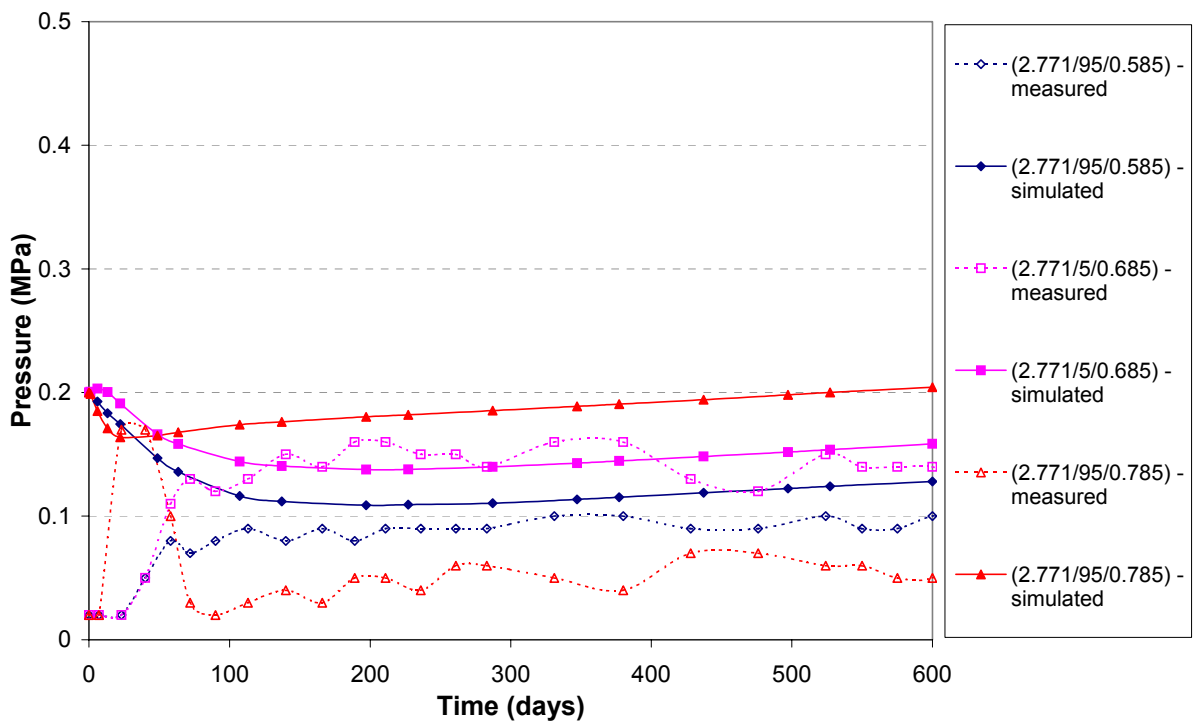


Figure 5: Measured and simulated total pressure plots for Borehole 3/Ring 5

Conclusions

A model for the coupled flow of heat, moisture, air and chemical solute in a deformable partly saturated soil has been presented. In particular inclusions of both the influences of the microstructure on the flow of moisture and geochemical interactions have been detailed. The model was then applied to simulate the coupled THM behaviour of the Prototype Repository. Comparison of the simulated behaviour with the experimentally observed behaviour found that the model is able to capture both the trends and patterns of behaviour in the system. The results illustrate that the temperature regime is well understood and represented in the system. It should be noted that inclusion of the three-dimensional configuration of the boreholes was essential to correctly capture the variation in the thermal response in the system. The simulated hydration rates in the system showed reasonable agreement with the experimental results measured. The simulation of the mechanical behaviour of the buffer captured the key features of the observed development of swelling pressures, although peak pressures close to the rock are under predicted possibly due to an over estimation of the compressibility of the pellet region.

References

- Alonso, E.E., Gens, A., and Josa, A., (1990)** “A constitutive model for partially saturated soils”, *Geotechnique*, **40**, No. 3., 405-430.
- Bear, J. and Verruijt, A., (1987)** “Modelling groundwater flow and pollution”, Kluwer Academic Publishers Group.
- Dahlström, L.O., (1998)** “Äspö HRL - Test Plan for the Prototype Repository”, SKB, HRL-98-24.
- EU (1999)** “Calculation and testing of behaviour of unsaturated clay”, Commission of the European Union, Contract Report, EC Contract FI4WCT950003.
- Goudarzi, R. and Börgesson, L., (2003)** “Äspö HRL – Prototype Repository. Sensors data report (Period: 010917-030601). Report No: 6”, SKB, IPR-03-31.
- Philip J.R., and de Vries D.A., (1957)** “Moisture movements in porous materials under temperature gradients” *Transactions, American Geophysical Union*, **38**, No 2, 222-232.
- Pusch, R., (1998)** “Microstructural evolution of buffer clay” In Proceedings of workshop on microstructural modelling of natural and artificially prepared clay soils with special emphasis on the use of clays for waste isolation, Lund, pp. 31-38.
- Swedish Nuclear Fuel Supply Co/ Division KBS, (1983)** “Final storage of spent nuclear fuel - KBS-3, III Barriers”, Swedish Nuclear Fuel Supply Co/Division, KBS Report: 9:1-16:12.
- Thomas, H.R. and King, S.D., (1991)** “Coupled temperature/capillary potential variations in unsaturated soil” *ASCE, Journal of Eng. Mech.* 117(11): 2475-2491.
- Thomas, H.R. and He, Y., (1995)** “Analysis of coupled heat, moisture and air transfer in a deformable unsaturated soil”, *Geotechnique*. 45(4): 677-689.

Thomas, H.R and He, Y., (1998) “Modelling the behaviour of unsaturated soil using an elasto plastic constitutive relationship”, *Geotechnique*, 48(5): 589-603.

Thomas, H.R. and Cleall, P.J., (1999) “Inclusion of expansive clay behaviour in coupled thermo hydraulic mechanical models”, *International Journal of Engineering Geology* 54: 93-108.

Thomas, H.R., Cleall, P.J. and Melhuish, T.A., (2002) “Simulation of the Prototype Repository using predictive THMCB modelling” UWC contribution to D34.

Thomas, H.R., Cleall, P.J., Chandler, N., Dixon, D. and Mitchell, H.P., (2003) “Water infiltration into a large-scale in-situ experiment in an underground research laboratory”, *Geotechnique* 53, No. 2, 207-224.

Yong, R.N., (1999) “Soil suction and soil-water potentials in swelling clays in engineered clay barriers”, *Int. Jour. of Engineering Geology* 54: 3-13.

4.6 A perspective of the modelling of Prototype Repository experiment

By Alberto Ledesma and Guangjing Chen
Tech. University of Catalonia, UPC, Barcelona, Spain

Abstract

Prototype Repository is a Large Scale Project managed by SKB and performed at the Äspö Hard Rock Laboratory (Sweden) with the aim of testing the KBS-3 Swedish concept of radioactive waste disposal. The project has been supported by the European Community in the context of the 5th Framework Research Programme, and several R+D groups have been involved in its development. The corresponding European Project has just finished, but the experiment will continue for many years and therefore some experience on the long term behaviour of the system will be obtained. This paper presents a view from one of the modelling groups involved in the project, summarizing the main results that have been achieved in the THM simulation of the experiment. The paper also emphasizes the modelling work that remains for the future. Although the limits of the problem seem to be well defined, there is still need for deeper understanding of the processes involved, especially regarding the long term behaviour of the system.

Introduction

Prototype Repository is the short name for “Full-scale test of the KBS-3 method for deep geological disposal of spent nuclear fuel in crystalline rock”. The KBS-3 method was initially developed in Sweden and refers to the following main characteristics:

- Copper canister with cast steel insert
- Buffer of bentonite clay surrounding the canisters
- Emplacement in vertical bore holes
- Repository depth of 400-700 m in crystalline rock
- Backfilling of deposition tunnels with bentonite-based materials

The test site is a 65 m long TBM-bored tunnel including six 1.75 m diameter deposition holes of 8 m depth. The outer 25 m long part has two holes and it is separated from the inner 40 m section including 4 holes by means of a tight plug. Details of the work plan may be found in Svemar & Pusch (2000).

The canisters were cylinders of 1.05 m diameter and 4.83 m height, installed in the deposition holes and surrounded by compacted bentonite rings 0.5 m height and 1.65 m of outer diameter. The gap between blocks and the rock was filled up with bentonite pellets. A small 1 cm gap was left between canister and bentonite blocks as a tolerance for installation purposes. The initial density of the bentonite blocks was 1.78 g/cm³, reaching 2 g/cm³ after saturation. The bentonite used was MX80 sodium bentonite from Wyoming.

After the installation of each heater, the bentonite blocks, the instrumentation and backfilling of the surrounding area, the corresponding system was switched on. That is, heaters were turned on according to the installation time schedule. First heater started last September 2001 (Goudarzi & Börgesson, 2003). Since that date, temperature, relative humidity, total pressure and water pressure from the instrumentation have been collected. Figure 1 shows the basic geometry of the experiment.

Here some typical results of the simulations regarding holes 1 and 3 are presented. A few groups were involved in the modelling work within the framework of a European Project supported by the EU. In general all groups were able to predict the main trends of the THM variables involved. However, it should be recognized that blind predictions were not very successful when the project started. Partly because of the initial conditions were difficult to define in advance, i.e. hole 1 was very wet from the beginning, whereas hole 3 was almost dry; but also because the basic parameters for the MX-80 bentonite were obtained from very few experiments.

The measurements available after 2 years of running the experiment were fundamental for calibrating the models and the parameters involved. As these calibrations may be problem dependent, it is crucial to improve our understanding on the physical processes that take part in the barrier, otherwise, any predictive THM analysis of a future repository may lead to odd results. In addition to that, an extrapolation to long term conditions is expected to be done in the near future and that exercise requires a very good knowledge of the physical problem. With this in mind, some needs for future research have been identified, and they are also described in the paper.

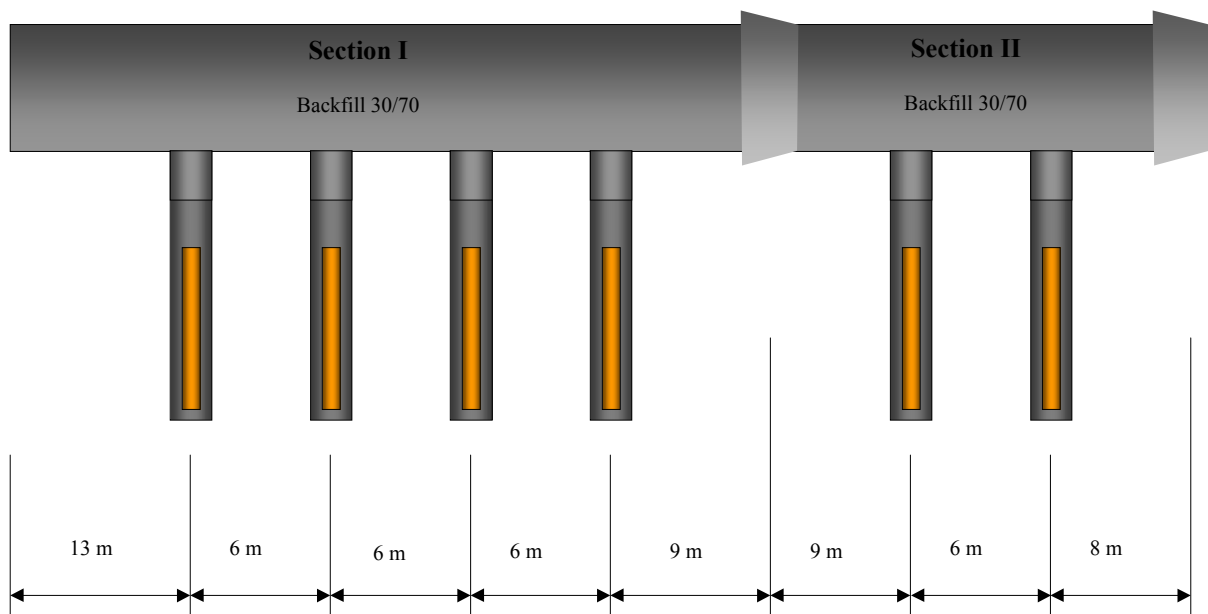


Figure 1. Basic geometry of the Prototype experiment. Hole number 1 is on the left hand side of the figure, in the inner part of Section I (Svemar and Pusch, 2000).

THM analysis of the experiment

All analyses performed by this group were carried out using Code_Bright, a finite element simulator developed in UPC to solve THM problems in this context. A description of the features of the code may be found in Olivella, (1996), and in deliverable D33 of the European Project (Pusch & Svemar, 2001).

The formulation considers a porous medium composed by solid grains, water and gas. Thermal, hydraulic and mechanical aspects are taken into account, including coupling between them in all possible directions. The problem is defined in a multiphase and multispecies approach. The three phases are solid phase (s), liquid phase (l , water + air dissolved) and gas phase (g , mixture of dry air and water vapour). The three species are solid ($-$), water (w , as liquid or evaporated in the gas phase) and air (a , dry air, as gas or dissolved in the liquid phase). On the other hand the program solves the mass balance equation of solid, water and gas, the momentum balance equation and the internal energy balance equation. At the end, displacements, pore water pressure, pore air pressure and temperature are the degrees of freedom of nodes.

The preliminary analyses developed by this group in the context of the Project were devoted to the understanding of the role of each parameter and geometry in the physical problem. As an example, figure 2 presents two of the geometries considered that were finally accepted for the final simulations. Note that a full 3D geometry may not be adequate when the bentonite buffer is studied in detail. In that case, a simpler geometry is more convenient, as it is possible to increase the number of elements in the barrier. It was shown that according to the geometry considered, the result in terms of temperature may lead to differences up to 100% (i.e., figure 3 presents the temperature evolution of a point on the canister surface for different models using different geometries). Therefore, symmetry assumptions and boundary conditions should be carefully defined to avoid those effects.

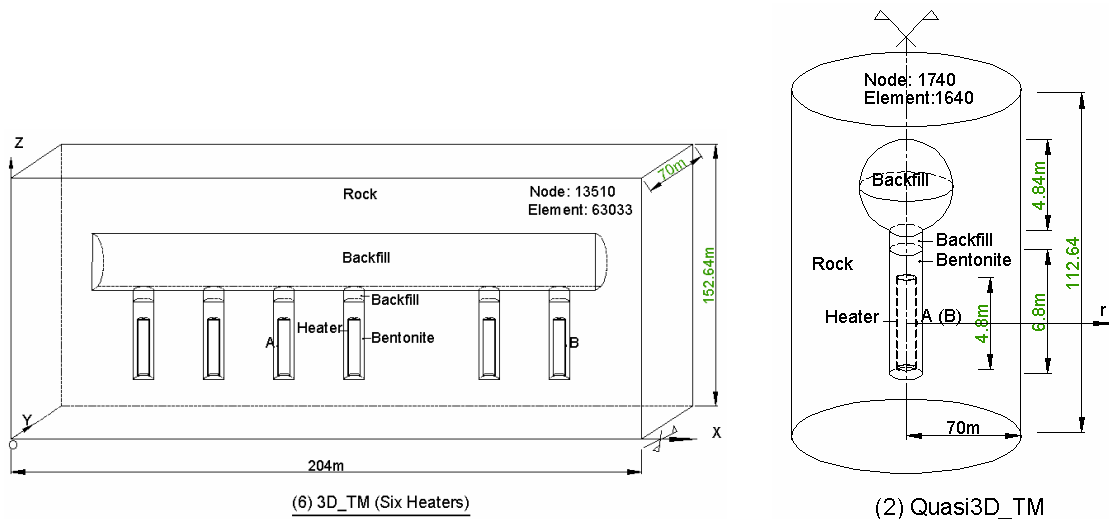


Figure 2. Left: Basic 3D geometry of the experiment used in the models. Right: axisymmetric representation of 1 single deposition hole, used in specific analyses.

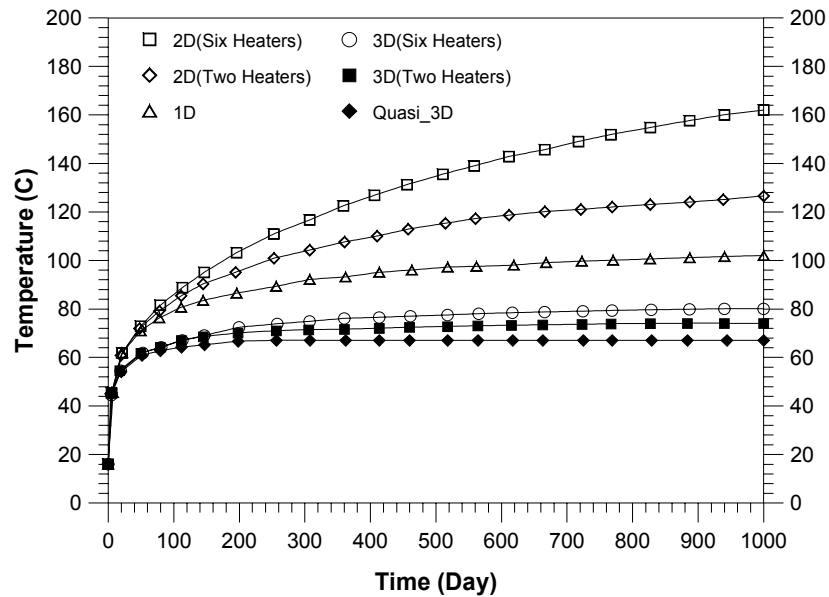


Figure 3. Temperature evolution at canister surface (point A in fig 2) assuming different geometries: 1D, 2D, axisymmetric (Quasi 3D) and 3D. The number of heaters considered depends on each case. Fully 3D and axisymmetric geometries have been used in the final analyses, and they have been presented in figure 2.

Analysis of hole nr. 1

Regarding hole number 1, figure 4 presents the time evolution of temperature and saturation degree for three points of the bentonite: one close to the heater ($r=0.585$ m), one close to the pellets and the rock ($r=0.785$ m) and a central one ($r=0.685$ m). All of them correspond to the mid plane of the heater.

It can be observed that the agreement is, in general, good. Temperature records may be eventually influenced by the installation of the rest of heaters. However, the trends and the temperature values seem to be consistent with measurements. For radius = 0.685 m, that is in the central area of the bentonite ring, there are two measurements available that show some scatter.

Saturation degree evolution has been reproduced reasonably. It should be pointed out that near the heater a wetting-drying cycle is observed, which is typical of coupled processes. The total pressure is presented in figure 5, and it is not reproduced with accuracy, but this is the case quite often due to different reasons, as described in Ledesma and Chen (2003b). One of the main aspects regarding this discrepancy is the existence of a gap between the heater and the bentonite rings. The swelling of the bentonite will eventually close the gap, and only after that point, stresses will be generated in practice. The simulation of this effect may be quite difficult in practice and in this case the mesh was changed after 35 days, when, according to the calculations, the bentonite inner boundary reached the heater.

An important aspect of this analysis is the evidence that initially the deposition hole was wet due to a conductive rock fracture. The initial water content of the gap became a fundamental parameter and had to be obtained by trial and error using the measurements for calibration purposes.

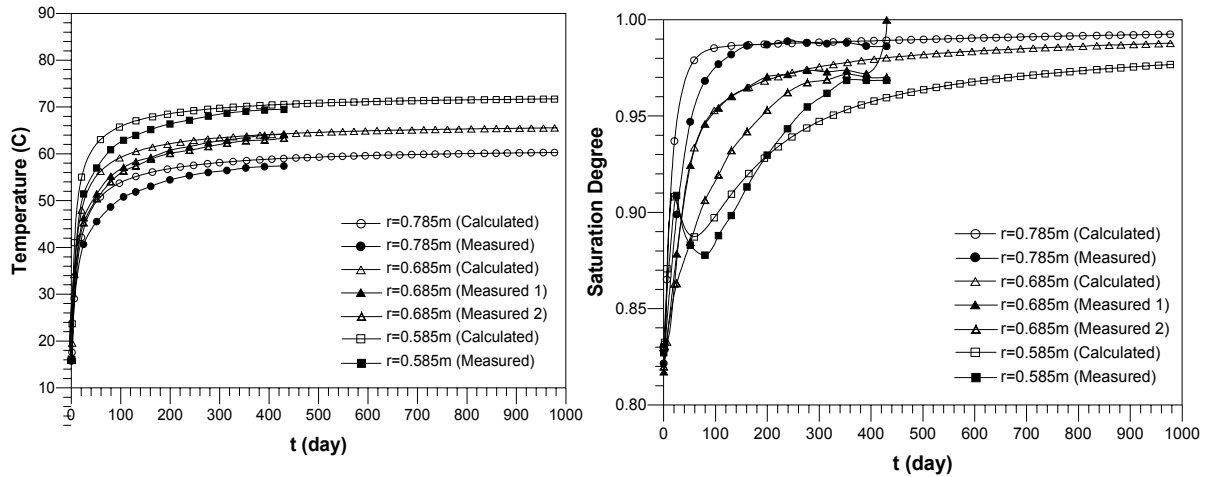


Figure 4. Mid section, hole nr. 1. Measured and computed variables. Left: Temperature. Right: Degree of saturation.

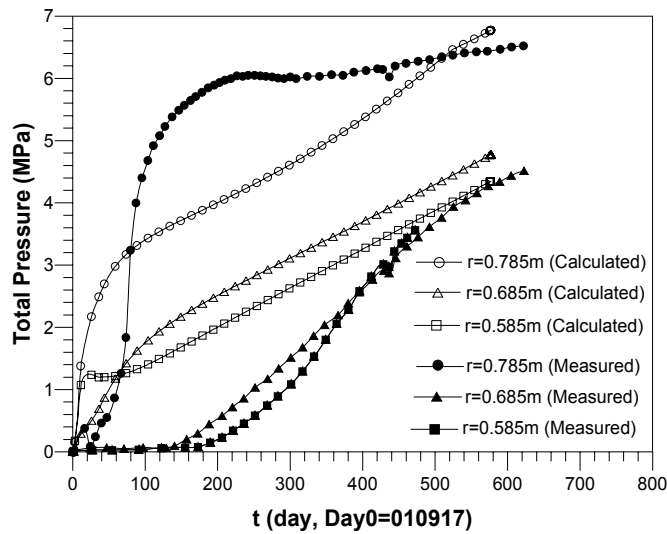


Figure 5. Mid section, hole 1: measured and computed total stresses in the bentonite buffer.

Analysis of hole nr. 3

The analysis of hole 3 is similar from a conceptual point of view than the previous case, except for the initial conditions, because in this case the deposition hole was almost dry. Figure 6 presents for the mid section of hole 3, the evolution of temperature and degree of saturation in the bentonite. Note that due to this effect, the saturation process after the first year of the experiment is very slow, and may be eventually almost negligible.

Figure 7 presents the evolution of total stresses for mid plane of this deposition hole. Note that due to the slow swelling rate of the bentonite, the stresses are still very low. In fact the gap between heater and bentonite seems to be open according to the analyses.

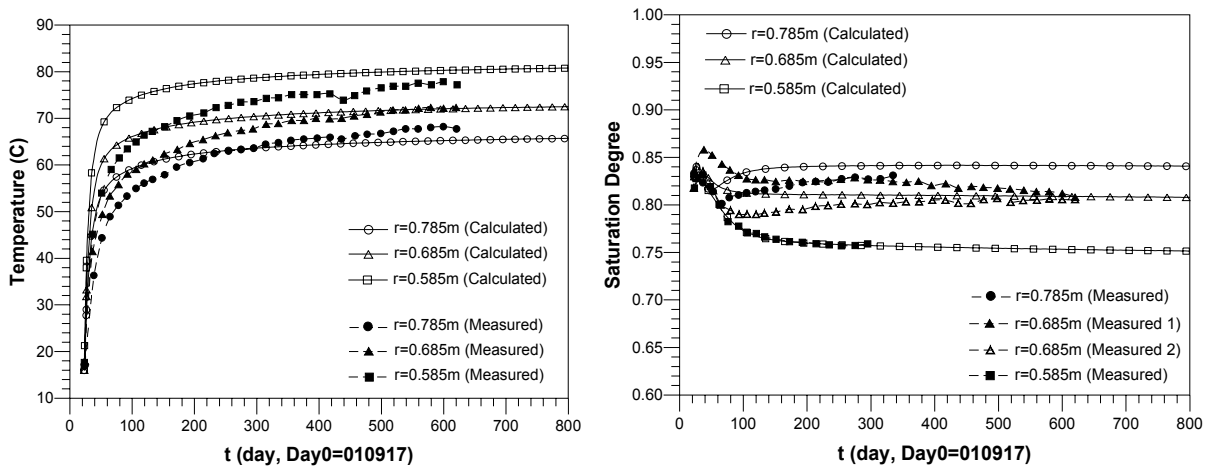


Figure 6. Mid section, hole nr. 3. Measured and computed variables. Left: Temperature. Right: Degree of saturation.

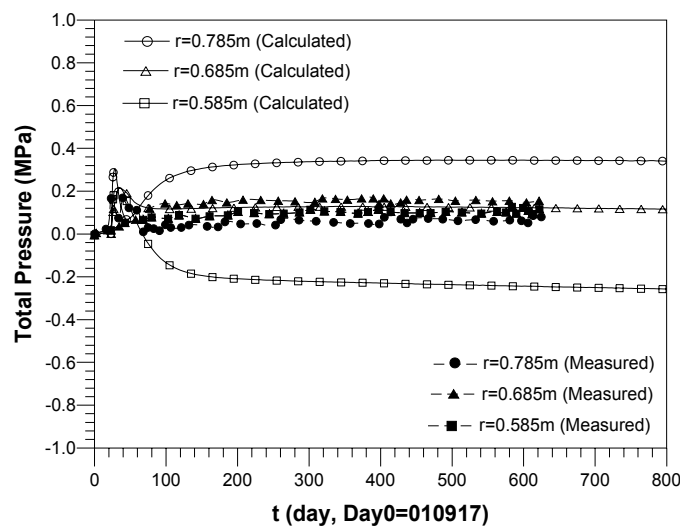


Figure 7. Mid section, hole 3: measured and computed total stresses in the bentonite buffer.

What is left for future developments?

Previous section is a summary of the main results obtained after 3.5 years involved in the Prototype Project. More details (including the parameters used in the analyses) may be found in Ledesma and Chen (2003a,b). From those results one may assume that THM formulations are well developed and that the final simulations have been very successful. Indeed the modelling groups have been able to reproduce the basic measurements in a consistent manner at the end of the Project. However, it should be pointed out that we can not make blind predictions of similar experiments in a real repository without some risk of missing some aspects of the problem. Despite that, the available THM formulations can define quite well the limits of the processes involved. Therefore, there is still room for further developments and some of them are indicated here.

An obvious development is the extension of the THM formulations to THMC (and even THMCB) schemes. This is an ongoing research process and some preliminary results are already available (Gens et al, 2004). However, perhaps this is not the main task to be developed. There are many aspects of the classical THM analyses that require further attention. They are in fact more specific:

a) A basic requirement is to improve our knowledge on the MX-80 bentonite. Some of the parameters involved in the analyses had to be defined by guess. The information is still scarce, and it seems that Äspö rock is better characterized than MX-80 bentonite so far. Laboratory experiments are now in process, but they are very slow and it will take time to improve this aspect. For instance, water retention curve should be obtained for other non-standard conditions (different densities, constant volume, and different temperatures). In addition to that, mechanical information regarding oedometer tests with suction control is not available, and that is important for stress and displacement analyses.

b) Regarding the simulation of the hydration of the bentonite, it seems that this process is well understood, but still some discrepancies between measurements and calculations are detected. Most of them may be superseded if the laboratory information is improved, and water retention plays an important role here. A final aspect that could become important is the effect of the osmotic potential on the flow within the bentonite. This is due to the fact that Äspö water is salty (between 6 to 12 g/l of NaCl and CaCl₂ at 50%/50% approx.) and that may create an osmotic suction that may be important close to saturation. This effect could explain why saturation rate is slower in practice than in the predictive calculations, although further analyses are required. Again, to the author's knowledge, there is not laboratory information about the osmotic properties of MX-80 for the conditions in a repository.

c) With respect to the mechanical problem, it is important to point out that there is still a lot of work to do. Constitutive laws for expansive soils are very complex, and only limited analyses for the Prototype have been attempted by the authors. Laboratory work is again a requirement regarding this aspect. On top of that, gaps and slots may constitute an additional perturbation element when comparing field measurements and calculations. Finite element codes should be able to incorporate those gaps or joints in a more consistent manner.

d) A long term THM analysis has not been performed properly. In general we have tried to reproduce current measurements, but a more long perspective will be eventually required. The extension of the Prototype experiment is an opportunity for continuing with this analysis and for performing that extrapolation.

e) Some of the experiments currently in operation at Äspö involve very high temperatures, above 100°C (i.e. “Temperature Buffer Test”). In general, the codes used so far have been tested for temperatures below that limit, and an additional effort is being performed in order to check the validity of the classical tools for this kind of problem. New developments will be probably incorporated in Code_Bright to deal with this particular aspect.

This list of remaining tasks regarding THM analyses is not intended to be exhaustive. But it indicates that despite the important developments carried out during last 10 years, additional work is still required in this area.

Conclusions

The paper reports some of the THM simulations carried out in the context of the Prototype Repository Project. The comparison between predictions and measured variables indicates that the main processes involved in the experiment have been taken into account. However, there is still room for future development and deeper understanding of the THM problem. In particular some parameters used in the models should be based on additional laboratory experiments. Also, the mechanical aspects need further development, as the comparison between measurements and calculations is not straightforward. Coupling the formulation with the chemical problem has been already performed in some cases, but more experience is required as well. Finally, a long term analysis of the repository should eventually become an issue, and this is in fact an extrapolation of the analyses performed so far. This is in fact one of the most important remaining tasks for the near future.

Acknowledgements

This work has been performed with the support of the European Union through Research Project FIKW-CT-2000-00055. Moreover, the support from ENRESA (Spanish Agency for radioactive waste disposal) and SKB is also gratefully acknowledged.

References

- Gens, A., Ledesma, A., Pusch, R., Börgesson, L., 2004.** THMC Processes in Engineered Barriers : The experience from Febex and Prototype Projects. Euradwaste Conference, Luxembourg, European Commission.
- Goudarzi, R.& Börgesson, L., 2003.** *Prototype Repository. Sensors Data Report (Period)010917-030301). Report n° 5.* Äspö Hard Rock Laboratory, International Progress Report IPR-03-23, SKB Sweden.
- Ledesma, A., Chen, G., 2003a.** T-H-M modelling of the Prototype Repository experiment at Äspö HRL, Sweden. Proc. Geoproc Conference, KTH, Stockholm (Sweden), p. 370-375.
- Ledesma, A., Chen, G., 2003b.** THM modelling of the Prototype Repository Experiment. Comparison with current measurements. Symposium Large Scale Field Tests in Granite. Sitges (Spain), UPC, Barcelona.
- Olivella, S., Gens, A., Carrera, J., Alonso, E.E., 1996.** *Numerical formulation for a simulator (CODE_BRIGTH) for the coupled analysis of saline media.* Engineering Computations, 13, n. 7, p. 87-112
- Pusch R, Svemar C, 2001.** Selection of THMCB models. AEspoe Hard Rock Laboratory. Int. Progr. Report IPR-01-66.
- Svemar, Ch., Pusch, R., 2000.** *Prototype Repository. Project description FIKW-CT-2000-00055.* Äspö Hard Rock Laboratory. International Progress Report, IPR-00-31. SKB, Sweden

4.7 Mechanisms in buffer hydration – are our modelling attempts OK?

Roland Pusch, Geodevelopment AB, Lund, Sweden

Richard Weston, Dept. of Mechanical Engineering, Lund Technical University, Lund, Sweden

Jiri Svoboda, Centre of Exp. Geotechnics, Czech Techn. Univ. in Prague, Czech Republic

Abstract

Current modelling of the rate of water saturation of the buffer clay that surrounds canisters with HLW assumes that suction in the buffer drives in water from the rock, the rate being determined by the transient hydraulic conductivity of the buffer and by the successively dropping suction potential. Microstructural examination suggests that hydration takes place by two parallel mechanisms; migration along particle surfaces from the wet outer boundary and condensation of vapour-transported water from the hot inner part of the buffer. Both processes are of diffusion-type implying that buffer saturation can be described as a quasi-diffusive process as exemplified by the Czech Mock-up test.

Background

Most repository concepts for storing highly radioactive waste make use of dense buffer clay as embedment of the metal waste canisters. The clay is not saturated from start but is wetted by taking up water from the rock. The rate of saturation is of great importance since slow wetting causes salt accumulation and risk of canister corrosion and chemical changes of the buffer. The driving force for saturation is the hydration potential of the unsaturated clay. It causes underpressure of several tens of MPa at low water contents but drops to zero at complete saturation.

Current modelling of the rate of water saturation assumes that suction drives in water from the rock at a rate that is determined by the transient hydraulic conductivity and successively dropping suction potential of the buffer. The present paper describes saturation of buffer clay by considering the diffusive character of the involved processes.

Clay microstructure – unsaturated state

Compaction of bentonite granules brings them into dense layering with voids of varying size. For low densities the voids make up continuous channels with constrictions while the voids are largely isolated in dense clays (Figure 1). Modelling of compaction of clay granules (Figure 2) has given the range of void sizes for densely compacted MX-80 clay in Table 1.

Table 1. Void size distribution in MX-80 with 10 % water content compacted to 1850 kg/m³ dry density (Pusch 2001). The effective porosity (representing voids excepting the interlamellar space) is 15 %.

Percentage of voids smaller than			
50 μm	7.5 μm	3.5 μm	2 μm
100 %	75 %	50 %	25 %

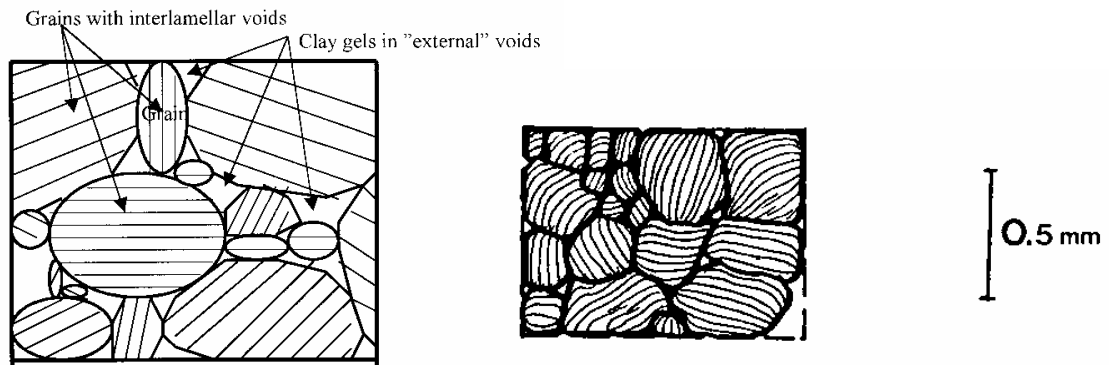


Figure 1. Arrangement of granules in compacted MX-80. Left: low dry density with voids between granules being up to a few hundred μm wide. Right: Dense condition at 100 MPa compaction with voids up to 50 μm . The granules contain numerous small, isolated voids.

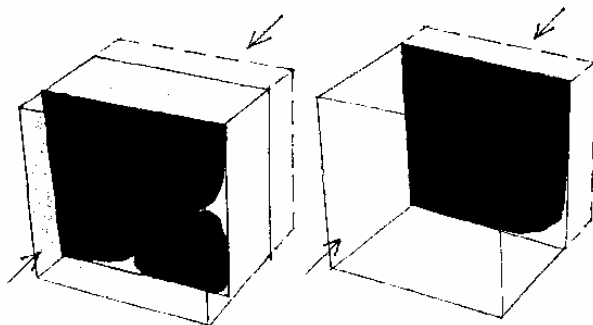


Figure 2. Two sections of cubical element with 175 μm side length of MX-80 granules uniaxially compacted under 100 MPa according to BEM modelling. The intersected voids (white) form tortuous paths with a size ranging from less than 2 μm to about 50 μm .

Clay microstructure – hydration stage

Smectite particles consist of stacks of lamellae that are separated by hydrated cations or positively charged molecules. Their size and charge and interaction with water molecules determine the interlamellar spacing. The number of lamellae is different in Na (3-5) and Ca clays (about 10), (Figure 3). No more than 3 interlamellar hydrate layers can be hosted in most smectites (Kawamura et al, 1999). The amount of adsorbed water is determined by the access to water and the number of interlamellar and extralamellar hydrates is hence a function of the RH at which the clay material is stored (Table 2).

There is a balance between the amount of water sorbed in interlamellar positions and on the outer surfaces of the stacks of lamellae (“external”). Most of the latter type of water is less strongly sorbed than the interlamellar hydrates and is rather easily driven off by heating that causes migration of water molecules from the interlamellar space to external positions until equilibrium between the two phases is reached.

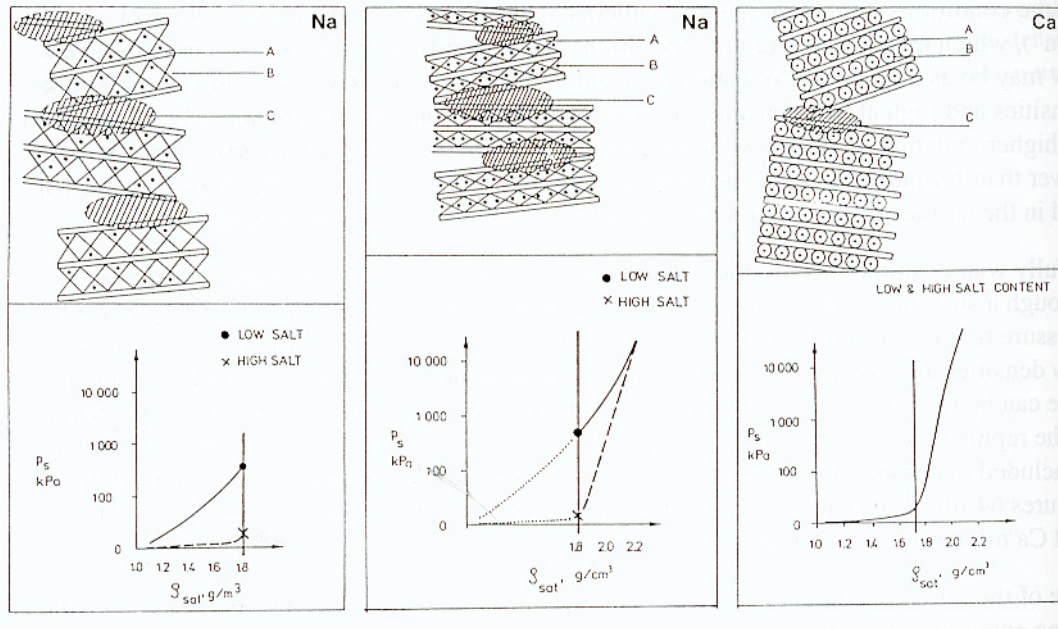


Figure 3. Schematic pictures of stack assemblages and influence of density at water saturation, expressed in g/cm^3 (1 g/cm^3 equals 1000 kg/m^3) and salinity for Na and Ca montmorillonite clay. A) Lamella, B) Interlamellar space, C) Stack contact region with interacting electrical double-layers [Pusch, 1994].

Table 2. Water sorbed on MX-80 powder stored in air of different humidity

RH, %	Water content, %	Number of inter-lamellar hydrates	Number of extralamellar hydrates
10	2	0-1	0-1 sorbed
40	8.5	1	1 sorbed
80	20	1-2	1-2 sorbed
100	25	2-3	2-3 sorbed
Capillary suction of liquid water	>25	2-3	2-3 sorbed, plus weakly bound water molecules, up to 10 layers

Clay microstructure – saturated state

At the end of the hydration period of buffer clay the microstructural constitution is as illustrated by Figure 4, showing a spectrum of void sizes. The heterogeneity is caused by incomplete expansion of the clay granules and contrasts to the homogeneous structure of natural smectite sediments with the same density. By time stress concentrations are relaxed by creep and total equilibrium with respect to the distribution of solids and fluids may take a very long time. This is a major reason for the delay in development of a stable effective pressure state in large-scale experiments.

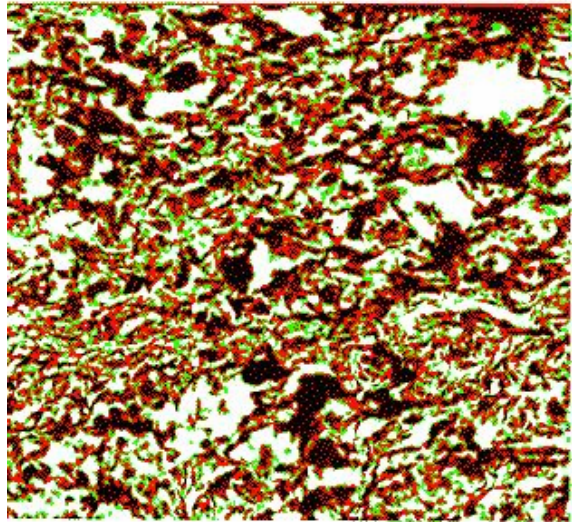


Figure 4. *Digitalized transmission electron micrograph of MX-80 clay with 1800 kg/m^3 at water saturation Black: rock-forming minerals; red: almost impermeable clay matrix; green: soft permeable clay matrix; white: open voids. Side length of the picture is $3 \mu\text{m}$.*

The transient clay microstructure of maturing buffer clay

Impact of porewater salinity on the hydration rate

The electrolyte content of the water that moves in from the rock has a significant impact on the saturation rate according to Table 3. It shows the outcome of 45 day laboratory tests with wetting with salt solutions from one end of 50 mm long cells with MX-80 clay. The temperature at the wet end was 30°C and 100°C at the opposite end. The clay had an initial water content of 10 % and a dry density of 1270 kg/m^3 . Experiments with distilled water give noticeable wetting only to 30 mm distance in this time, hence showing that the microstructure of hydrating clay is affected by the solutes.

Table 3. Water saturation of MX-80 clay samples exposed to a temperature gradient of 14°C/cm and a water pressure of 50 kPa at the cold end for 45 days (Karnland 1995).

Distance from cold end, mm	Water content after 45 days for 3.5 % NaCl solution	Water content after 45 days for 3.5 % CaCl ₂ solution
10	47	45
20	45	41
30	32	38
40	12	33
50	8	28

These effects are explained by colloid chemistry: Thus, Figure 3 demonstrates that Ca causes contraction of the stacks of lamellae yielding larger pore space, and double-layer theories show that coagulation takes place in salt water (Figure 5). They combine to give a higher hydraulic conductivity when clay sorbs Ca-dominated salt water than when electrolyte-poor water is taken up. In the latter case the content of mobile water is lower (Figure 6).

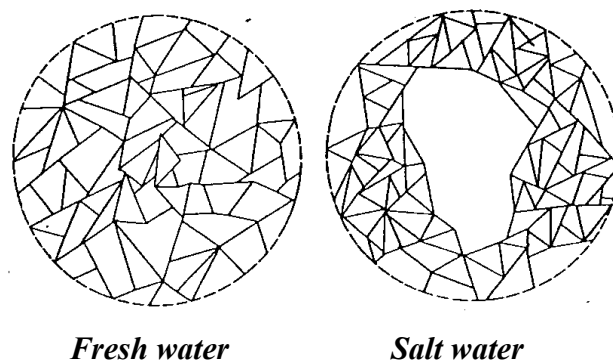


Figure 5. Impact of salinity on the microstructure of clays through coagulation.

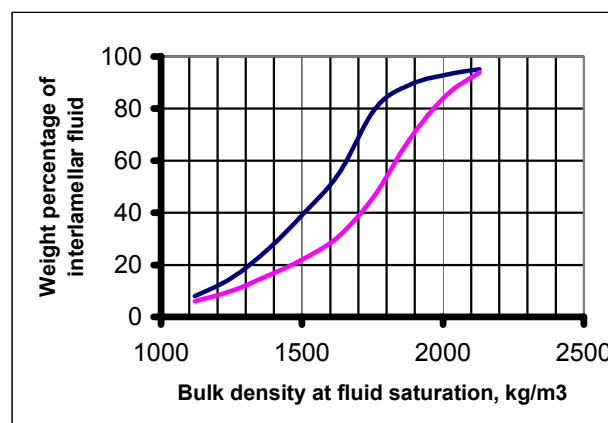


Figure 6. Relative amounts of interlamellar (immobile) water and free, mobile water. The upper curve represents Na MX-80 and the lower MX-80 clay with Ca in exchange positions (Pusch 1994).

Impact of water pressure on the hydration rate

Experiments show that water at a pressure of 0.6 MPa enters dense MX-80 clay with 50 % saturation by a few centimeters in a few minutes and then stops (Pusch 2001). This suggests that continuous systems of larger voids between granules are quickly filled to a certain shallow depth but that expansion of the clay matrix surrounding these channels closes them and prevents further quick penetration of water.

Impact of temperature on the hydration rate

There are two effects of a rise in temperature: 1) the viscosity of water entering the buffer clay is reduced, 2) the hydration potential is affected. The first effect speeds up flow and diffusion and the second involves increase in the d-spacing of smectite when the temperature is raised (Kawamura et al, 1999), which means that the sorption energy drops. Hence, the driving force for hydration of the buffer decreases with increasing distance from the rock.

The hydration process

Major mechanism

The tremendous hydration potential of smectites is the reason for the wetting of buffer clay. There are two regimes: the interlamellar and the extralamellar space, representing different conditions.

Mineral surfaces exposed in voids carry electrical double-layers, representing the *osmotic* potential, while the interlamellar space has the highest hydration potential (*matric* potential). Water entering dry clay is first sorbed on “external” surfaces from which it migrates into the interlamellar space causing expansion.

The *matric* potential is extreme: 200 MPa pressure is required to squeeze out the last monolayer but drops to zero for fully expanded clay, corresponding to hydrates in Ca clay and 3 layers in Na clay. The *osmotic* potential is lower but is noticeable even at several tens of hydrate layers. One can not distinguish between the two potentials by measurement for water contents lower than 30-40 %. Above this interval the osmotic potential rules alone.

Interaction of microstructure and water migration under closed conditions

Figure 7 illustrates the presence and migration of water on the microstructural scale. The upper picture represents isothermal conditions of buffer before water is sorbed with a system of interconnected voids forming channels with constrictions representing contacts between compressed granules. The lower picture illustrates the conditions when the canister produces heat but no water is yet taken up from the rock.

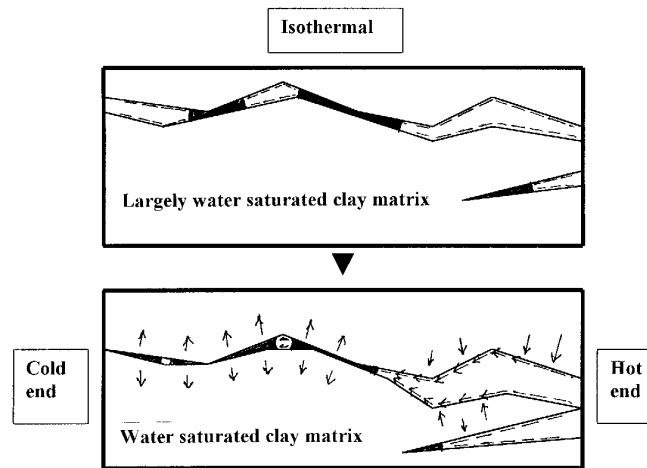


Figure 7. Schematic drawing of porewater migration and associated microstructural changes in buffer clay. Upper: Initial isothermal state with largely water-saturated clay matrix and systems of isolated voids forming channels that is water-filled at the constrictions (granule contacts). Lower: State with thermal gradient. Movement of water from the clay matrix to the channels in the drying zone causing widening of the channels and water migration towards the cold end by film transport and vapour flow.

Water that is initially sorbed on the external surfaces of the stacks of lamellae in the drying part of the buffer is vapourized and starts moving in gaseous form towards the colder parts of continuous channels, where the vapour pressure is lower and condensation hence takes place. Furthermore, the lower sorption energy of the hotter clay causes surface diffusion – film transport - along the channels towards the cold end and accumulation at their water-filled ends. From this local “over-saturated” zone the surrounding drier clay matrix sucks water and expands. The heat-related difference in sorption potential prevails also in all the isolated voids across which there is a gradient in temperature and hence in sorbed water, causing migration to the cold ends until equilibrium is reached between the amounts of interlamellar and extralamellar water. The migration mechanism is film transport by surface diffusion along the void boundaries and a second type of diffusive transport from the external water hulls to the interlamellar space. The redistribution of water is associated with microstructural strain of creep-type, which is more or less of log-time type and hence diffusion-like (Pusch 1994).

The migration of water is not a flow phenomenon and not controlled by the hydraulic conductivity. Instead, the transport is diffusive of at least two different types determining the time required for reaching equilibrium.

Interaction of microstructure and water migration under “wet” conditions

With access to non-pressurized water at the cold end water migration takes place both from the drying end as in Figure 7 and from the cold boundary. Wetting from the cold side causes film transport by surface-diffusion of water molecules along the walls of channels and isolated voids with the difference in sorption energy, or simply the gradient in water concentration, as driving force. Like in the earlier case there is first an increase in the content of “external” water at the cold end of the voids and concomitant diffusion of water molecules from there into the adjacent drier clay matrix. In comparison with the buffer near the canister the thermal gradient will be lower in the outermost buffer but it will still have some effect, i.e. to drive water from the hotter part. This will retard the wetting from the cold side where the sorption potential is highest but the effect is believed to be small although of some importance when the wetting has proceeded significantly towards the hot side.

For the case of pressurized water at the cold side the conditions are somewhat different. Water will be quickly pressed into the largest open channels, especially at high electrolyte contents, but the clay matrix will suck water from them to form firstly “external” and subsequently interlamellar water in the thereby expanding clay matrix and slow down further penetration. The rate of wetting for this case is partly controlled by the hydraulic conductivity of the largely water-saturated outer part of the buffer. Hence, for the case with high water pressure both flow and diffusion determine the wetting rate.

Examples

The Czech Mock-up experiment will be taken here as an example of interpreting the wetting process. In the KBS-3-type test arrangement a steel tube with 0.8 m diameter contains a circumferential filter and RMN smectite-rich buffer blocks of 85 % smectite, 10 % quartz and 5% graphite, the dry density being 1700 kg/m^3 and the water content 10 %. The heater temperature is maintained at 95°C . Clay powder is in the 50 mm gap between the filter and the blocks. The test program implies closed conditions for 5 months, and subsequent water uptake under 60 kPa pressure. After 2.5 years a gas experiment is planned.

Figure 8 shows the actual and predicted degree of water saturation after 0.75 years. The predicted wetting was based on a diffusion coefficient of $2\text{E-}9 \text{ m}^2/\text{s}$ and agrees very well with the recordings.

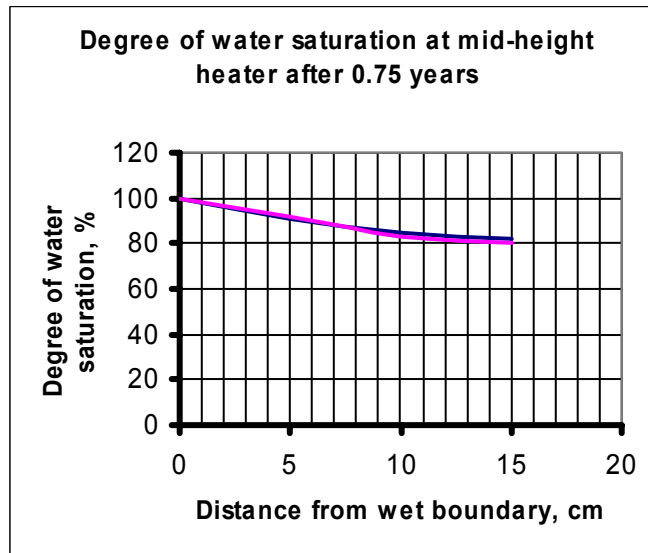


Figure 8. Evaluated degree of water saturation at mid-height heater 0.75 years after the start of wetting. The black curve represents analyses of extracted samples and the violet predicted values assuming the hydration to be diffusion with $D=2E-9 \text{ m}^2/\text{s}$.

For the level just below the heater the agreement is equally good as demonstrated by the recorded degree of saturation in Figure 9 and the predicted evolution in Figure 10.

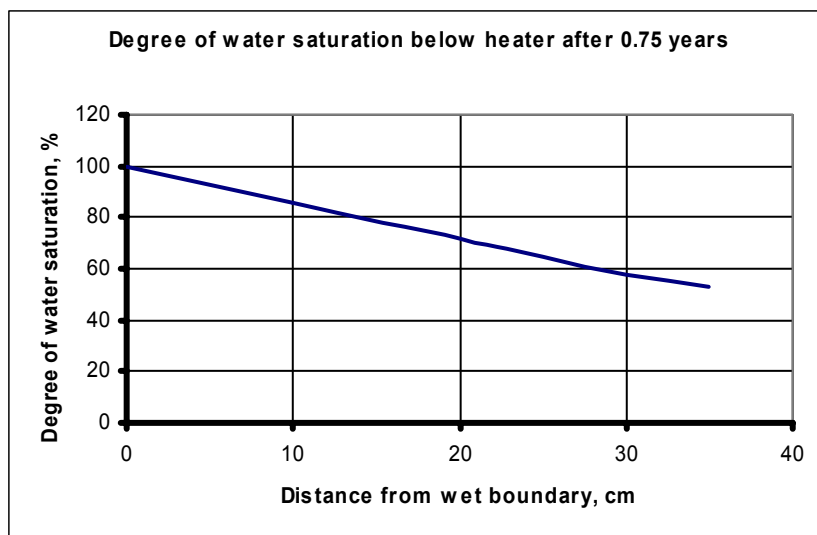


Figure 9. Actual degree of water saturation 25 cm below the center of the base of the heater after 0.75 years as evaluated from extracted samples.

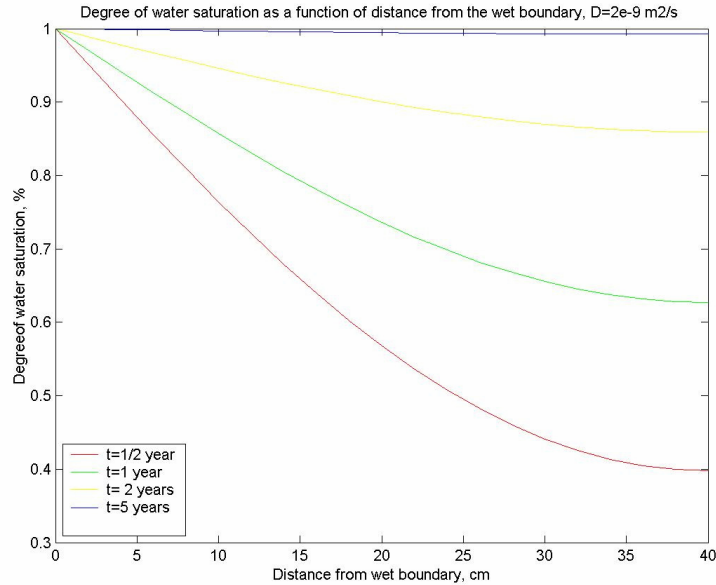


Figure 11. Predicted water saturation by diffusion for $D=2E-9$ m²/s saturation 25 cm below the heater. After 0.75 y the degree of saturation below the center is 50 % (R.Weston).

Conclusions

- While the common buffer hydration models take flow as the main transport mechanism we believe that diffusive transport dominates. This concept is physically most relevant.
- The agreement between the actual and theoretically calculated wetting rates is striking and shows that diffusion theory can be used for prediction of the wetting. Although the true hydration process is believed to involve at least two diffusion-controlled mechanisms and be very complex because of structural reorganization, a generalized quasi-diffusive model with only one diffusion coefficient appears to apply. Estimates show that the diffusion coefficient depends on the density and smectite content (Börgesson, 1985)
- The fact that the temperature gradient was 2.1°C/cm at mid-height heater and only 0.2 °C/cm below the heater in the Czech Mock-up test indicates that the temperature and temperature gradient have no significant impact on the water distribution rate.

References

Börgesson L, 1985. Water flow and swelling pressure in non-saturated bentonite-based clay barriers. *Engineering Geology*, Vol.21 (pp.229-237).

Karnland O,1995. Salt redistribution and enrichment in compacted bentonite exposed to a thermal gradient. *SKB Arb. Rapp.* 95-31.

Kawamura K, Ichikawa Y, Nakano M, Kitayama K, Kawamura H, 1999. Swelling properties of smectite up to 90°C. In situ X-ray diffraction experiments and molecular dynamic simulations. *Engineering Geology* Vol. 54 (pp.75-79).

Pusch R, 1994. *Waste Disposal in Rock, Developments in Geotechnical Engineering*, 76. Elsevier Publ. Co, ISBN: 0-444-89449-7.

Pusch R, 2001. Can the water content of highly compacted bentonite be increased by applying a high water pressure?. *SKB Technical Report TR-01-033*. SKB, Stockholm.

4.8 Proposal of an alternative re-saturation model for bentonite buffers - the conceptual model, the numerical model and the data base

Contribution to the
MEETING ON BUFFER & BACKFILL MODELLING IN LUND 2004
Klaus-Peter Kröhn, GRS Braunschweig, Germany

Introduction

This paper presents results of a project of GRS which was concluded in autumn 2003 (Kröhn, 2004a). The project aimed at a simplified re-saturation model for application in the framework of long-term safety analyses. Looking into the concepts and equations of the already established THM-codes revealed some deficiencies in their hydraulic part (Kröhn, 2003) which triggered

- some own considerations of the microstructure of bentonite and processes occurring on this observation level during re-saturation
- the development of a macroscopic model of re-saturation including
- conceptual model
- equations
- code development
- laboratory experiments to constitute a data base for testing re-saturation codes

Emphasis in this paper is laid on three points which coincide thematically with first three sessions of the meeting (in reverse order):

- results of re-saturation experiments with Äspö-solution and with saturated water vapour using compacted MX-80 bentonite
- description and test of a new numerical vapour diffusion model
- conclusions and description of an alternative conceptual model that explains re-saturation mainly by vapour diffusion in the pore space

At the moment these results refer to re-saturation at ambient conditions meaning room temperature and atmospheric pressure. A final chapter will summarize the work that is considered necessary to confirm the new model for conditions in an underground repository for radioactive waste.

Laboratory data

Experimental equipment and measuring procedure

Air-dry MX-80 bentonite with an initial water content of about 10% was filled into cylindrical steel cells illustrated in Fig. 4.1. The specimen had a length of 10 cm and a diameter of 5 cm. The bentonite was compacted layer wise in order to minimize density changes due to wall friction and the resulting initial average dry density was about 1500 kg/m^3 . In order to mirror the conditions at the Äspö Hard Rock laboratory the bentonite was saturated with water from the Baltic Sea. Starting in a burette the Äspö solution flowed with minimal hydraulic pressure through a flexible tube into the cylinder where it was distributed by means of a system of circular and radial grooves on the surface of the locking solid cylinder and a frit. Thus a uniform and continuous water supply over the front plane of the cylindrical bentonite specimen was achieved which allows to describe the water uptake as a one-dimensional process. The interface between frit and bentonite is called “inlet” further on. The amount of water drawn into the bentonite was measured over time using the burette. Water uptake took place under a constant temperature of $20 \text{ }^\circ\text{C}$.

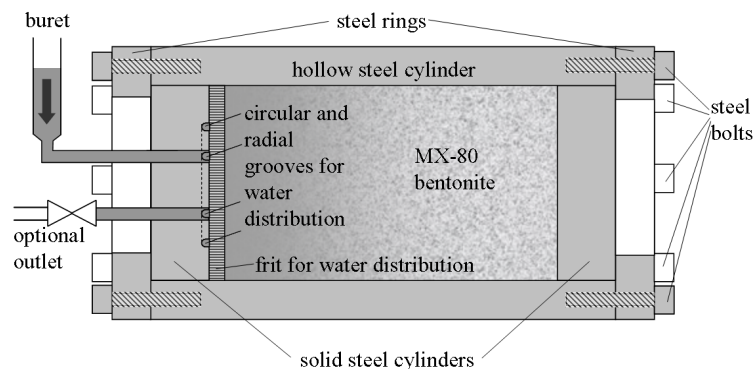


Fig. 4.1 Principal sketch of the measuring cell

After a predefined period of time the water-carrying tube to the measuring cell was disconnected. The cell was opened and the bentonite specimen was pushed out of the cell. During this process bentonite slices with a thickness of a few millimetres were cut off. The thickness of each slice was measured before cutting. The slices were weighed, dried 24 hours at a temperature of $105 \text{ }^\circ\text{C}$ and weighed again in order to assess the mean water content and the mean dry density. These values were assigned to the midpoint of the respective slice for the graphical representation of the data.

Each individual uptake test yields one profile for a specific time period. In order to check the accuracy of the measuring procedure most tests were repeated. The agreement of corresponding test results was notably satisfying. The longest test period was about half a year.

Uptake experiment with water vapour

A second series of uptake tests was performed in which the measuring cells described above were used to investigate the dynamics of uptake of water vapour. Five cells, five gas washing bottles and a pump were coupled in a series connection with flexible tubes constituting a closed gas circuit with highly vapour saturated air as illustrated in Fig. 4.2. The test procedure as well as the duration of each individual test corresponded to the experiment with Äspö-solution.

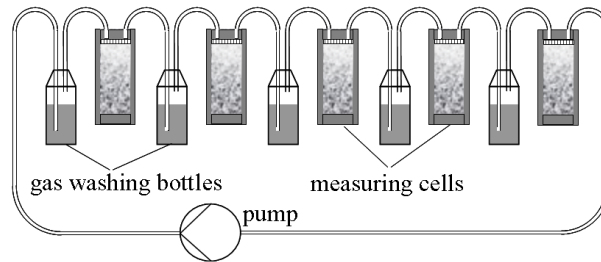


Fig. 4.2 Connection diagram of the measuring cells for the vapour uptake tests

Vapour diffusion model

Processes considered

The main water transport mechanism in the new vapour diffusion model is assumed to be the diffusion of water vapour in air. The flow rate of water between the pore space and the interlamellar space, called “hydration rate” further on is assumed to be finite and to depend on the differences of the chemical potential of pore water and hydrated water. The corresponding decrease of porosity is considered in the model as well.

Balance equation

The case of water flow in an unsaturated bentonite can be regarded as a flow in a porous medium with a locally varying porosity Φ and a locally varying sink r for the water. In the vapour diffusion model the porosity is assumed to be a function of the water content which is calculated separately integrating the local hydration rates over time. While the porosity and the vapour partial density ρ are variables in time and space the coefficient D for binary gas diffusion is a constant under the isothermal conditions that are considered here. For the sake of simplicity the tortuosity τ is assumed to be constant as well. The resulting mass balance equation for the vapour in the pore space reads:

$\frac{\partial(\Phi\rho)}{\partial t} - \tau D \frac{\partial}{\partial x} \left(\Phi \frac{\partial \rho}{\partial x} \right) = r$	(4.1)
---	-------

Quantification of the sink term mainly requires the calculation of the local hydration rate. This has been done in detail by (Kröhn, 2004a,b) using the following assumptions:

- the local hydration rate is a linear function of the difference between the chemical potential ψ_p of the water vapour in the pore space and the chemical potential ψ_i of the interlamellar water,
- the adsorption isotherm for MX-80 is a linear function, and
- the diffusion coefficient as well as the tortuosity are constants.

Comparison of experimental and modelling results

Fig. 4.3 shows that the time dependent moisture distribution in the experiments for uptake of water vapour could be reproduced to a certain extent with the vapour diffusion model. The amount of hydrated water as well as the trend of the distributions coincides well with the measured data. Only the uptake dynamic seems to be somewhat off. Considering that the vapour diffusion model at the present stage incorporates several simplifications the agreement is satisfying.

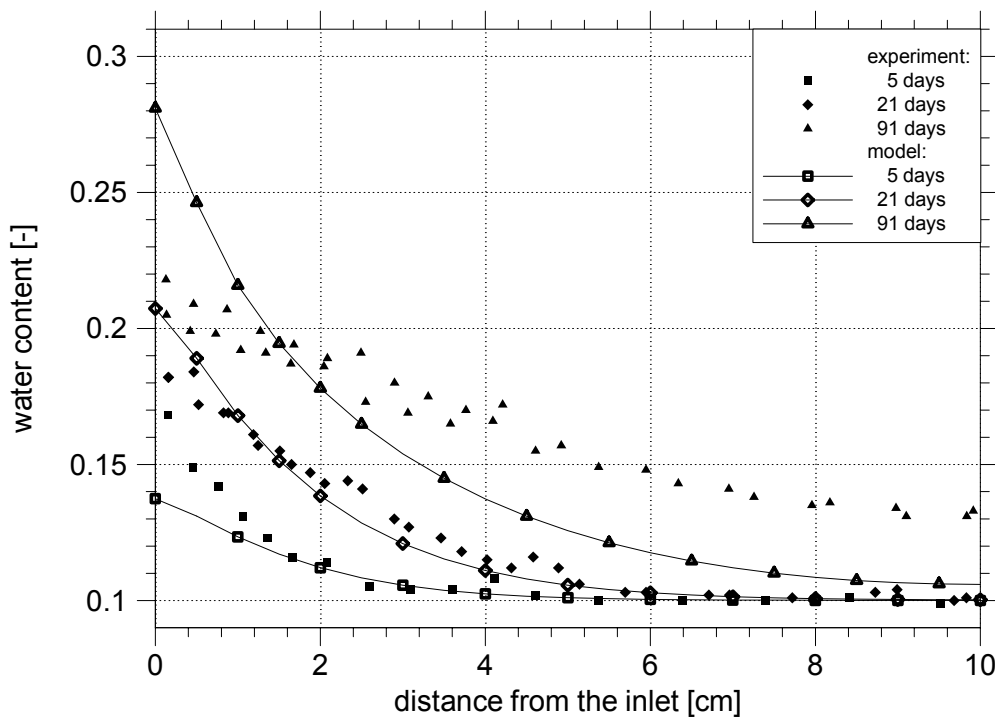


Fig. 4.3 Water content as a function of penetration depth; re-saturation with water vapour; from (Kröhn, 2004b)

Alternative conceptual model

Interesting conclusions can be drawn from a comparison of the results of the vapour diffusion model with the data from the uptake experiment with liquid water as illustrated in Fig. 5. It shows that about one half of the hydrated water can be explained by means of binary gas diffusion. This means at least that a considerable part of the water uptake is due to vapour diffusion. Assuming for instance that vapour diffusion fades to Knudsen-diffusion in an advanced stage of saturation the bentonite saturation could be explained exclusively by vapour flow due to an increased diffusion coefficient.

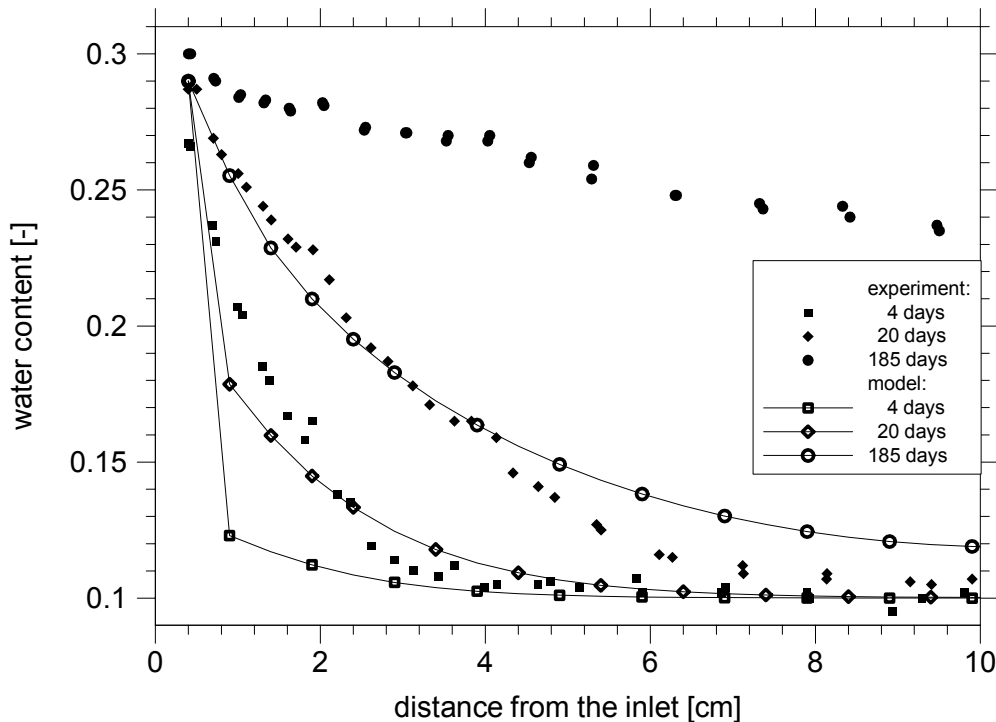


Fig. 4.4 Water content as a function of penetration depth; re-saturation with liquid water; from (Kröhn, 2004b)

Based on these results the following alternative to the conventional two-phase flow approach for bentonite re-saturation appears to be reasonable in which a main phase is preceded by a pre-stage and possibly followed by an abandonment stage:

The pre-stage begins with the contact of water with the bentonite. In a short period of time water is sucked into the pore space rather fast, mainly by capillary forces. With the liquid water present in the pore space hydration kicks in. The reduction of pore space caused by the swelling of the minerals goes in hand with a dramatic reduction of permeability. Since uptake of liquid water by clay minerals is a fast process, too (Pusch and Yong, 2003), water penetrates very little into the bentonite before further water inflow is hindered very effectively due to the low permeability. This view is supported by the experimental evidence of (Kröhn, 2004a) which shows exclusively for the slice adjacent to the inlet unproportionally high water content and a particularly low dry density.

Parallel to the uptake of liquid water evaporation takes place in the pore space at the interface of the fluid and the gas phase. This becomes significant when the influx of liquid water is low after the first stage because progress of the water/air-interface in the pore space is slowed down even further by this process. A rough estimation of the flux densities at the end of the first stage shows that the supply of liquid water through the narrow, already saturated zone equals the following vapour flow further into the bentonite (Kröhn, 2004a). Thus the saturation with liquid water is temporarily limited to the wetted bentonite surface. The measurements of (Pusch and Kasbohm, 2002) indicate that the stage of capillary water uptake takes time on the order of minutes rather than hours or even days.

The main stage is a phase in which no two-phase flow occurs at all. All the water entering during this stage evaporates at the established interface between liquid water and air. Water transport further into the bentonite takes place only by means of vapour diffusion in the gas phase. The low density of the vapour is here compensated by the high process velocity of the gas diffusion. The effectiveness of this process has been demonstrated with the help of the vapour diffusion model in chapter 0.

During the second stage the vapour flux at the water/air-interface decreases as the gradient of the relative humidity decreases. Concurrently the water vapour increases the amount of hydrated water next to the interface. This reduces the suction and thus the liquid water flow through the thin saturated zone at the inlet. It is therefore quite probable that the water/air-interface move very little for quite some time.

In the *abandonment stage* two-phase flow could commence again when the vapour flux eventually drops below the likewise decreasing liquid water flux. But by then the suction forces would have been reduced considerably due to re-saturation via water vapour. Additionally, the permeability would be very low in an advanced stage of re-saturation. The significance of this third stage is therefore not clear at the moment.

Final note: this model is consistent with a statement in (JNC, 1999) where it is indicated that water movement in the pore space at low water contents is dominated by vapour transport while transport of liquid water is predominant at high water content. Unfortunately, the primary literature is in Japanese so the background of this remark could not be checked.

Future work

The main problem of the identification of the relevant transport processes from experiments lies in the fact that it is still hardly possible to measure pore water and hydrated water separately. One way to tackle this problem is to investigate the re-saturation via water vapour more closely because it is not influenced by uptake of the liquid phase. As soon as this process is understood, the impact on re-saturation with liquid water can be identified. Since very little is known about the dynamics of vapour uptake especially at increased temperature and increased pressure referring investigations are needed, too.

Acknowledgement

This paper is based on work funded by the German Federal Ministry of Economics and Labour (BMWA) under the contract no. 02 E 9430.

References

- Japan Nuclear Cycle Development Institute JNC:** H12 Project to Establish Technical Basis for HLW Disposal in Japan, Supporting Report 2, Repository Design and Engineering Technology. JNC-Bericht JNC TN1 400 99-012, Draft, May 1999.
- Kröhn, K.-P.:** New conceptual models for the resaturation of bentonite. Proceedings of the Workshop on "Clay Microstructure and its Importance to Soil Behaviour" held in Lund, 2002, Applied Clay Science, Vol. 23, 2003.
- Kröhn, K.-P.:** Modelling the re-saturation of bentonite in final repositories in crystalline rock. Final report of the BMWA-project 02 E 9430, GRS-report (in preparation), 2004a.
- Kröhn, K.-P.:** Results and interpretation of bentonite resaturation experiments with liquid water and water vapour. Proceedings of the International conference on unsaturated soils in Weimar 2003 (accepted for publication), 2004b.
- Pusch, R., Kasbohm, J.:** Can the Water Content of Highly Compacted Bentonite be Increased by Applying a High Water Pressure? SKB, Technical Report 01-33, 2001.
- Pusch, R., Yong, R.:** Water saturation and retention of hydrophilic clay buffer - microstructural aspects. Proceedings of the Workshop on "Clay Microstructure and its Importance to Soil Behaviour" held in Lund, Applied Clay Science, Vol. 23, 2003.

4.9 Prediction of geochemical changes in the Prototype Repository tunnel backfill

By Ari Luukkonen, VTT Building and Transport, Espoo, Finland

Abstract

The study deals with geochemical changes during the wetting of tunnel backfill, and the time-dependent changes at the tunnel boundaries of a repository engineered barrier system (EBS). The tunnel volume is divided to uniform subsequent reaction cells. There is no quantitative coupling to hydrological flow, but the modelling assumes instant full saturation of a cell volume as soon as infiltrating water first time enters the studied cell. The calculations are batch reaction oriented, and follow the equilibrium thermodynamic assumption. A water parcel introduced into a reaction cell is expected to stay within the cell until liquid and solid phases are fully equilibrated.

The tunnel backfill is assumed to consist of sodium bentonite (30%), and crushed Äspö diorite (70%) components. The backfill composition has been estimated in accordance with mineral quantities present in the components of the backfill mixture. The initial groundwater sucked into the EBS at the repository boundaries is Na-Ca-(HCO₃)-SO₄-Cl-water having a reference to brackish seawater origin.

The reactions considered are cation exchange, surface complexation, and dissolution/precipitation of certain minerals. As an initial condition, the undersaturated pore volumes of backfill contain entrapped air. The speciation and dissolution/precipitation equilibria are considered at 40°C.

Introduction

Temperature in the tunnel backfill is expected to stay below 40–50°C during the execution of experiment (King et al., 2001; Pusch & Börgesson, 2001). The first wetted cell volumes of backfill are created at the tunnel boundaries. These porewaters are sucked deeper into the undersaturated cell volumes of backfill, and represent the first wetting of the tunnel EBS. At the same time, new porewater compositions are repeatedly generated at the EBS boundary. The equilibrium modelling illustrates how the geochemistry evolves in the EBS interior and boundaries as a function of batch reaction cycles.

Tunnel backfill properties

The tunnel backfill consist of 30% bentonite mixed with 70% crushed Tunnel Boring Machine (TBM) muck. Based on Börgesson & Hernelind (1999) an initial compacted backfill cell with a 1-dm³ pore volume contains 0.58 dm³ of water and 0.42 dm³ of air in its pores. When this cell saturates with external water, the gas phase is assumed to disappear. The initial 0.42-dm³ volume of air in a compacted cell gives a 6.56-dm³ volume, and a weight of 11.48 kg, of water and backfill. The weight of backfill is 10.90 kg.

The composition of TBM-muck can be estimated based on Patel et al. (1997). Äspö diorite contains frequently narrow fracture and broader hydrothermal alteration zones. These increases the amount of secondary minerals (e.g. goethite, calcite, and quartz) compared to the fresh rock composition. There are several tabulations available on the composition of MX-80 bentonite (e.g. Bruno et al. 1999; Bradbury & Baeyens 2003). The cation exchange capacity (CEC) for bentonite is around 787 meq/kg (Bradbury & Baeyens, 2003). The specific surface area in MX-80 bentonite available for surface complexation is around 31.5 m²/g (Wieland et al., 1994; Bradbury & Baeyens, 2002). For the current purposes, the judged relevant mineral quantities for backfill and its components are presented in Table 1.

The CEC of TBM muck is at the most 5-10% of the CEC of bentonite. Therefore, in a 70/30 mixture, bentonite is still mostly responsible (more than 80%) of the exchange properties of the backfill. Currently, the cation exchange properties and surface geochemistry of backfill are based on the bentonite fraction only. The amounts of potentially reactive species in the 10.90 kg of backfill are presented in the last column of Table 1.

Geochemical reactions

The fractures of the near-field bedrock feed external water into EBS. The external water used in the calculations is a salinity median of the samplings March '98 – June '99 (Andersson & Säfvestad, 2000) from the near field of the Prototype repository drift. The concentrations in water are shown in Table 2.

The first intrusion of external water into a cell volume differs from all subsequent cycles. An undersaturated backfill cell contains 3.3 mmol O₂ and 0.006 mmol CO₂. Oxygen is consumed during the first batch cycle (dissolution of pyrite) and CO₂ gas is available, if needed for further reactions. The modelling tries to take into account both cation exchange and surface complexation. The constants for equilibria are presented in Table 3. The surface complexation follows a mechanistic approach presented by Bradbury & Baeyens (2002). The pH dependent surface processes affect to surface charges of solids and charge balances in solutions.

The calculations equilibrate the porewater compositions to following solids: calcite, gypsum, halite, quartz, pyrite and goethite (cf. Muurinen & Lehikoinen, 1999; Bruno et al., 1999). Concentrations of these solids in the initial backfill cells are presented in Table 1.

Calculations attempt to take into account the effect of elevated temperature (40°C). With the current knowledge, temperature dependencies are available for gas-phase and aqueous speciation calculations, and for dissolution/precipitation reactions of calcite, gypsum, quartz and pyrite (Parkhurst & Appelo, 1999). However, the cation exchange and surface reactions (Table 3), and goethite precipitation are estimated with equilibrium constants defined at 25°C only.

Table 1. Reactive solids of the tunnel backfill in the modelling calculations.

	Unit wt g/mol	TBM-muck mol/kg	Bentonite mol/kg	70/30 Backfill mol/kg	70/30 Backfill mol/(1dm ³ water)
Quartz	60.1	2.19	1.66	2.03	22.2
Pyrite	120	0.03	0.03	0.03	0.30
Goethite	88.9	0.07	-	0.05	0.57
Calcite	100	0.04	0.14	0.07	0.77
Gypsum	136	-	0.02	0.01	0.08
Halite	58.4	-	1.35e-3	4.05e-4	4.41e-3
Cation occupancies in the exchange sites					
Ca ²⁺			0.13	0.04	0.43
Mg ²⁺			0.08	0.02	0.26
Na ⁺			0.67	0.20	2.18
K ⁺			0.01	0.00	0.04
Surface site capacities					
≡S ^{w1} OH			0.04	0.01	0.14
≡S ^{w2} OH			0.04	0.01	0.13

Table 2. The main composition of sample KA3542G02/2587 (Andersson & Säfvestad, 2000). The pe value is estimated. All concentrations are in mg/l except pH and pe values.

pH	7.4	pe	-3.0
Na ⁺	1620	HCO ₃ ⁻	188
K ⁺	9.5	Cl ⁻	3890
Ca ²⁺	624	SO ₄ ²⁻	296
Mg ²⁺	79.4	HS ⁻	0.0
Fe ²⁺	0.23		
Si ⁴⁺	7.8		

Table 3. Exchange and surface parameters for the thermodynamic models considered

Parameter	Reaction	Value
<i>Cation exchange</i> ^(a)		
logK	Ca ²⁺ + 2NaX ⇌ CaX ₂ + 2Na ⁺	0.41
logK	Mg ²⁺ + 2NaX ⇌ MgX ₂ + 2Na ⁺	0.34
logK	K ⁺ + NaX ⇌ KX + Na ⁺	0.60
<i>Surface complexation</i> ^(b)		
logK	≡S ^{w1} OH + H ⁺ ⇌ ≡S ^{w1} OH ₂ ⁺	4.5
logK	≡S ^{w1} OH ⇌ ≡S ^{w1} O ⁻ + H ⁺	-7.9
logK	≡S ^{w2} OH + H ⁺ ⇌ ≡S ^{w2} OH ₂ ⁺	6.0
logK	≡S ^{w2} OH ⇌ ≡S ^{w2} O ⁻ + H ⁺	-10.5

^{a)}According to Wersin (2003), Gaines-Thomas convention.

^{b)}According to Bradbury & Baeyens (2002)

Modelling approaches

In the backfill interior case (Fig. 1a), porewater parcels are transported through successive backfill cells. The calculation starts from the EBS boundary. The system is equilibrated and then porewater is transported into a next undersaturated material cell deeper in the EBS. In the repeated process, porewater equilibrates with successive cell volumes, and approach attempts to simulate the first wetting of the EBS.

In the backfill boundary studies (Fig. 1b), the calculations consider porewater and solid phase evolution in one cell at the EBS boundary. Repeated parcels of external water fill the pore spaces of an edge-cell volume. At start of modelling, the first parcel of external water fills the undersaturated cell. After the first cycle, next refills occur into the saturated cell. The porewaters created in successive cycles are sent deeper into the EBS.

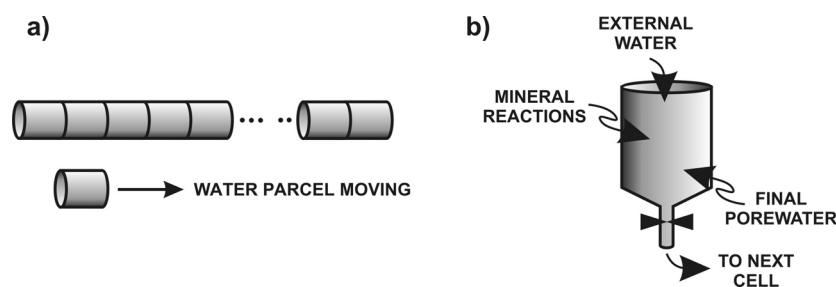


Figure 1. Illustration of the modelling methods for backfill interior (a), and boundary (b).

Modelling results

Backfill interior

The backfill interior diagrams (Fig. 2) illustrate how porewater composition and solids evolve as wetting front advances as a function of cell number. The initial water (Table 2) and the initial amounts of solids (Table 1) are shown on the left borders of diagrams.

Oxygen gas in each undersaturated cell is consumed with pyrite dissolution. The pyrite dissolution stabilises to a constant level causing as well the stabilisation of pe and pH. Significant part of the Fe input is removed from porewater with goethite precipitation. The first cells indicate distinct dissolution of gypsum. Dissolution increases SO_4^{2-} concentrations in water to the level of gypsum saturation. Later, cells precipitate small amounts of gypsum. The input of CO_2 during the first reaction cycles causes an increase in alkalinity of porewater. All cells dissolve small amounts of calcite. However, significant amount of CO_2 does not stay in water but speciates in the gas phase.

There is a slight increasing trend among major cations due to dissolution of halite. Because of halite dissolution, there is a clearly increasing trend of Cl as a function of wetting. Other anions (HCO_3^- and SO_4^{2-}) indicate slightly decreasing trends due to CO_2 partitioning in the gas phase and precipitation of gypsum. Quartz dissolves to its solubility limit in the first cell, and then practically nothing happens in the subsequent cells.

Backfill boundary

Figure 3 illustrates the results of 40-time-refill of an EBS boundary cell (cf. Fig. 1b) with external water (Table 2). The first reaction cycle is similar to the first cycle of the previous wetting front study (Fig. 2), i.e. water reacts with entrapped air, pyrite is dissolved, goethite is precipitated, and pH is dropped to a lower level. All subsequent cycles occur in the anoxic saturated conditions without pyrite and goethite reactions.

During the first two reaction cycles gypsum is dissolved to its solubility limit leading to production of dissolved sulphate and Ca in water. The role of cation exchange is significant during Ca production. Cation exchange is a partial sink for produced Ca and it releases other major cations into solution. As soon as gypsum runs out, all major cation and sulphate concentrations drop to a lower level in porewater. Contemporaneously, as sulphate runs out from porewater, the pe values have a chance to find a lower level. The dissolved Fe is a simple function of pe.

During the first cycles (Fig. 3), dissolving calcite causes sharp increase in alkalinity and an increase in pH. Later, the backfill boundaries precipitate small amounts of calcite. This is possible because of Ca in the external water. Due to temperature rise to 40°C calcite becomes supersaturated in respect to the external water composition (Table 2). This causes calcite precipitation at the EBS boundaries and concordant pH drop.

It can be concluded that the 40 batch cycles, in most cases, have negligible effect on the mineral amounts available in the cells. The exception is gypsum that is dissolved away from the backfill boundary during the simulations.

Concluding remarks

In addition to bentonite cation exchange properties, also TMB-muck contains silicate surfaces and exchange sites that can adsorb cations. However, in the current calculations more difficult problem possibly arises from anion adsorption/exclusion. In the compacted backfill, anion processes likely become effective. Therefore, the trends for dissolved anions presented in Figure 2 are speculative.

The effect of temperature was partially taken into account in the calculations. However, elevated temperatures may have unexpected effects to the systems because batch reaction times are potentially extensive. Considering the silicates available in the backfill, there are several phases susceptible for partial alteration or gradual decomposition (e.g. montmorillonite, illite, amphibole, plagioclase, and K-feldspar).

At the beginning of the repository operation, batch cycles follow each other more quickly than at the later stages of operation. External water infiltration causes high porewater pressures at the repository boundaries creating strong gradients in the saturated part of EBS, and drives water deeper into EBS (Börgesson & Hernelind, 1999). At the same time, there are high negative porewater pressures in the undersaturated EBS. The initial suction gradients are possibly strong. Later the gradients begin to diminish and finally vanish. At later stages of the system, the thermal/geochemical gradients are probably the significant driving forces. Near the saturation level, porewater moves only by diffusion meaning very slow transport.

BACKFILL WETTING FRONT

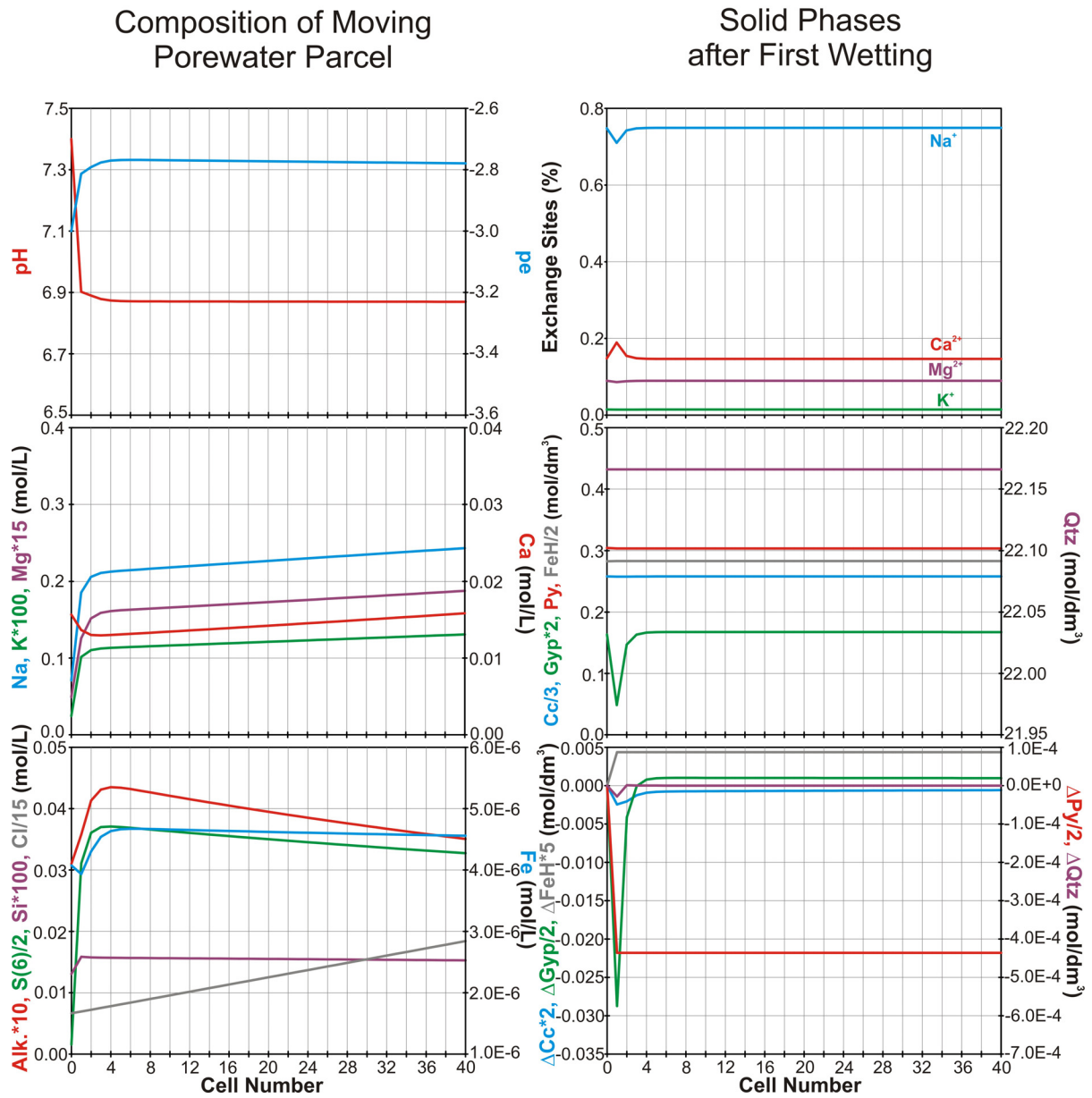


Figure 2. Geochemical evolution of moving porewater parcel and compositions of material volumes after first wetting of backfill. The porewater parcel is transferred 40 times to a new undersaturated backfill cell. The equilibrium temperature assumption is 40°C. Cc = calcite, Gyp = gypsum, Py = pyrite, FeH = goethite.

BACKFILL BOUNDARY EVOLUTION

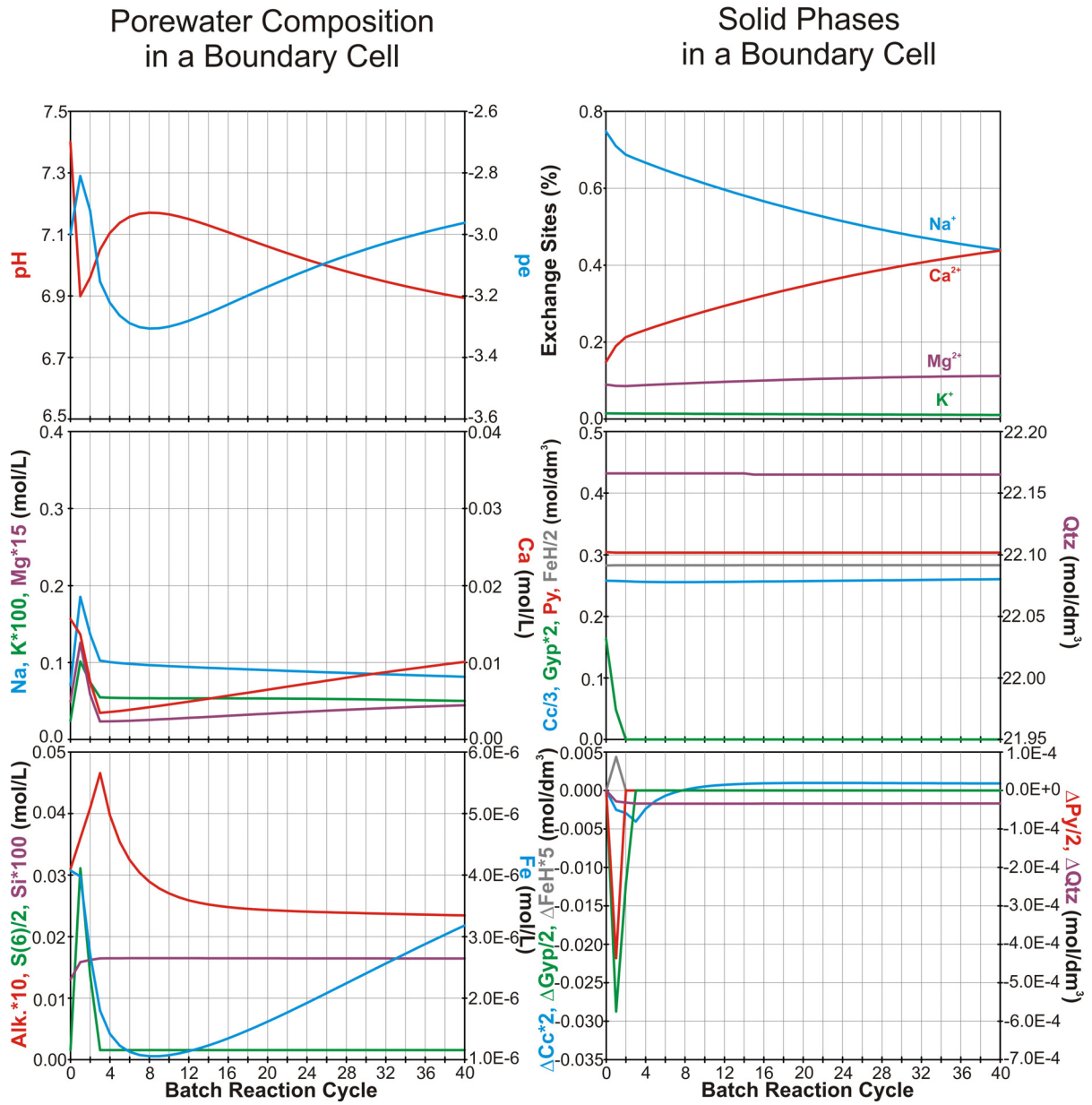


Figure 3. Geochemical evolution in material properties and resulting porewater compositions in an EBS cell volume at the rock-backfill boundary. The cell volume is refilled 40 times with water presented in Table 2. The equilibrium temperature assumption is 40°C. Cc = calcite, Gyp = gypsum, Py = pyrite, FeH = goethite.

References

- Andersson C & Säfvestad A, 2000.** Äspö Hard Rock Laboratory. Compilation of groundwater chemistry data from the Prototype repository. March 1998 – June 1999 (unpubl. report). Svensk Kärnbränslehantering AB (SKB), Stockholm, Sweden. International Technical Document 00-04: 6 p.
- Bradbury MH & Baeyens B, 2002.** Porewater chemistry in compacted re-saturated MX-80 bentonite: Physico-chemical characterisation and geochemical modelling. Paul Scherrer Institute, Villingen, Swizerland, PSI Bericht 02-10: 41 p.
- Bradbury MH & Baeyens B, 2003.** Porewater chemistry in compacted re-saturated MX-80 bentonite. *Journal of Contaminant Hydrology* 61: 329–338.
- Börgesson L & Hernelind J, 1999.** Äspö Hard Rock Laboratory. Prototype Repository. Preliminary modelling of the water-saturation phase of the buffer and backfill materials. Svensk Kärnbränslehantering AB (SKB), Stockholm, Sweden. International Progress Report 00-11: 99p.
- Bruno J, Arcos D & Duro L, 1999.** Processes and features affecting the near field hydrochemistry. Groundwater-bentonite interaction. Svensk Kärnbränslehantering AB (SKB), Stockholm, Sweden. Technical Report 99-29: 56 p.
- King F, Ahonen L, Taxén C, Vuorinen U & Werme L, 2001.** Copper corrosion under expected conditions in a deep geologic repository. Svensk Kärnbränslehantering AB (SKB), Stockholm, Sweden. Technical Report 01-23: 176 p.
- Muurinen A & Lehtikoinen J, 1999.** Porewater chemistry in compacted bentonite. Posiva Oy, Eurajoki, Finland. Posiva Report POSIVA 99-20: 46 p.
- Parkhurst DL & Appelo CAJ, 1999.** User's guide to PHREEQC (Version 2) – A computer program for speciation, batch-reaction, one-dimensional transport, and inverse geochemical calculations. U.S. Geological Survey, Denver, Colorado. Water-Resources Investigations Report 99-4259: 312 p.
- Patel S, Dahlström L-O & Stenberg L, 1997.** Äspö Hard Rock Laboratory. Characterisation of the rock mass in the Prototype Repository at Äspö HRL, Stage 1 (unpubl. report). Svensk Kärnbränslehantering AB (SKB), Stockholm, Sweden. Progress Report HRL-97-24: 62 p.
- Pusch R & Börgesson L, 2001.** Äspö Hard Rock Laboratory. Prototype Repository. Instrumentation of buffer and backfill in Section I. Svensk Kärnbränslehantering AB (SKB), Stockholm, Sweden. International Progress Report 01-60: 28 p.
- Wersin P, 2003.** Geochemical modelling of bentonite porewater in high-level waste repositories. *Journal of Contaminant Hydrology* 61: 405–422.
- Wieland E, Wanner H, Albinsson Y, Wersin P & Karnland O, 1994.** A surface chemical model of the bentonite-water interface and its implications for modelling the near field chemistry in repository for spent fuel. Svensk Kärnbränslehantering AB (SKB), Stockholm, Sweden. Technical Report 94-26: 64 p.

List of Appendices

Title	Author	Appendix no
Relevant THMC Phenomena and Mathematical description	A. Gens, Technical university of Catalonia	1
Modelling the Thermal-Hydraulic-Chemical-Mechanical (THMC) behaviour of bentonite buffer	H. R. Thomas, P. j. Cleall, T. A. Melhuish and S. C. Seetharam, Geoenvironmental Research Centre	2
Hydraulic Rock-Buffer Interaction	Richard Weston, Lund University Dept. Production and Materials Engineering	3
Conclusions	R Pusch, Geodevelopment AB	4
Influence of water penetration rates on heterogeneous buffer	E. Alonso, Cimne	5
Code-Bright: A THMC numerical simulator	A. Gens, Technical University of Catalonia	6
Numerical Simulation of coupled Heat, Moisture and Salt Transfer in porous Materials	Heiko Fechner, University of Technology	7
A new numerical tool for analysis of coupled far-field near-field processes	Viktor Popov, Wessex Inst. Of Tech.	8
AECL Experiences with HM modelling: Tunnel Sealing Experiment	D. Dixon, R. Guo, AECL	9
A perspective of the modelling of Prototype Repository Experiment	A. Ledsema, G. J. Chen, Cimne	10
Proposal of an alternative re-saturation model for bentonite buffers	Klaus-Peter Kröhn, GRS	11
Pressure distribution versus excavation Disturbed zone in a filled deposition hole - non isothermal two-phase flow in Porous media	Lutz Liedtke, BGR	12
Problem statement and course of work	Lennart Börgesson, Clay Technology	13
Coupled modelling with Rockflow/Rockmech – Current Status	T. Nowak, BGR	14

Title	Author	Appendix no
Predicting Thmc Behaviour Of Febex Bentonite At Different Scales	A. Gens, Technical university of Catalonia	15
Modelling gas migration in clay buffers	E. Alonso, Cimne	16
Prediction of geochemical changes in the Prototype Repository tunnel backfill	A. Luukkonen, VTT	17
Proposal for continued modelling work	E. Alonso, UPC	18
Modelling Underground Mines For Rock Stability Assessment Using Boundary Elements A New Approach For Large Scale Problems	Viktor Popov, Wessex Inst. Of Tech.	19
Agenda	C Svemar / R Pusch	20
List of Participants		21